Degradation of a Polymer Electrolyte Membrane Fuel Cell Under Freeze Start-up Operation

by

Christopher Rea

A thesis

presented to the University of Waterloo

in fulfillment of the

thesis requirement for the degree of

Master of Applied Science

in

Chemical Engineering

Waterloo, Ontario, Canada, 2011

AUTHOR'S DECLARATION

I hereby declare that I am the sole author of this thesis. This is a true copy of the thesis, including any required final revisions, as accepted by my examiners.

I understand that my thesis may be made electronically available to the public.

ABSTRACT

The polymer electrolyte membrane fuel cell (PEMFC) is an electrochemical device used for the production of power, which is a key for the transition towards green and renewable power delivery devices for mobile, stationary and back-up power applications. PEMFCs consume hydrogen and oxygen to produce power, water and heat. The transient start-up from sub-zero freezing temperature conditions is a problem for the successful, undamaged and unhindered operation. The generation and presence of water in the PEMFC stack in such an environment leads to the formation of ice that hinders the flow of gases, causes morphological changes in the membrane electrode assembly (MEA) leading to reversible and irreversible degradation of stack performance.

Start-up performance is highly dependent on start-up operational conditions and procedures. The previous state of the stack will influence the ability to perform upon the next start-up and operation. Water generated during normal operation is vital and improves performance when properly managed. Liquid water present at shut-down can form ice and cause unwanted start-up effects. This phase change may cause damage to the MEA and gas diffusion media due to volume expansion. Removal of high water content at shutdown decreases proton conductivity which can delay start-up times. The United States Department of Energy (DOE) has established a set of criteria that will make fuel cell technology viable when attained. As specified by DOE, an 80 kWe fuel cell will be required by 2015 to reach 50% power in 30 seconds from start-up at an ambient temperature of -20°C.

This work investigates freeze start-up in a multi-kilowatt stack approaching both shut-down conditioning and start-up operations to improve performance, moderate fuel cell damage and determine the limits of current stack technology. The investigation involved a Hydrogenics Corporation 5 kW 506 series fuel cell stack. The investigation is completed through conditioning the fuel cell start-up performance at various temperatures ranging from -5°C to below -20°C. The control of system start-up temperature is achieved with an environmental chamber that maintains the desired set point during dwell time and start-up. The supply gases for the experiment are conditioned at ambient stack temperature to create a realistic environment that could be experienced in colder weather climates. Temperature controls aim to maintain steady ambient temperatures during progressive start-up in order to best simulate ambient conditions. The control and operation of the fuel cell is maintained by the use of a fuel cell automated test station (FCATS™). FCATS supplies gas feeds, coolant medium and can control temperature and reactant humidity in reactants according to a prescribed procedure for continuous operation. The

collection of data occurs by the same system recording cell voltage, temperatures, pressures, flow rates and current densities. A procedural start-up and characterization are conducted in order improve start-of performance and examine reactant flows, coolant activation time, stack conditioning and the effects by freezing temperatures. The resulting degradation is investigated by polarization curves and various ex-situ measurements. In this work, it was found that freeze start-up of a fuel cell stack can be aided and managed by conditioning the stack at shut-down and applying a procedure to successfully start-up and mitigate the damage that freezing can cause.

ACKNOWLEDGEMENTS

I would like to acknowledge the Natural Sciences and Engineering Research Council (NSERC) for their financial support as well as Hydrogenics Corporation for their financial aid, use of their facility and equipment.

I would like to thank my supervisor, Michael Fowler for his support in arranging for this opportunity and guidance leading me along the way. Thank you also to my supervisor at Hydrogenics, Rami Abouatallah for his guidance and assistance.

I would like to thank Natasha Beydokhti for her assistance in building and operating the fuel cell. All my colleagues, and special note of Vengatesan Singaram for his time and help operating the scanning electron microscope.

My appreciation goes out to Dr. Mark Pritzker, Dr. Zhongwei Chen and Dr. Michael Fowler for taking the time to act as readers for this thesis.

I would also like to thank my parents and family for their generous support. Lastly, but not at all least, my fiancée Taryn Bingley who helped to encourage me and provided me with a beneficial distraction.

TABLE OF CONTENTS

LIST OF FIGURES

LIST OF TABLES

NOMENCLATURE AND ABBREVIATIONS

Symbol	Description	Units
A	Active area of Cell	cm^2
DOE	United States of America Department of Energy	-
CCL	Carbon Catalyst Layer	-
CCM	Catalyst coated membrane	-
e^-	Electron	-
EASA	Electrochemical active surface area	-
E^0	Standard chemical potential	V
F	Faradays constant	$C \cdot mol^{-1}$
FC	Fuel Cell	-
GDM	Gas Diffusion Media/Membrane (Gas Diffusion Layer (GDL))	-
i	Stack operating current density	$A \cdot cm^{-2}$
	Electric kilowatt	KWe
MEA	Membrane Electrode Assembly	-
n	Number of cells in fuel cell stack	-
n_e	Number of electrons transferred in a reaction	-
OCV	Open Circuit Voltage	-
P	Pressure	kPa
P_{Stack}	Stack Power	W
PEM	Polymer Electrolyte Membrane	-
PEMFC	Polymer Electrolyte Membrane Fuel Cell	-
PFSA	polyflourosulphonic acid	-
PTFE	polytetrafluoroethylene	-
e-PTFE	expanded polytetrafluoroethylene	-
Q	Volumetric gas flow rate	slpm
t	Time	hour, min, sec
T	Absolute temperature	K
slpm	Standard Litre per minute	-
y_i	Molar gas fraction for species i in the mixture	-
V	Stack Potential voltage	V
V_{Cell}	Cell Potential voltage	V
η	Polarization overpotential	V
λ	Stoichiometric coefficient	-

INTRODUCTION

1.1. Objective

Fuel cells will have to be superior to established technology in order to become commercially viable for everyday use. Fuel cell (FC) technology is an environmentally clean, increasingly renewable and a step towards sustainable energy systems. Various technical aspects are impeding utilization of this technology in today's society. Governments, various industries and academia which seek to overcome current barriers by improving this technology and incorporate it into daily life. This project seeks to aid in the development of FC technology by examining the influences of cold weather and sub-zero temperatures on the current state of available technology. Specifically, the objective of this thesis is start-up operation of a polymer electrolyte membrane fuel cell (PEMFC) from freezing conditions. Suppressed temperatures influence the ability to generate power and from the water freezing and forming ice. Experiments are conducted with various procedural changes to measure their effect on performance and develop improved practices. More specifically the goals of this project are to improve freeze start-up performance, measure modes of degradation that can occur due to ice and sub-zero start-up and operation, and develop potential strategies that can mitigate or reduce their effects.

1.2. Format of the Thesis

This chapter breaks down the subject of PEM fuel cells by describing their basic theory, components and systems that are used to operate and produce power. In 0the subject of water, the critical role and reason it is necessary within the fuel cell is reviewed. 0further investigates the role of water but in reference to freezing where water can form ice and the methods that can be used to mitigate damage. 0discusses degradation that occurs from operating the stack both as a result of normal operation and from a sub-zero freezing environment. 0introduces the experimental instrumentation and procedures used to condition and start-up the PEMFC in sub-zero environments. 0presents the results of the experimental testing and highlights and discusses key findings. Finally, 0 will provide conclusions and recommendations on the current work that has been completed.

1.3. **Transition to Fuel Cells**

Hydrogen has recently been described as a key resource for use in society: to transition towards a more secure, environmentally sustainable, economically viable and vital energy future [1]. FC adoption has been forecasted as a means to stem and reverse the effects of global climate change and move towards improved environmental and sustainable practices. The versatility of hydrogen is illustrated in terms of its many different forms of generation and its ability to generate power. Hydrogen fuel can generate power without carbon emissions in various forms to reduce greenhouse gas emissions. The adoption of hydrogen as a resource has been coined the "hydrogen economy". The role of the fuel cell in a hydrogen-fueled economy is equivalent to the internal combustion engine in today's petroleum-based economy.

The advantages of FC technology make it promising for implementation. First, the generation of power by an electrochemical reaction produces electricity. Thermal combustion systems seek to produce primarily heat to drive a mechanical piston or motor. The motion of the motor can then be used to produce electricity. At each stage of conversion some of the generated power is lost. The efficiency of combustion engine is governed by the Carnot cycle which yields the maximum attainable power produced from combustion. Theoretically FC power generation can surpass this limit by the direct conversion of electrochemical energy to electrical energy. Secondly, the reaction inside the fuel cell produces pure water only and a small amount of waste heat. The power generation is therefore very clean with no harmful emission or by-products produced. Third, a FC can be flexibly designed to suit large scale installations in the megawatt range for multiple homes or smaller personal devices in the watt range. Fourth, the operation of the FC is quiet with no moving parts which lowers maintenance requirements and improves reliability.

Various types of fuel cells exist such as alkaline, polymer electrolyte membrane, solid oxide, molten carbonate which are classified in terms of the nature of the electrolyte. The selection of the appropriate type of FC is based on the operating criteria and desired fuel utilization. PEMFC are desired for their ability to be used in any setting, from powering large scale installations to small scale devices in stationary or mobile applications.

The future vision of an economy powered by hydrogen is feasible and in reality a step towards an environmentally sustainable future. Engineers and scientists seek to aid in the research and development necessary for its successful introduction into society. Hydrogen FC technologies have

dramatically improved cell performance by increasing power density, reducing costs and improving operating ranges [2]. The increase in operating temperatures has reduced the need for cooling and led to better operating performance [3]. Increasing performance while decreasing precious metal loading and substituting different catalysts on electrodes decreases manufacturing costs [4,5]. Reducing production costs will ease the adoption of FC technology, making it more accessible and favourable. It is inevitable that performance will degrade during the life of a fuel cell due to irreversible decay of electrode materials. Fuel cell durability was a major problem initially, but has recently improved so that lifetimes of more than 5,000 hrs for mobile applications and 40,000 hrs for stationary applications have been achieved [6]. The current state of FC technology has made substantial progress from its initial stages so that the objective of producing a stable and economically viable technology for implementation is close to realization.

1.4. Operation of PEM Fuel Cell

The basic operation of the fuel cell system and in-situ measurements of performance are described in the following sections.

1.4.1. Principles of Fuel Cell Operation

The state of water in a fuel cell is important for its performance. If the water produced is a vapour, then less energy is generated by the process. (0-1 shows the standard enthalpy change and cell electromotive force for the production of liquid water, while (0-2 shows the corresponding values when vapour is generated. These differences show that the production of liquid water releases more energy.

$$H_2 + \frac{1}{2}O_2 \rightarrow H_2O_{Liquid} \qquad \Delta H° = -285 \text{ KJ mol}^{-1} \qquad E^O = 1.23V \tag{0-1}$$

$$H_2 + \frac{1}{2}O_2 \rightarrow H_2O_{Vapour} \qquad \Delta H° = -241 \text{ KJ mol}^{-1} \qquad E^O = 1.18V \tag{0-2}$$

The measure of performance of the fuel cell is critical for qualifying and quantifying effects of various factors such as activation losses, ohmic losses and concentration overpotential. The electrochemistry of fuel cells is similar to that of batteries, except that batteries contain a fixed amount of material that is used in the production of power. On the other hand, reactants are not stored in fuel cells and instead are continuously supplied. In this way, they operate

continuously to produce power and do not require recharging or replacement of the power source.

A fuel cell is made up of three elementary components known as electrodes, an electrolyte and a load. The electrolyte transports the necessary protons for the reaction. Hydrogen oxidation to protons and electrons occurs at the anode. The reaction between protons, oxygen and electrons occurs at the cathode. A simplified schematic of these reactions is shown in Figure 0-1 . The electrons generated at the anode are conducted to the cathode through an external load to power a device.

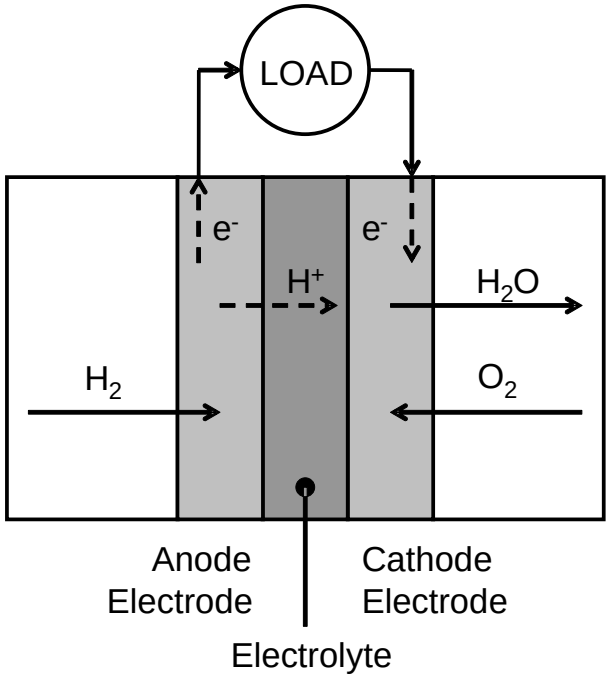

Figure 0-1: Galvanic cell representative of the PEMFC

Hydrogen is continuously fed to the anode to react at a precious metal catalyst to form protons and electrons by the half-cell reaction:

$$2\mathrm{H}_2 \rightarrow 2\mathrm{e}^- + 2\mathrm{H}^+_{(\mathrm{aq})} \qquad E^o_{25^oC} = 0\ V_{SHE} \qquad (0\text{-}3)$$

The electrolyte is electrically non-conductive which allows the electrons to be directed through an external circuit. The protons travel through the electrolyte to the cathode where they react with oxygen and electrons to form water according to the half-cell reduction reaction given in (0-4:

$$O_2 + 4H^+_{(aq)} + 4e^- \rightarrow 2H_2O_{(Liq)} \qquad E^o_{25^oC} = 1.223\ V \qquad (0\text{-}4)$$

The two half-cell reactions (0-3 and (0-4 combine to yield the overall fuel cell reaction:

$$2H_2 + O_2 \rightarrow 2H_2O_{(Liq)} \qquad E^o_{25^oC} = 1.223\ V \qquad (0\text{-}5)$$

In theory, the maximum cell voltage potential of an operating cell is 1.223 [V]. This potential is related to the activity of products and reactants by the Nernst (0-6:

$$E = E^\circ - \frac{RT}{2F} ln\ \frac{P_{H_2O}}{P_{H_2} P_{O_2}^{1\ 2}} \qquad (0\text{-}6)$$

The actual voltage generated in an operating fuel cell drawing current is always lower then this value. Loss occurs as a result of electrical resistances, overpotentials (activation, ohmic and mass transport) and reductions in thermodynamic driving force that inhibit the generation of power and lower the performance.

1.4.2. PEMFC Performance

The performance of the system differs from the ideal as a result of operational losses. The processes in a fuel cell involve transport, adsorption, diffusion, reactions and desorption, all of which contribute to a decrease in performance. The kinetics of the oxygen reduction reaction (ORR) at the cathode is slow and tends to be rate determining and control the resistance in the fuel cell operation [7]. The cathode can be supplied with pure oxygen, although air is typically used. The use of air at the cathode lowers the partial pressure of oxygen and reduces the extent of adsorption. Therefore, the reduction in performance is confounded by the decrease in concentration since the ORR is already rate determining. Water is also generated at the sites where oxygen adsorbs. Water must leave and/or evaporate to free the catalyst site before the reaction can resume at the site. The GDM that assists gas transfer can also hinder the reaction, since water can fill pores and block the transport of fresh gas to active reaction sites. The GDM can become so water-filled that flooding of the diffusion media leads to a lack of available pathways for gas transport. Since flooding leads to poor performance or even cell failure, attention to thermal management and water management (0) is necessary for fuel cell performance.

One of the main metrics of FC performance is a polarization curve (PC). Figure 0-2 shows the relationship between the current density and the output cell voltage. A PC normally exhibits three main regions where activation polarization, ohmic polarization and concentration polarization become dominant. Activation polarization is dominant at low current densities (Area 1). At increasing current density, both activation polarization and ohmic polarization start to effect power generation (Area 2). At sufficiently high current densities concentration polarization becomes important as the current approaches a limiting level (Area 3).

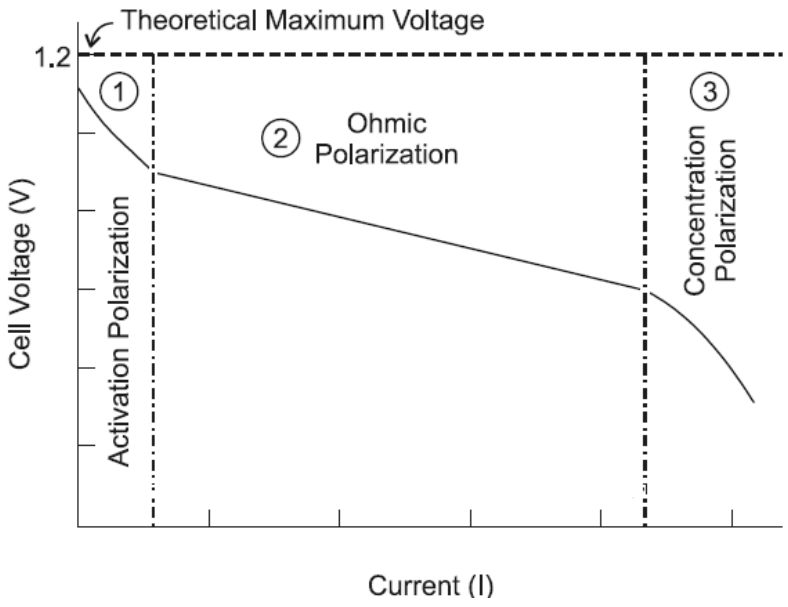

Figure 0-2: Polarization curve performance of a fuel cell

1.5. Introduction to Polymer Electrolyte Membrane Fuel Cell

This section introduces the basic principles and components of a polymer electrolyte membrane fuel cell (PEMFC) system in order to understand its basic operation.

1.5.1. Fuel Cell Components

A FC system contains the components shown in Figure 0-3. This includes a bipolar plate typically with channels routed or moulded into the plate for gas transport and distribution. The plate also acts as a current collector and distributes charge across the surface. The gas diffusion media (GDM) is a layer situated next to the bipolar plate. The GDM distributes and removes reactants and products while providing mechanical support to the membrane. The local areas around the

channels where the bipolar plate and the GDM contact each other are known as lands. The GDM is a porous material that delivers gas into the fuel cell. The pores/channels carry the gas and distribute it across the surface of the PEM. On the other side of the GDM is a gas-impermeable PEM with an 'electrode' surface composed of carbon support for a platinum precious metal composite catalyst. The side of the PEM is the electrode (anode or cathode) where one of the electrochemical reactions takes place. The membrane conducts protons from the anode assembly to the cathode assembly and inhibits electrical conductivity between the two sides to keep the reaction from short-circuiting. The combination of the membrane, anode layer and cathode layer is commonly referred to as the 'catalyst coated membrane' (CCM). The combination of the membrane, electrodes and GDM is commonly called the 'membrane electrode assembly' (MEA). Each side of the CCM is in contact with a GDM and bipolar plate for support and gas delivery. This sequence of components creates a cell. Cells are layered upon each other to form multiple cell systems known as a stack. The number of cells in the stack is designed to meet the desired application.

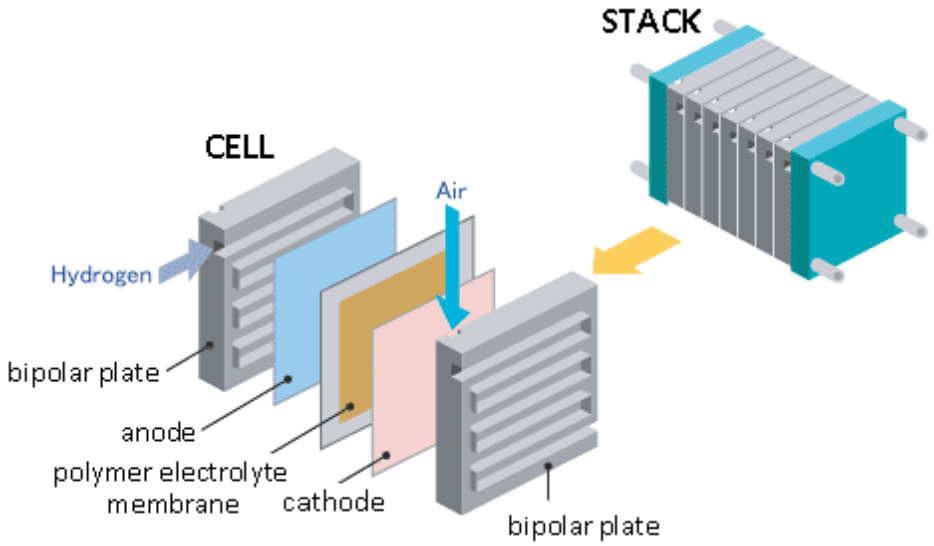

Figure 0-3: PEM fuel cell stack geometry **[**8**]**

1.5.2. **Endplates**

Two endplates of the fuel cell, whether it contains one or more cells, are necessary to provide the desired structure and rigidity of the stack. The endplates get their name for being at the outer ends of the stack. Endplates also enable connections for supply and removal of reactant

and products by a gas manifold. Endplates are also used to compress the stack at the desired force and prevent any structural damage that may occur as the internal components are more susceptible to shock and damage. The stack is compressed to increase electrical contact between components and prevent internal material components from warping. Typical endplate materials are stainless steel, aluminum, magnesium or other alloy or carbon-based composite materials. The type of material used is an important consideration as the endplates make up the majority of the weight of the fuel cell stack.

1.5.3. Insulator

An insulating material is placed inside the fuel cell stack between the endplates and the current collecting plate to prevent passage of any electrons. Insulators keep the endplates from generating any potential or transferring current to the surroundings. The insulator is generally a plastic material that is light and easily manufactured at a relatively low cost.

1.5.4. Bus Bar

Two bus bars or current collectors are located between the insulator and the first and last bipolar plate. The bus bar is the interface between the current generated in the stack and the external load that is being supplied with electrical power. The bus bar is an excellent electronic conductor which is necessary to transfer all the electrons generated from the reaction taking place. The contact between the bus bar and the bipolar plate must be uniform with no separation as any spaces or gaps will increase resistance and losses in power delivery. Copper, brass or highly conductive material is commonly used. The bus bar can be gold-plated for increased performance (i.e. greater conductivity and corrosion resistance) depending on the cost and performance desired.

1.5.5. Bipolar or flow field plate

The bipolar plate is positioned along the bus bar and cell internal components, repeated between subsequent cells in the stack. The desired light weight bipolar plate material is typically graphite, a coated metal or composite material. Bipolar plates provide rigidity and mechanical structure for the cells to be compressed evenly. The electrical conductivity of the material provides conductance in series to other cells that make up the stack. The material must be chemically stable to reducing and oxidizing environments for durability. Low gas permeability

keeps the fuel and oxidant separate while distributing the gases evenly over the cell and removing by-products in the flow fields. The bipolar plate typically has formed channels and pathways for the gas to flow in various patterns: interdigitated, meandering, parallel, serpentine or other types of flow path configurations. Coolant can be circulated into the bipolar plates that have internal channels to remove and distribute the generated heat.

1.5.6. Gas Diffusion Media

The gas diffusion media (GDM) is a porous structure typically made from carbon paper or carbon cloth [9]. The GDM enables the distribution of the gas reactant over the interfacial area of the membrane and controls the movement of water by having both hydrophilic and hydrophobic properties. GDM conducts electrons from other cell reactions towards or away from the bipolar plate for the process to propagate. The GDM consists of a three phase boundary where water, gas reactant and solid phase interact. The porous nature of the material enables transport between the bipolar plate and membrane surface. Water is transported away from the membrane while gas reactant is transported to the membrane. The pores in the GDM are distributed in size and shape, causing regions of the pores to be water-filled or open to gas transport. The GDM can be chemically treated to inhibit or assist in the removal or retention of water. One type of treatment for hydrophobicity is with materials such as polytetrafluoroethylene (PTFE) [2] which cause water to be removed faster through the media and improve the performance at higher reaction rates. Water content in the cell is controlled by the cell components and the amount of supplied humidity in gas reactants. The GDM is typically treated along the layer that lies against the membrane with a special layer known as the microporous layer. The main purposes of the GDM are to control the reactant distribution to the electrodes and aids in management of the water content of the membrane.

1.5.7. Microporous Layer

The microporous layer (MPL) is a component between the GDM and the catalyst layer (CL). The MPL beneficial improves fuel cell performance [10]. The purpose of the MPL is to facilitate removal of water from the CL in and thereby increase the electrochemical active surface area (EASA) [11]. The typical material selected is a highly hydrophobic material such as PTFE. The MPL assists in the separation between the CL and GDM pores where water may collect. This

separation allows for operation at higher temperatures or pressures so that more evaporation and easier transport of water can occur.

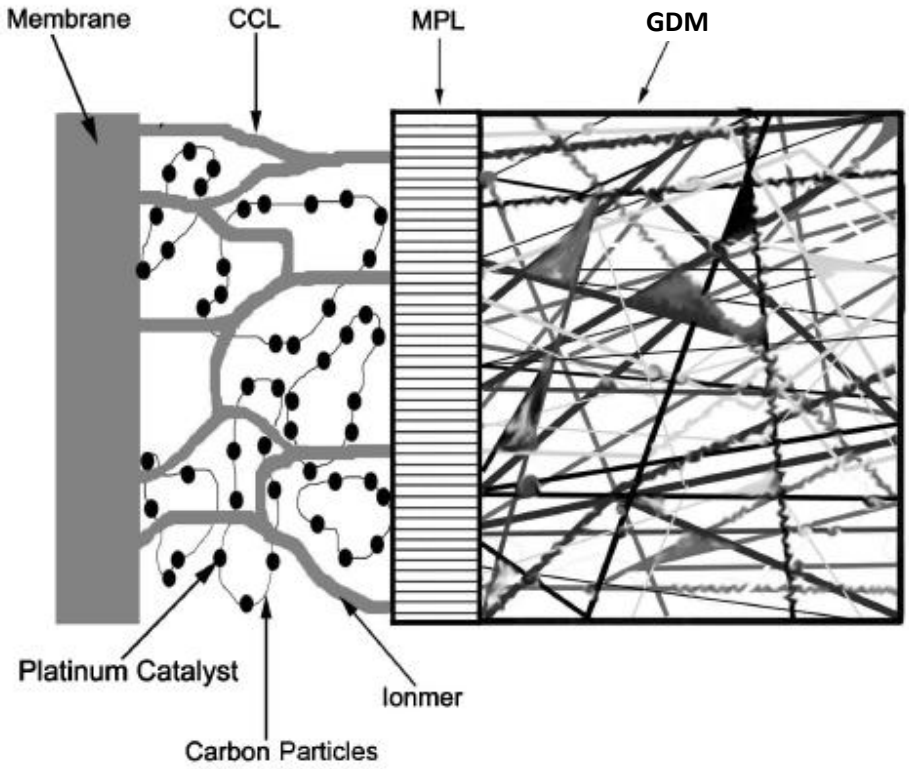

Figure 0-4: PEM cell internal showing microporous layer along gas diffusion media and membrane electrode assembly [12] (with permission from Taylor & Francis)

1.5.8. **Membrane**

The membrane in PEM fuel cell is a solid polymer with strong acidic (e.g. sulphonate) side groups. A typical material is sulfonated tetrafluoroethylene-based fluoropolymer-copolymer (PFSA). In the presence of water, the membrane hydrates and conducts protons for the reactions to occur. The membrane controls the movement of ions from electrode to electrode, separates gas reactants and electrically insulates the electrodes from shorting. If the electrons were to flow across the membrane, then all the generated electrical power would remain contained in the cell. The membrane must be chemically stable in both a reducing and oxidizing environment. The membrane material should have mechanical strength in order to survive pressure spikes or gradients to which it may be subjected.

1.5.9. **Catalyst Layer**

The membrane is treated with a catalyst layer (CL) at which the oxidation and reduction reactions occur (Figure 0-5). The catalyst can be incorporated by different methods with various components, but is most commonly made of platinum and other precious metals. Platinum is the best catalyst at the low operating temperatures of PEMFCs and is used at both electrodes. The CL next to the anode enhances the oxidation of hydrogen to protons and transfers them to the membrane by structured support sites. The cathode CL allows protons and oxygen to combine with electrons to form water. The catalyst is generally applied to the membrane on a carbon support structure that immobilizes the catalyst particles.

The active sites in the cell are located at three-phase interfacial regions where the supported catalyst contacts carbon for electrical conductivity, ionomer for proton conduction and gas diffusion pathways for hydrogen and oxygen. These areas where the reactions occur are known as the Electrochemical Active Surface Area (EASA).

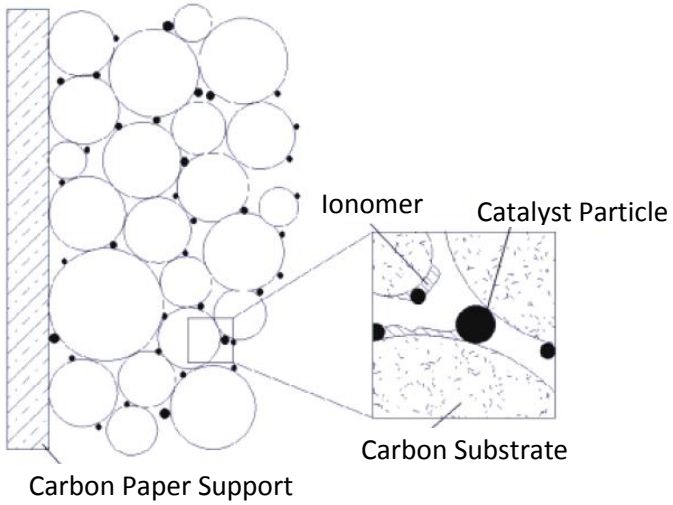

Figure 0-5 Catalyst layer structure

1.6. **System Operation**

Various systems are used to maintain and manage the state of operation: air supply, fuel supply, thermal management, water management and power conditioning. The process diagram is displayed below in Figure 0-6. Each of these system components must be integrated together in order to operate and maintain the FC stack.

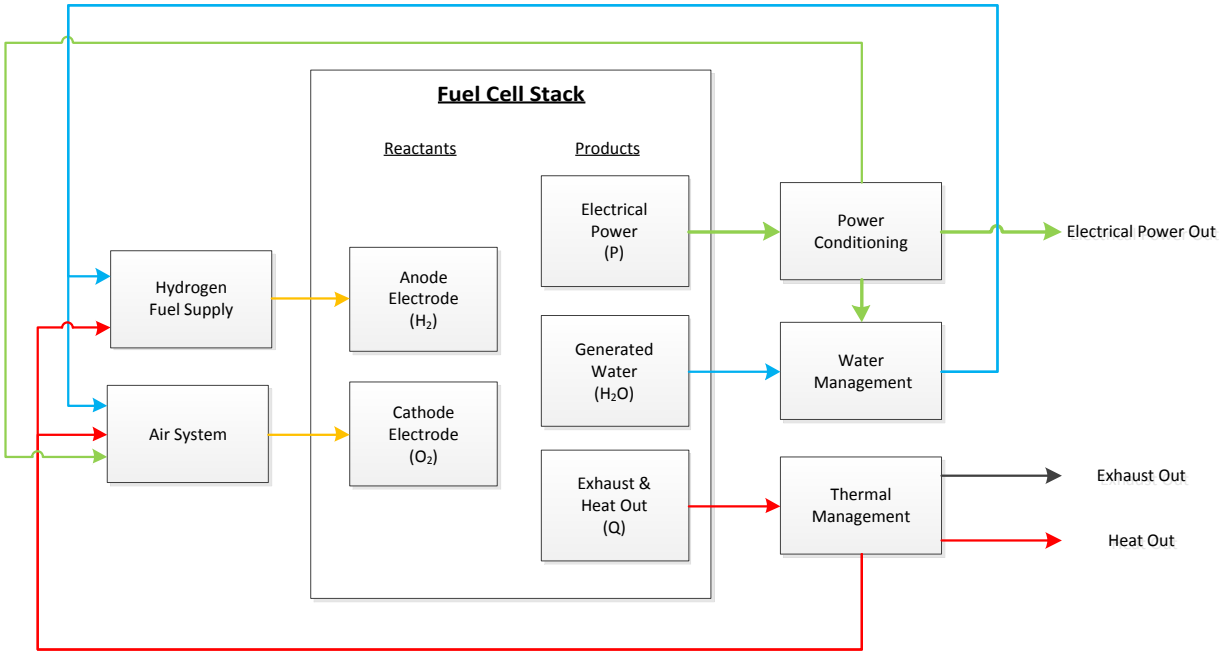

Figure 0-6: Fuel cell systems

1.6.1. Air Supply System

The use of air as a source of oxygen reduces storage requirements and reduces energy usage for fuel processing. Air is directed to the cathode by a blower in smaller systems or by gas compressors in large systems [13]. The pressure of the system varies depending upon the desired power density for the mode of application. The air can be hydrated to control the relative humidity and water content of the system.

1.6.2. Thermal Management System

FC operation generates heat as one of the products of the reaction. Improperly managed heat can raise the system temperature leading to performance loss and degradation. The thermal management system is used to cool and maintain safe operating temperature. Channels are machined into the graphite bi-polar plates to permit the circulation of a fluid to remove or introduce heat depending on the system state and design. The thermal management system can contain a heat exchanger, pump, de-ionized (DI) water polisher, particulate filters and flow meter. This enables heat to be captured and used to meet the desired needs of the application or emitted to the surroundings.

1.6.3. Water Management System

The presence of water in the fuel cell stack is necessary for the reaction and can be fed to the stack by various, internal or external methods which will be discussed in 0 [13]. Hydration of the stack is necessary for durability and performance as water is used as part of the electrolyte. The fuel can be humidified in order to deliver water to the stack. Water is discharged from the stack by outlet gas flows and/or into the coolant when using porous plates [14]. Discharged water is typically captured by a device to deliver humidified gas or water at a future time or in other applications.

1.6.4. Power Management System

The power generated by the operating FC creates a direct current (DC) that can be distributed directly to suitable applications. Scaling the size of the fuel cell system can be done to deliver power variations as required. Power converters are used to modify voltage when the delivered stack voltage does not match the applications requirements. An inverter can be employed to convert the output to alternating current (AC) for applications requiring this form of power. The use of a power management system also aids the FC by adding a level of protection and isolation of the fuel cell and its load [2].

WATER MANAGEMENT

One of the major benefits of fuel cell technology is that water is essentially the only emitted product. The generation of water in the fuel cell has many drawbacks as well as benefits. If improperly managed, water accumulates in the cell(s) and/or stack hindering operation and performance [15]. The PEMFC is generally operated at ambient pressures and temperatures lower then 100°C [2]. As the temperature of the fuel cell stack approaches the boiling point of water, water tends to vaporize. The presence of water is necessary for PEM durability, transport of protons through the membrane and the electrochemical reaction to occur [12]. Management and control of the amount of water present is therefore necessary for optimum cell performance.

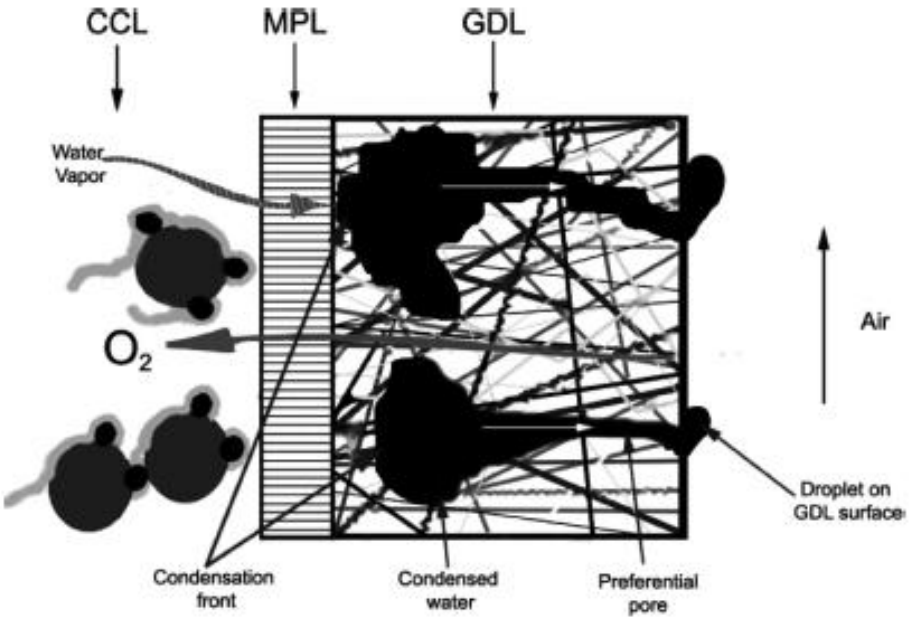

Figure 0-1: Water transport in fuel cell components [12] (with permissions from Taylor & Francis)

Water generated inside the fuel cell can accumulate in the MEA, gas delivery channels or inside the gas manifold (Figure 0-1). The rate of water production at the cathode is proportional to the operating current (I). An increase in the power draw causes an increase in the rate of water production according to Faraday's law ((0-1). When the heterogeneous catalyst sites become blocked by water the resistance due to the chemical reaction will increase. A decrease in flux to the electrodes reduces the concentration of reactive species causing a decrease in the yield of the reaction.

$$N_{Water,production} = \frac{I}{2F} \tag{0-1}$$

Water content in the cell is to be maintained at or within a certain range for optimal performance [12]. The operating temperature can also control the distribution of water in the stack. At lower temperatures the amount of liquid water present will increase. Areas of the fuel cell that become inactive due to flooding cause other local areas in a cell to operate at higher current densities in order to maintain the overall current. When the supply of reactant to the local area halts, the reaction may proceed in the reverse direction. Cell reversal causes operation as an electrolyser producing hydrogen and oxygen instead of their consumption. The adjacent cells may drive the reversed cell providing the necessary power. At high operation temperatures, water will evaporate and enable faster transport. As the ability to transport water increases, the rates of water removal will increase. However, if this becomes excessive, drying can occur and reduce proton conductivity and thus increase the cell resistance. As the membrane dries out, the gas permeability rate is affected. An increase in gas crossover between electrodes will reduce the efficiency of fuel utilization [16]. Optimal operation requires that the appropriate amount of water be present in the fuel cell.

The movement and location of water in the fuel cell components is an important factor for the water balance. Four main factors affect the content of water in the fuel cell: generation, electro-osmotic drag, back diffusion and humidification, which will be discussed in Section 1.7.

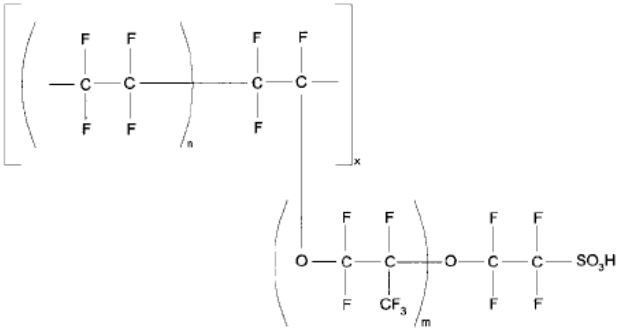

Figure 0-2: Example polymer membrane structure of PTFE with PFSA copolymer

The PEM material, perfluorosulphonic acid (PFSA) (Figure 0-2) contains hydrophilic groups as well as hydrophobic groups. The PFSA polymer can be described by in terms of two components: the backbone and the side chains. The membrane backbone which is related to polytetrafluoroethylene (PTFE) is highly hydrophobic. The sulphonic functional side chains are hydrophilic and will saturate in the

presence of water and form water-filled regions (Figure 0-3). The water-filled regions create channels and pores that can carry protons across the membrane. The water-filled areas become acidic environments from the donation of the sulphonic acid proton.

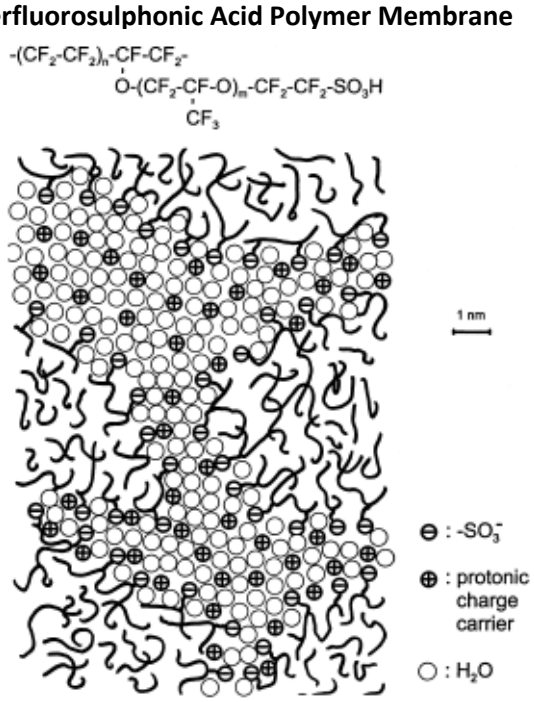

Figure 0-3: Hydrated PFSA membrane structure [17] (with permission from Elsevier)

Water can be managed by choosing the appropriate materials or treatments on the components in a fuel cell and by proper operation of auxiliary components in the system [18,19]. Stacks are constructed with cooling plates between or along a number of cells to control temperature during the electrochemical reaction. The coolant temperature can be controlled by auxiliary equipment, allowing for the removal of heat during operation. When gaseous reactants are recirculated for increased fuel utilization, a gas purge is conducted to remove impurities that can accumulate during operation. The exhausted gases contain a high level of water and are generally supersaturated with liquid droplets.

The control and management of water is necessary for maintaining continuous operation, as the membrane is required to stay hydrated for achieving long lifetimes [12]. Cycling humidity levels lead to repeated drying and swelling of the polymer membrane. Repeated swelling and contraction of the membrane polymers lead to mechanical wear and can reduce membrane integrity. Water management becomes critical during environmental effects with exposure to freezing temperatures.

1.7. **Water Content**

Water content helps to improve stack performance by decreasing resistance due to poor oxygen electrocatalysis, an increase in the resistance in the catalyst layers and an increase in membrane ionic resistance [20]. The amount and transport of water are mainly controlled by four different mechanisms (Figure 0-4). Water is formed at the cathode during power production, 'generation'. Water travels from anode to cathode via the second mechanism of water migration, i.e. 'electro-osmotic drag'. The increase in water concentration between cathode to anode gives the third mechanism of 'back diffusion'. The fourth mode of humidification is controlled externally by the presence of water in the gas reactant streams which carry water into the cell and the product stream which carry water out of the cell. These mechanisms must be understood for the proper operation of the fuel cell in both normal and freezing environments.

Generation

The generation of water occurs at the cathode locally at a three-phase interface between stack components. Generated water can reside at the CL active site, move into and hydrate the membrane or migrate into the GDM and out of the cell. Increasing current density increases the rate of water generation and therefore increase the necessary water flow rate ((0-2), i.e.

$$N_{H_2O} = \frac{I}{2F} \tag{0-2}$$

Electro-osmotic Drag

Protons are necessary to complete the reaction ((0-3) and are transferred from the anode to the cathode. The transfer of protons through the membrane occurs in conjunction with water. The protons positive charge attracts the waters dipole. Therefore, protons move across the membrane and drag water molecules along with them. The electro-osmotic drag coefficient gives a measure of the number of water molecules that travel across the membrane per proton. Zawodzinski *et al.* estimated that 0.9 to 3.4 [H_2O $(H^+)^{-1}$] are dragged (or pulled) across the membrane depending upon the type of membrane employed [21].

Back Diffusion

The concentration of water at the cathode is higher than at anode due to generation, and electro-osmotic drag. The concentration gradient creates a situation where water will travel back across the membrane from cathode to anode in order to equalize the gradient. The net movement of water molecules is from the anode towards the cathode due to the electrochemical reaction. Back diffusion is undesired as it inhibits the desired movement of protons from anode to cathode.

Back diffusion can be managed by component material selection and water management. Selecting a thinner membrane will decrease the required path lengths making it easier to travel across the membrane, decreasing the internal resistance. A thinner membrane aids in the transport of protons from side to side and, but also decreases the membrane resistance to gas pressure differentials and aging. The GDM can be selected with wetting properties to enhance water retention. Humidification of the anode electrode also directly increases the water content at the anode. All of these can increase the concentration at the anode and decrease the gradient.

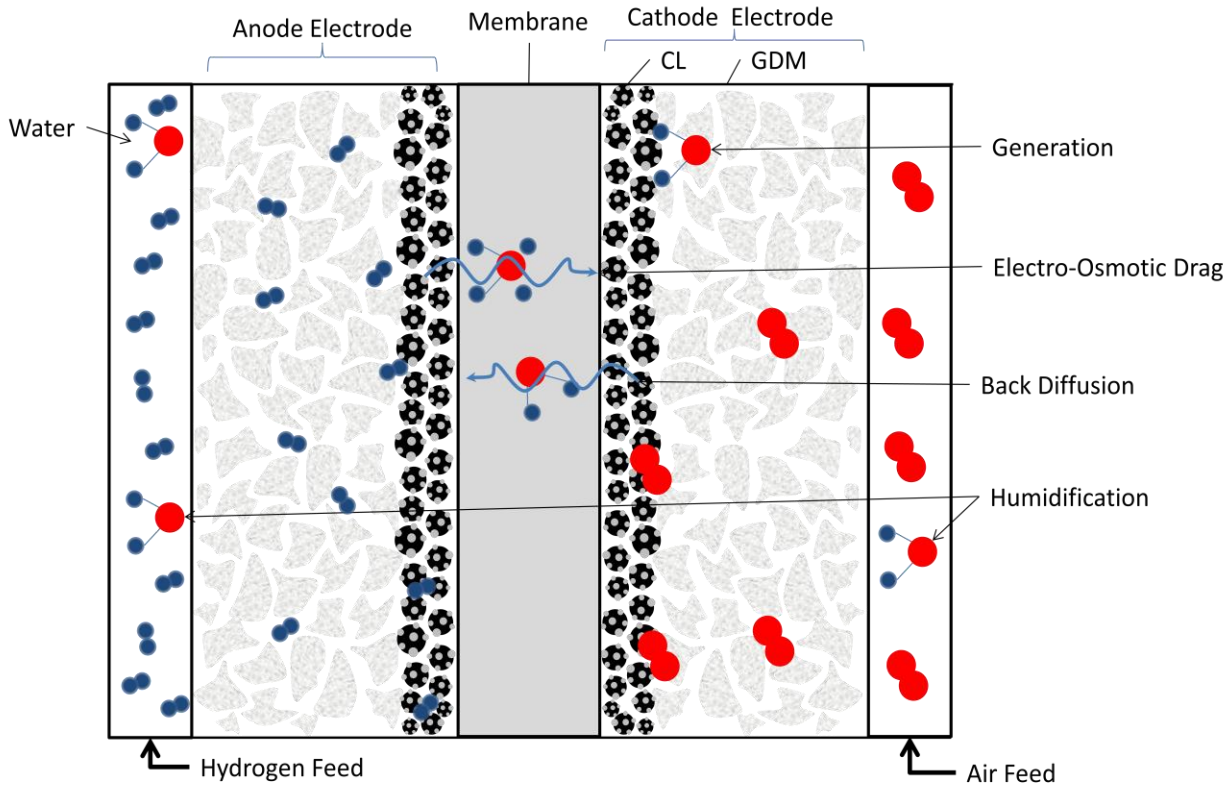

Figure 0-4 Water movement across PEMFC membrane

Humidification

Water in the gas reactant is necessary for proper water management depending upon the desired stack application and the components used. Water can be supplied and removed from the fuel cell by the inflowing gas reactant. To encourage the general propagation of the reaction, humidity is supplied to keep water levels high within the membrane. The flow of gas reactant into the bipolar plates causes conditions to differ between inlet to outlet. Inlets typically see the driest and coldest flows. As the gas flows through the channels and across the MEA, it can pick up heat and water. This causes the water content and temperature to change across the MEA surface. Local changes of temperature and water content across the membrane surface affect local performance and membrane life. Humidifying inlet gases can aid in equalizing the water gradient across the MEAs surface and decreases these effects. The anode is generally humidified to a greater extent than at the cathode to increase the overall net transfer of protons, aiding electro-osmotic drag, decreasing back diffusion, and preventing the anode from drying out. A fuel cell stack is operated with excess reactants. If the excess reactant is below 100% RH, then it can aid in water removal.

FREEZE MANAGEMENT

Environmental temperatures are an obstacle to PEMFC operation and implementation since the conditions surrounding the stack can cause residual or generated water in the stack to freeze. As previously discussed in Chapter 2, water management is extended here in the context of freeze management. Operation will be obstructed if water forms ice within the stack. Therefore, proper management of start-up, operation and shut-down of the stack prevents the accumulation of water and the formation of ice in the stack.

The formation of ice impedes operation, in turn causing reversible and irreversible degradation and the possibility of structural damage. Start-up operation of a fuel cell with the hardware within the stack below the freezing point of water is of particular interest since any water that comes into contact with the stack may freeze. The temperature of the stack components must rise above the freezing point in order for water to exist in the system in a liquid state. The ability of the stack to start-up and operate at sub-zero conditions is limited, as ice inhibits gas reactant delivery as well as blocking water removal.

The presence of ice in the stack can block reactant channels and pores in the GDM, and/or remain on the catalyst layer (CL). Figure 0-1 shows the GDM layer with liquid present distributed throughout the media [22]. The current technology within the stack can allow for water to freeze in and along particular stack components with variable temperatures. The CL and the membrane are of particular interest as these components interact with water and affect the formation of ice.

Freezing point suppression occurs in the CL as a result of the Gibbs-Thomson effect. The Gibbs-Thomson effect arises due to the fact that small crystals of a liquid freeze at a lower temperature than the bulk liquid. The freezing point depression is inversely proportional to the pore size, as smaller water-filled pores remain in a liquid state while larger pores will freeze. Ge and Wang [23] investigated the influence of freezing temperatures at start-up on the CL and found that water can remain in a liquid state even if the temperature deviates by as much as 1.0 ± 0.5°C from the normal freezing point.

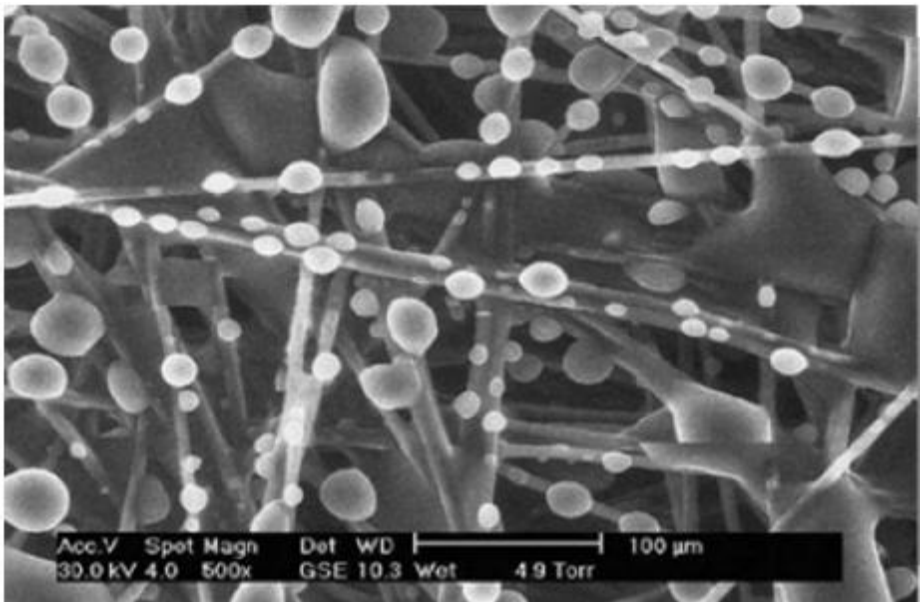

Figure 0-1: Water present on gas diffusion media [22] (with permissions form Elsevier)

The adsorption of water in the PEM will vary with temperature leading to multiple states of hydration [24]. This leads to multiple points within the membrane where ice may formation. The various pore sizes and structures of the membrane lead to the water freezing at different temperatures. Water in small pores and/or channels inside the PEM will not freeze due to the presence of the sulphonate groups preventing water from forming its crystal structure. Yoshida and Miura [25] investigated and classified the water in the membrane, and found that it can exist as three different states: free-water, freezing-bound water and non-freezing water. Free-water behaves as bulk water and freezes at sub-zero temperatures. Freezing-bound water forms ice after a minimum sub-zero temperature has been achieved. Non-freezing water remains in a liquid state and allows start-up of the PEMFC at sub-zero temperatures.

The membrane has a distribution of pores and channels that can fill with water and freeze depending upon their size and temperature [26]. Nucleation of water occurs near the centre where the influence of the sulphonate groups is weakest. Crystal growth causes a freezing-front to expand towards the outer edges increases the acidic content of the remaining liquid water. The non-freezing water that remains present conducts protons at temperatures down to -120°C. Free-water provides the proton conductivity in the PEM enabling start-up. These results were confirmed by Ge and Wang [23] who also measured the high frequency resistance (HFR) of the membrane during exposure to sub-zero temperature exposure. Ge and Wang found that HFR resistance increases as temperature decreases, indicating that there are variations in the freezing point of water within the membrane. This is an important factor as

liquid water remaining in the PEM at multiple temperatures enables operation to occur even at substantially low sub-zero temperatures. Mukundan *et al.* [27] observed that during low temperature conditions the membranes proton conductivity will increase at lower water contents. This may be the result of a low water content increasing the ratio of sulphonate groups causing more pathways for transport to be available.

The important issue for freeze operation is directly related to the amount of water that the fuel cell contains at shut-down and the necessary time to heat the fuel cell stack above freezing conditions. Elimination of free-water, freezing-bound and non-freezing water from the fuel cell will increase the PEM water capacity at start-up and reduce the necessary enthalpy requirement for heating. For a successful transient start-up the temperature of the stack must rise above the latent heat of freezing before the level of accumulated ice hinders the supply and exhaust of gas reactant. Success in a freeze start-up is related to the cathode CL and the cathode GDM ability to remove product water before and during sub-zero temperature exposure [28]. Water removal at the cathode is the main factor as the ORR limitation can become compounded during start-up by the generation of ice that further inhibits catalyst activity by blocking active catalyst sites [29]. The pore volume on the cathode CL has been shown to be linked with the water generation rate and the ability to start-up under sub-zero temperatures [28].

As gases are circulated through the fuel cell, water is carried away from the CL and cools. It may be possible to remove generated water prior to the formation of ice. Water may exist as super-cooled liquid on the CL depending on the state of the system and stored latent heat that will facilitate transportation [23]. Water can be removed as a vapour, but the amount of water that can be carried away will be reduced by the temperature of the gas. Transportation of exhausted water from the CL into and through the GDM can occur by ordinary diffusion and/or by Knudsen diffusion of gas reactant flow. Knudsen diffusion occurs when the species travelling through a pore frequently contacts the surface walls, leading to a greater amount of heat transfer. The slower diffusion will increase the amount of time available for heat transfer and may lead to contact with ice or the formation of ice seed crystals along the channel or pore wall.

Areas where ice occurs may grow as a result of the water movement and ice agglomeration. Areas that exhibit ice growth are known as ice lens or frost heaves (as water expands as it freezes). The transition of water to ice causes a volumetric expansion forcing an expansion of the local area. The frost heave

stresses the surrounding cell components and can lead to permanent separation of the layers and changes in the pores/channel structure.

The management of water at shut-down when exposed to freezing conditions is best approached by the removal of water from the PEMFC during operation. Water can be removed from the cell by reactant humidification flows and gas outlet recirculation. A gas purge with a high concentration of dry gas reactant can remove residual water by humidifying the outlet gases. The removal of water occurs in sequence from the bi-polar plate channels, GDM, and CL until substantially dry, at which point the membrane will dehydrate. The removal of water by gas reactant purge has been shown to occur at a constant linear rate until most of the water has been removed, and the evacuation of water from anode to cathode is rate limiting [30]. Ito *et al.* examined the removal of water from the GDM and MEA and found that it occurs in a sequence of stages: through plane and in-plane drying of the GDM, in-plane drying of the GDM and drying at the channel interface between the GDM and membrane (MPL/CL), and then removal of water from the membrane [31].

If sufficient heat can be generated during start-up of the PEMFC before water begins to freeze, the FC can reach non-freezing temperatures allowing full operation. Figure 0-2 shows the start-up process where water is initially produced along the EASA and freezes within the pores. The main factors influencing the start-up are the start-up temperature and the shut-down conditions of the fuel cell stack. A balance is necessary between the rate of water generation and the required time to get above sub-zero temperatures. Temperatures can be low enough that no start-up is attainable as the generated water will freeze at the generation site and not warm the area sufficiently. The Department of Energy (DOE) in the United States of America has established a set of targets, which lay the groundwork for the successful adoption of fuel cell technology [6]. The DOE's 2015 target for FC adoption is for an 80 kWe FC to start-up and reach 50% power in 30 seconds at an ambient temperature of -20°C.

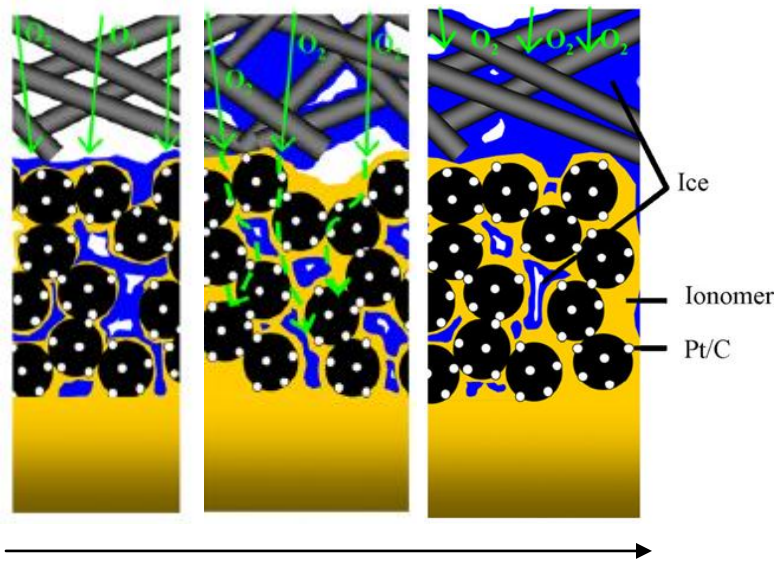

Figure 0-2: Freeze start-up ice formation along cathode electrode [32] (with permission from Elsevier)

To enable the rapid start-up of PEMFC the investigation of different start-up and shut-down conditions is necessary. The knowledge developed in understanding sub-zero start-up and operation can be used to devise engineering principles and practices to mitigate and/or eliminate forms of decay. The objective of this work is to review the behaviour of cold start-up of fuel cells, specifically map areas of the current freeze start-up ability and determine the degradation that can occur.

Initial start-up operation of FC system from sub-zero conditions can lead to the formation of ice in the pores and channels in the membrane electrode assembly (MEA). The generation of heat aids in start-up operation of the fuel cell system from sub-zero temperatures, and may enable full operation without preheating of the coolant, reactants, or heating the stack with some type of external heater. Depending on the state of water capacity at shut-down and the rate of generated water during start-up, the temperature gain may be insufficient to mitigate the formation of ice.

Degradation of the stack materials can result from exposure to freezing conditions but may be mitigated by applying management procedures and devices. The management of sub-zero start-up will be discussed in Section 3.2 and the degradation that results from exposure to freezing conditions will be discussed in Section 3.1.

1.8. **Freeze Degradation**

Fuel cell performance can be negatively affected by the degradation from exposure to freeze-thaw cycles or start-up and operation in sub-zero temperatures. The freezing of water causes the expansion of pores, channels and delamination between cell layers and cell components. This can cause reversible and irreversible damage to the components, spalling of catalyst and/or cracking of the CL.

Reversible and irreversible degradation and morphological effects are all the result of unwanted ice in the fuel cell. The ice that forms can inhibit fuel cell operation by decreasing the electrochemically active surface area and preventing the flow of reactants to active catalyst sites (Figure 0-3). The blockage of water or ice at the CL sites causes reversible loss which can be recovered by higher temperature exposure. When the fuel cell reaches sufficient temperature, ice in the PEM, CL, GDM and bipolar plates melts and opens up blocked pathways and catalyst sites.

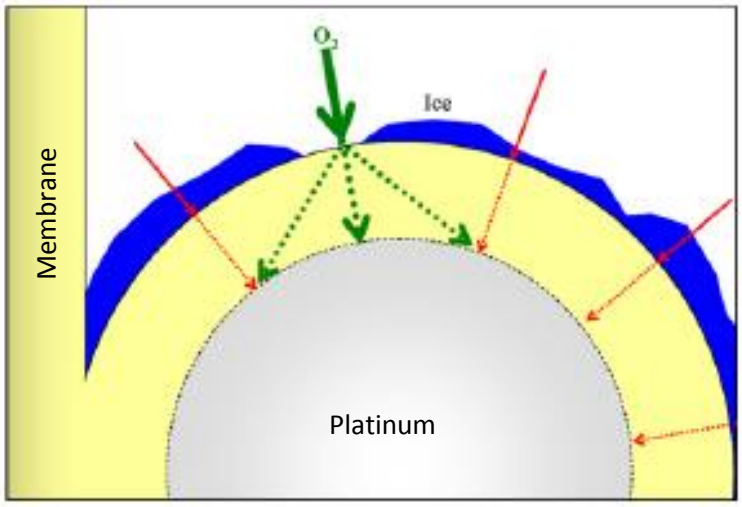

Figure 0-3: Cathode catalyst layer platinum particle undergoing freeze start [32] (with permission from Elsevier)

The result of water freeze-thaw in the membrane can cause morphological effects and wear due to volume expansion of 9% with the formation of an ice lattice structure [33], but this will depend on the temperature range cycled. It has been found that purging with dry gas to remove residual water in the stack will mitigate the degradation that can occur.

During a conditioned sub-zero start-up of a PEMFC, the state of the system has been characterized in three different stages [29]. The first stage takes place at the cathode CL, where water production at the catalyst sites hydrates the membrane. Water absorption into the membrane will occur if it has been

dehydrated by prior purging. Thompson *et al*. [7] have studied the temperature effects of water uptake on the membrane and found that a PFSA membrane can hydrate up to a maximum of approximately 14 H_2O molecules per SO_3 molecule at -20°C. After the membrane has become saturated, stage 2 occurs involving the outward migration of water, its cooling and eventual freezing within the cathode GDM. During stage 3 the ice melts if sufficient heat is generated, allowing diffusion to occur and transport of the water away.

An initially dry gas-purged stack also may have problems when starting up from sub-zero temperatures depending on the start–up procedure and initial temperature of the stack. A balance must exist between the reaction generating water and water diffusing away from the reactive catalytic sites. The balance between heat and water generation rate must be accounted for in order to carry heat into the cell components and allow them to be heated above the freezing point [34]. If initial stack operation is conducted at high current densities in an attempt to rapidly deliver power or heat, then the resulting water production rate will be too fast for enough heat transfer to transport liquid water completely from the stack. Ice has been shown to exist below saturated water conditions, but the formation of ice is a different matter. Supersaturation of water in air or the presence of a frost front is required to form ice. The resulting frost front acts as a point where water being discharged from the stack forms ice and accumulates in the GDM. A frost front can cause damaging separation of components within the GDM, especially for carbon paper.

Ge and Wang [35] have studied the effects of ice by cyclic voltammetry during fuel cell start-up. They showed that degradation will occur when fuel cells are started up, but after an elapsed time the degradation can be recovered. The experimental procedure involved halting the start-up after a certain amount of water has been generated and then allowing it to freeze. This demonstrated where water can form ice and cover the catalyst to affect the performance of start-up as the temperature is decreased.

The formation of ice in the PEMFC has been shown to change the morphological structure and the hydrophobicity of the GDM [36]. Porosimetry measurements conducted by mercury intrusion on virgin MEAs and on MEAs after exposure to freezing show signs of this deformation. The presence of water causes degradation in the form of catalyst layer cracking, interfacial delamination as well as contributing to other catalyst ageing effects [37]. Severe catalyst domain segregation and cracking were found upon exposure to water during subfreezing temperatures [38]. The freezing liquid water in the GDM pores and channels causes compressive and expansion forces in areas that would not normally be exposed to

these stresses. Experimental observations have shown that the effect of sub-freezing cycling operation causes pores in the GDM to change, making otherwise water resistant or non-wetting pores and capillaries open and accessible to water (Figure 0-4). Water-filled pores will then cause blockages where an otherwise gas-filled pore/channel would have existed. The in-plane and through-plane gas flows in GDMs have been shown to change after exposure to freezing water. The freezing water also results in the loss of smaller pores which under normal conditions would not fill with water. Upon freezing, water can be forced into or cause smaller pores to collapse. The effect of freezing in a small water-filled pore causes it to grow in size [39]. An increase in the amount of larger pores makes water management more difficult during higher current density operation.

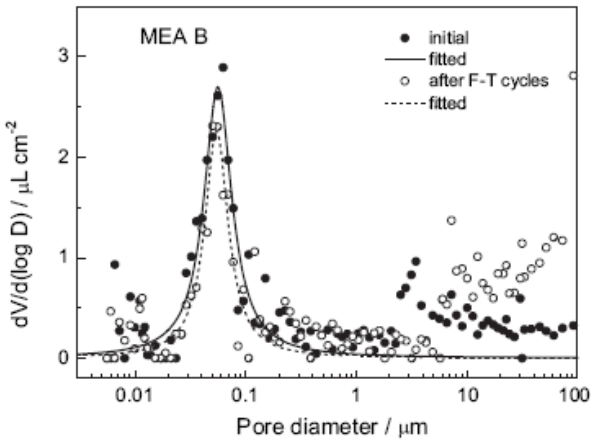

Figure 0-4: Result of GDM freeze with water filled pores [40] (with permission from Elsevier)

Freeze-thaw cycling has been shown to affect the microstructure of the MEA depending on the mode of manufacture. Lee *et al*. investigated five different MEAs with freeze-thaw cycling. Various structural changes were observed: void formation, delamination (Figure 0-5), CL cracking, porous structure variations and undesirable effects on performance mainly due to ohmic losses. Activation polarization degradation did not occur after 120 freeze-thaw cycles [40]. Kim and Mench investigated the effects of freezing on a conditioned stack (i.e. purged stack), where water was removed prior to freezing. Their findings demonstrate that conditioning a stack prevents observable electrochemical or physical damage from occurring [41].

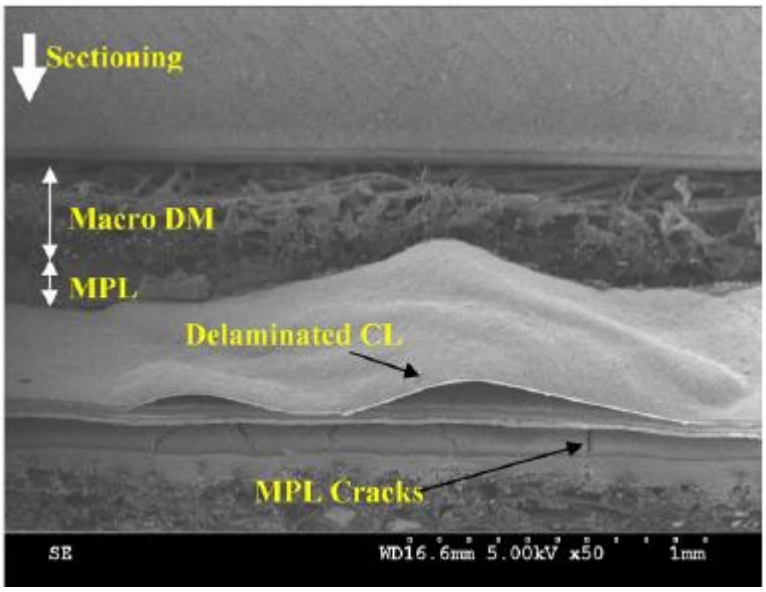

Figure 0-5: PEMFC catalyst layer delamination [41] (with permission from Elsevier)

Water at low temperatures can cause interfacial delamination of MEA layers, by the creation of what is known in geological formations as a frost heave. He and Mench [42] developed a model to describe the formation of a frost heave in a PEMFC and found that the most likely places (Figure 0-6) for a frost heave to form and expand is likely in one of 3 areas within the channel (Area 1), between the CL and GDM (Area 2), or between the CL and the membrane (Area 3). Area 9 is also a candidate which is under the land at the PEM/CL interface. A frost heave can also cause delamination due to the volume expansion stressing the local surrounding area.

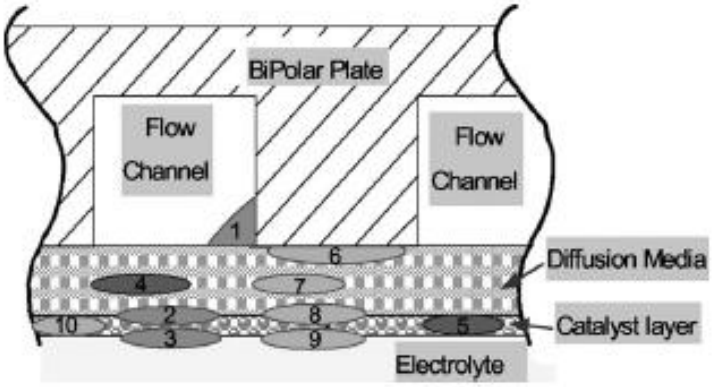

Figure 0-6: PEMFC MEAs cross-section during transient thermal start-up, showing areas where ice formation most likely to occur (i.e. areas 1-3 and 9) [42]

Kim and Mench [41] investigated membrane degradation that occurred as a result of freeze-thaw and which demonstrated how crack propagation through the CL occurs. CL cracking can be categorized into

two different shapes: inverted (Figure 0-7 on left) and non-inverted V-shapes (Figure 0-7 on right). The type of crack can accelerate its formation by the way future ice will form and expand. An inverted V-shape will increase stresses between the CL and the membrane and increase the likelihood of delamination.

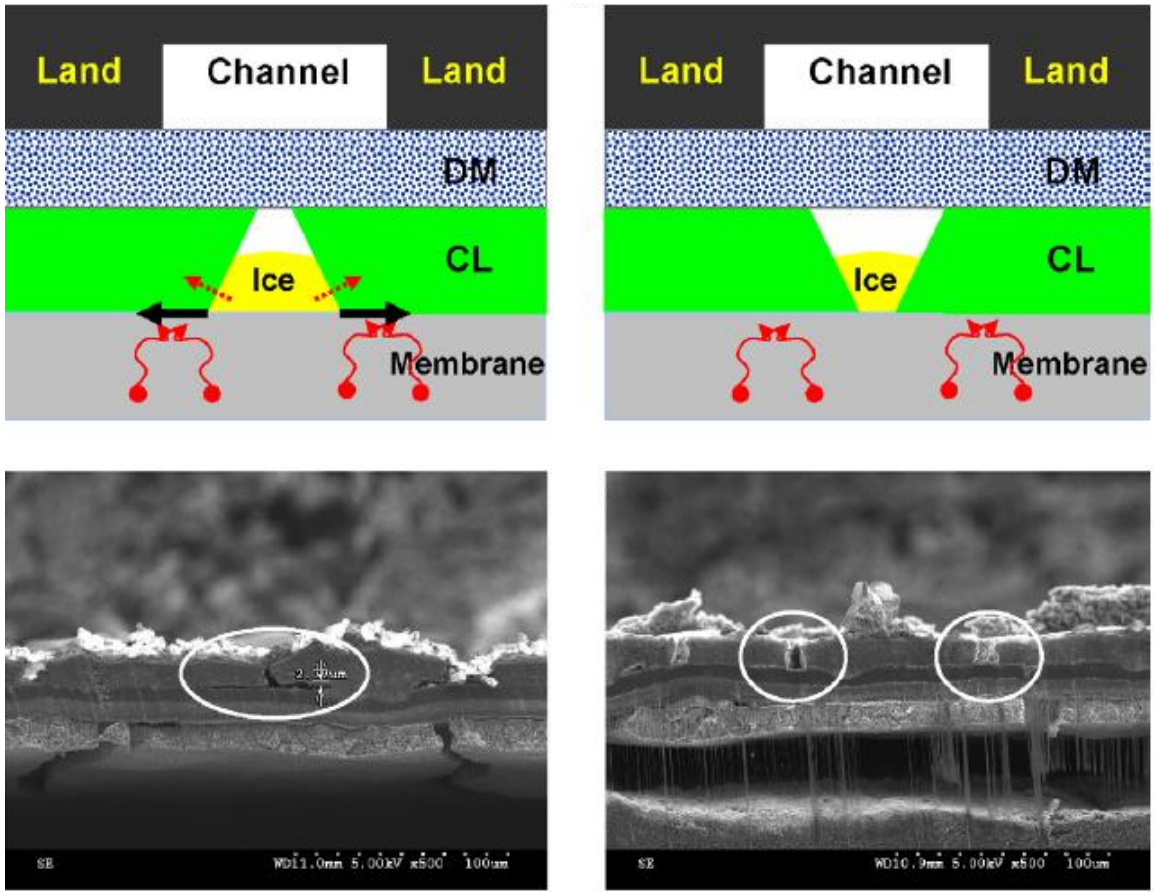

Figure 0-7: PEMFC freeze-thaw investigation on CL cracking, inverted and non-inverted V-shape [41] (with permission from Elsevier)

Delamination and cracking of the CL degrade the PEM leading to the formation of pinholes in the membrane (Section 1.10). The degradation by the evolution of pinholes or tiny allowances in the membrane enables gas crossover between electrodes and degrade fuel cell performance. The start-up procedure of fuel cells can cause local stresses due to non-uniform humidity levels, current distributions, stretch and strain by ice formation, all of which have the potential to lead to gas crossover though the MEA [43]. The degradation that results from freezing may be controlled by limiting the amount of remaining water in the stack and using the appropriate start-up procedure.

1.9. Mitigation of Failed Start-up

The frequency of failed start-ups can be minimized through proper start-up management procedures, the use of proper active components, or shut-down conditioning protocols. Understanding freeze management protocols help to mitigate the degradation, damage and performance loss that can result from sub-zero freezing.

1.9.1. PEMFC Freeze Stack Conditioning

At stack shut-down, the remaining water may freeze when environmental conditions yield a temperature below the freezing point of water. Since the stack is warm at shut-down, it will take time for the stack to actually reach freezing temperatures (i.e. cool-down time). Lee *et al.* [44] investigated the characteristics of water removal from a PEMFC and found that with a fixed amount of purge gas an increase in flow rate leads to a lower remaining water. Lower overall lower water content within the fuel cell will lessen the necessary energy requirement to raise the temperature to non-freezing conditions. Water removal can be accomplished using flowing dry gases at shut-down or by pumping out the stack using a vacuum purge procedure. A stack conditioning protocol should be required in all situations where freezing can occur.

The removal of water and drying of the membrane is one method to prevent ice formation in the stack. Ice formation can also be prevented by adding anti-freeze solutions to the stack. Additives that inhibit freezing improve proton conductivity, improve start-up performance and prevents the formation of ice. However the anti-freezing solutions can decrease proton conductivities above sub-zero temperatures (9). Therefore, additives should only be employed in situations where freezing is likely to occur, because they will reduce the performance of the PEMFC system after start-up. The use of freeze inhibitives allows liquid water to remain in the stack, which also adds to the thermal mass of the FC at start-up.

1.9.2. Start-up Operation

To minimize the start-up response in sub-freezing conditions, a structured protocol can be employed to increase the amount of heat generation. In order to initiate operation, the generated heat must warm the stack above freezing temperature before all voids and vacancies in the porous media have become water/ice-filled. This report seeks to improve the start-up and shut-down procedures in order to gauge the stack start-up response.

Meng [45] have developed a simulation model for freeze start-up of a PEMFC. Their results indicate that the cathode gas flow should be high to remove water vapour, prevent ice formation and improve the overall start-up. The rate of ice growth is found to be greatest at the cathode CL and the interface between the CL and GDM. The PEM is shown to absorb water from a dehydrated state which can be beneficial to start-up by lowering the water content in the CL.

To improve start-up of the stack, heat generation must be maximized to warm the stack above freezing temperature before ice halts operation. Heat produced at start-up occurs from entropic heats of the reaction, irreversibilities of the electrochemical reaction, electrical resistances, and as well as condensation of water vapour [46]. In order to adopting the condensation and formation of ice in the stack, start-up should be managed by either shorting the stack (to drain excess protons and hydrogen) or with a specialized load protocol. A shorted stack is the condition where all the produced current is routed back into the stack. This will cause all the produced power to generate heat in the stack components. Shorting the stack does reduce start time and degrade stack performance, which leads to the development of a load operation profile. Amperostatic or potentiostatic operation can be applied. Amperostatic operation involves maintaining a constant current on the stack and Potentiostatic operation maintains a constant voltage. Amperostatic operation during start-up can supply the load with the required current but cell voltages may not be at the required performance levels to maintain operation. A decrease in cell voltages can cause cell reversal and/or corrosion of the catalyst support due to their lowered performance. Potentiostatic operation during start-up may allow for greater control of degradation and warm-up potential. Potentiostatic operation would require an additional configure in order to monitor and control the applied load on the stack to maintain a low cell requirement during start-up.

The reactant fuel supply can be modified by stopping or cycling the reactant flows into the FC to allow starvation to occur causing heat generation. Fuel starvation is detrimental to fuel cell stack durability and will result in corrosion of the catalyst support. The generation of heat in the stack can also be supported by applying a controlled amount of crossover of hydrogen to the cathode causing combustion to occur locally at the CL sites, see Section 1.9.4.

The Relative Humidity (RH) at stack start-up is generally low or not supplied at all in an order to decrease and remove product water that may form ice. The freezing environment may cause

damage to the device or mechanism that attempts to supply that humidity, which should be addressed.

1.9.3. Keeping the Stack Warm

Freezing of FC stacks can be mitigated by employing a warming strategy with a heater or a partial start-up procedure to maintain the stack above freezing conditions. Insulation can also be added to the surroundings of the fuel cell stack to maintain and delay freezing, thereby increasing the cool-down time that the stack would require to reach sub-zero temperatures. Insulation may lead to a future problem with thermal management, as the operation of a fuel cell stack at a high ambient temperature condition may exceed temperature controls (i.e. the stack could overheat during operation and certainly would have an increase in cooling demand). The amount of energy required to keep the stack above freezing temperature will vary depending on the geographical region and energy requirement.

1.9.4. Assisted Start-up

In order to start under freezing conditions, the time at sub-zero temperatures should be minimized. The use of an auxiliary warming device can increase temperature, thereby decreasing start time and improving performance while avoiding degrading effects. As discussed earlier, the use of freeze inhibitors has also been one method suggested to prevent water from forming ice. Various electric heaters can be used in internal or external devices.

Coolant heating can be used to supply the stack with a coolant that is above the internal temperature of the system and homogenize the temperature within the stack cells and across the cell surface. If the initial gas flow is low, a large central heat zone in the centre of the cells can exist. The circulation of coolant in a by-pass loop has been recommended as one way to apply coolant heat. A reduction in the amount of coolant will increase the temperature response of the coolant. The required implementation of a non-freezing coolant medium is required to enable proper circulation.

Endplate heaters and/or cell heaters can be used to respond to local heat generation in the cell. The endplates that holds the cells together are typically made of a metallic material, which makes them a large thermal sink that will keep the end cells at a lower temperature relative to internal central cells, which are warmed by adjacent cell heating. Adding heat to the ends cells

can be effective. The incorporation of heaters at the end cells or between cells will assist start-up from colder sub-freezing temperatures, although these additions increase costs of fabrication and make operation at start-up more complex.

Pre-heating the gas supply can be used to heat reactants above freezing temperatures or above the stack temperature will help to prevent ice formation. Implementation of gas heaters can be used in different ways. For example, catalytic combustion of hydrogen external to the stack or allowing a small crossover of hydrogen or oxygen can generate heat. The amount of crossover allowable should be low to avoid a possible ignition or explosion. The use of gas pre-heaters will aid in the start-up of the FC from decreased temperature environments, although the heat capacity of the gas is low making it a poor medium for heat transfer. Gas pre-heating may increase the range over which a fuel cell can start unassisted but will moderately increase the start-up time and performance of operation. The response time of any heater is still a problem for rapid start-up times. Any type of heater or heating device is also a drain on energy and thus overall efficiency.

1.9.5. System Design Modifications

The overall system and integration of these strategies can greatly mitigate freeze degradation of the stack. Overall the system can be modified in order to better manage the heat that the system produces by decreasing the thermal mass of the system. Components can be modified to improve the thermal mass and modify the thermal conductivity of the stack. A coolant system which makes use of a reduced bypassed loop can reduce the amount of overall required volume that is heated by the stack in operation.

DURABILITY AND FAILURE MODES

Fuel cell durability is critical for performance, cost and life. The management of stack operation is necessary for the desired life and performance of a PEMFC. Cells are susceptible to various forms of degradation and failure which can lead to an end-of-life (EOL) [47]. The weakest component in a fuel cell is the membrane electrode assembly (MEA) as it is susceptible to the most forms of degradation and is often the cause of shut-down and decommissioning (i.e. MEA failure is stack failure). The degradation to the MEA can be accelerated by operation outside of the desired parameters and modes of operation. Temperature, humidity and operation load cycling leads to mechanical and chemically related degradation but if properly controlled and managed these decays will be minimized. Characterization and knowledge of the forms of degradation can lead to proper management and mitigation. For this work, causes of fuel cell performance loss occur during normal operation, exposure to freezing conditions and from sub-zero temperature start-up.

1.10. Non-Freezing Operation Durability and Failure Modes

Several modes of degradation of the MEA are shown in Figure 0-1. The MEA decay cycle can result from regular operation and can be accelerated by operating parameters being outside of normal operation. Operation of the fuel cell can lead to different forms of decay resulting in degradation of stack performance: fuel starvation, gas crossover (pin holes and hot spots), cell reversal, peroxide formation and carbon catalyst support corrosion.

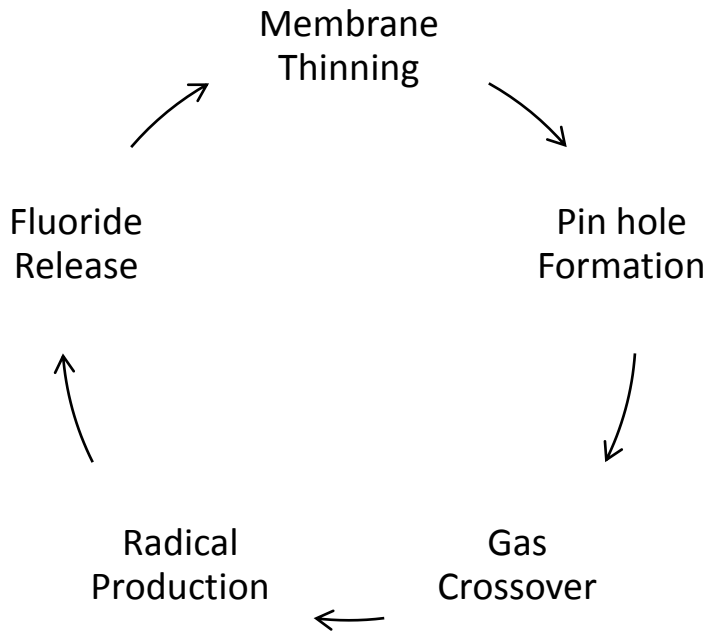

Figure 0-1: Degradation of PEMFC membranes

1.10.1. **Fuel Starvation**

Fuel is delivered to the cell by piping and channels that distribute gas reactants along the GDM. Gas circulation keeps the cell reactant concentration high and removes products and impurities. Changes of the stack during operation or start-up can cause inconsistent gas delivery or circulation resulting in variations of reactant availability. Fuel starvation as a result of flow blockage by an obstruction or if flooded can result in carbon corrosion and/or cell reversal. Areas of an electrode where fuel is insufficient will cause low cell potential and may lead to reversal in electrode polarities (i.e. cell reversal), allowing both the anodic and cathodic reactions at the same electrode or between both electrodes.

1.10.2. **Gas crossover**

A purpose of the membrane is to provide an impermeable gas barrier between the anode and cathode. Gas separation is crucial for performance and useful utilization of fuel. Hydrogen and/or oxygen may transport directly from one electrode to the other resulting in the reaction taking place at a single electrode. This causes an inefficient consumption of fuel, as the local reaction will no longer generate and deliver electrical power. Cell voltages may decrease as a

result of gas crossover and will be weaker (lower performance at higher current densities), possibly allowing for easier occurrence of cell reversal. Operation at higher current densities requires larger gas reactant delivery to maintain sufficient gas concentrations at the electrodes. Local reactions near gas crossover sites will also lead to other forms of failure, since temperatures will increase in these areas. A high level of gas crossover is one cause for stack end-of-life (EOL) as the cells may not be able to operate sufficiently and waste fuel.

Pin hole formation

Gas crossover is caused by the formation of pathways transporting gas reactants across the membrane. As those pathways become larger, they form a visible pinhole in the membrane. Pin holes will increase in size as the gas crossover continues. This in turn increases the rate of gas crossover.

'Hot spots'

The electrochemical reaction in a fuel cell in conjunction with combined gas crossover can generate excess heat in a localized area. Direct combustion of the hydrogen and oxygen will lead to a large release of heat, increasing the local temperature. High temperatures result in a decrease in water content, which may free more pathways for gas crossover.

1.10.3. Cell Reversal

In multi-kilowatt stacks, variations of water content and temperature can lead to a situation where one or more cell(s) become flooded and receive insufficient gas reactant. As a result, cell voltage decrease and can potentially lead to a situation where cell reversal can occur (0-1). Cell reversal is a condition where it is overwhelmed by an adjacent cell causing reversal of its polarity or for both the anodic and cathodic half cell reactions to occur on the same electrode. Hydrogen then will be generated at the cathode and oxygen generated at the anode.

$$H_2O \rightarrow \frac{1}{2}O_2 + H_2 \qquad (0\text{-}1)$$

The mixing of hydrogen and oxygen can then lead to a combustible environment, but typically the generated gases are consumed rapidly. The operation of the cell is then no longer producing

power but consuming as an electrolyser. The stack can still operate and deliver power but will continue to drive the electrolysis by diverting generated energy. Cell reversal can lead to corrosion of the catalyst support, a waste of fuel and shut-down of the system.

1.10.4. **Peroxide Formation**

The PEM is susceptible to various forms of chemical degradation by attack of the membrane monomers [47]. The generation of free radicals can chemically attack the PFSA backbone or side chains of the polymeric structure. This 'radical attack' can cause the release of fluoride ions, which are directly measured in the discharged water. The loss of membrane material directly leads to membrane thinning. The generation of free radicals can be caused by unreacted gas crossover, incorrect operation leading to cell reversal or the ORR at the cathode:

$$O_2 + 2H^+ + 2e^- \rightarrow H_2O_2 \quad (0\text{-}2)$$

$$H_2O_2 \rightarrow 2OH\cdot \quad (0\text{-}3)$$

The presence of oxygen and protons lead to the formation of hydrogen peroxide (Equation (**0-2**), which can be one of the intermediates of the PEMFC reaction. Hydrogen peroxide can proceed to form hydroxyl radicals (**0-3**) that can oxidize components of the membrane polymers and cause their release. This thins the polymer membrane and thereby weakens its integrity.

1.10.5. **Corrosion of the Carbon Support**

Chemical degradation can also occur as a result of fuel starvation during operation of the fuel cell. In situations where insufficient gas is supplied to the cell other components of the cell such as carbon can be oxidized. Equation (0-4 shows how the carbon support will corrode to replace the required reactant for the reaction. Carbon dioxide and protons are produced while delivering the required electrons for the reaction to continue.

$$C + 2H_2O \rightarrow CO_2 + 4H^+ + 4e^- \quad (0\text{-}4)$$

The chemical attack on the membrane leads to the loss of carbon support and catalyst material, therefore decreasing the available active catalyst sites. Platinum and other catalyst metals can either dissolve away or redeposit elsewhere such as in the membrane.

1.11. Durability in Freezing Environments

In addition to the normal operational conditions that the stack endures, freezing temperatures and sub-start-up will decrease stack durability and may accelerate the loss of stack life. The transition in temperature from sub-zero to full operating temperatures may stress and result in mechanical degradation of the cell components. Degradation of the stack components arises due to the presence of ice, the thermal differential in changing from sub-zero to a normal operating temperature and the thermal expansion associated with the materials.

Freeze start from a lower water condition with little or no humidity supplied is desired in order to maximize heat production and reach sufficient cell temperatures before the accumulation of ice hinders operation. This causes a large change in relative humidity supplied to the stack, which causes swelling and contraction of the PEM. The formation and expansion of ice within the stack may cause delamination, between the CL and GDM or CL and the membrane. Any formation of ice occurring within a cell component can cause a morphology change.

1.11.1. Delamination

Water can be present in the membrane after shut-down and reside between the CL and the GDL or between the CL and the PEM. When exposed to cold enough conditions, water can freeze and expand affecting both the GDM pore size and the interfaces between the CL layer and GDM or the membrane. These effects can be found mainly at the cathode side of the fuel cell since water generation occurs locally at the electrode.

The water trapped by freezing between the cell components causes a frost heave to occur, where the materials are forced apart by the ice expansion. Subsequent melting of this ice leaves voids where there has been intimate contact between these materials. The degradation caused by physical delamination is an irreversible form of degradation.

1.11.2. Catalyst Layer Degradation Effects

The transport of oxygen occurs through gas-filled pores in the GDM. The size distribution of pores in the GDM leads larger ones to be wetting, while smaller pores are non-wetting (i.e. gas-filled). During the freeze or sub-zero start-up process, water can be forced into gas-filled pores forcing expansion by freezing and crushing adjacent pores. Pores will remain water-filled during operation until a temperature is reached where they are dehydrated. A decrease in the number

of available pathways for gas transfer leads to a decrease in the delivery of reactants. Since the water-filled pores can be recovered by dehydrating the membrane, this is a reversible form of degradation.

The loss of electrochemical active catalyst sites can result from cracking of the CL where the formation of ice lenses or frost heaves and causes it to break into pieces. Cracks in the CL lead to voids that can fill with water and can grow during sub-zero temperature freezes. Water freezing in the catalyst layer can also cause spalling of the catalyst as a result of freezing stresses. Cracking and spalling are both irreversible forms of degradation.

1.11.3. Ice blockage

Water that has remained within the bipolar plate channels and along the GDM when frozen can block and impede the transfer of gas into and out of the stack. During start-up, if the membrane is not fully hydrated the water that is generated at the cathode will hydrate the membrane until it has become saturated. After the membrane is saturated but still below freezing, any water generated by the reaction freezes if it remains in the cell. The electrochemical surface area at the electrodes may diminish as a result. The frozen water will impede or disrupt the distribution of fresh gas reactant. Blockages can lead to a build-up of gas pressures within the channels and cells. The build-up of pressure on one side or within a blocked area of the cell leads to large differentials across the membrane, which can eventually rupture or tear the membrane.

1.11.4. Loss of Porosity

The formation of ice within the stack can cause morphology changes to the GDM. Pores within the GDM can enlarge due to freeze expansion of water. The GDM has a range of pore sizes that cause some to remain gas-filled while other larger become water-filled. Cho *et al.* found that freeze thermal cycling with water present caused the GDM pore size distribution to change [33]. Pores smaller 25nm were reduced in number, while pores that larger then 25nm increased in quantity. The water-filled pores during freezing underwent a forced volume expansion. Air-filled pores adjacent to water-filled pores were crushed as a result of the stress.

EXPERIMENTAL

1.12. General

The object of this work is to start-up a PEMFC stack from sub-zero temperatures (i.e. a frozen stack), measuring the response time and gauging methods to improve and mitigate damaging effects that can occur during start-up. A Hydrogenics Corporation™ PEMFC stack was utilized with a special setup to measure and control various environmental and operating parameters. The experimental testing was located and conducted at the Hydrogenics Testing facility. The test hardware associated consisted of three main components: a Hydrogenics 4 kW fuel cell stack, a Fuel Cell Automated Test Station (FCATS™) and an environmental chamber.

1.13. Fuel Cell Stack

The FC system selected for this work consisted of a Hydrogenics 20 cell stack. Each cell in the stack has an active area of approximately 500 cm^2. The bipolar plates were graphite with a proprietary gas distribution flow field. The stack is designed to operate at low pressures with a “dry-dry” capability. “Dry-dry” is where the stack anode and cathode reactants require little or no humidification. The cathode is dry with no auxiliary humidification beyond what is normally present in the air. The anode electrode is operated between 15 and 25% relative humidity. Operation of the fuel cell system is in a horizontal upright position with a counter current flow to enable a higher degree of heat and reaction homogenization across the active cell areas. The cells are numbered according to their sequence moving from the “wet endplate” to the “dry endplate”. Cell 1 lies against the “wet endplate” where the stack manifolds and connections are located. The voltage measurements are attained by adding a wire harness affixed to the top of the bipolar plate, enabling real time single cell voltage measurements. Three load cables are attached between the bus bar and the load box. An ultra-thin thermocouple is inserted between the bipolar gas seals and directed into a coolant channel, in order to measure temperatures directly from the middle of the stack. ***Figure 0-1*** shows the side of the stack as well as the ultrathin thermocouple inserted between the bipolar plates.

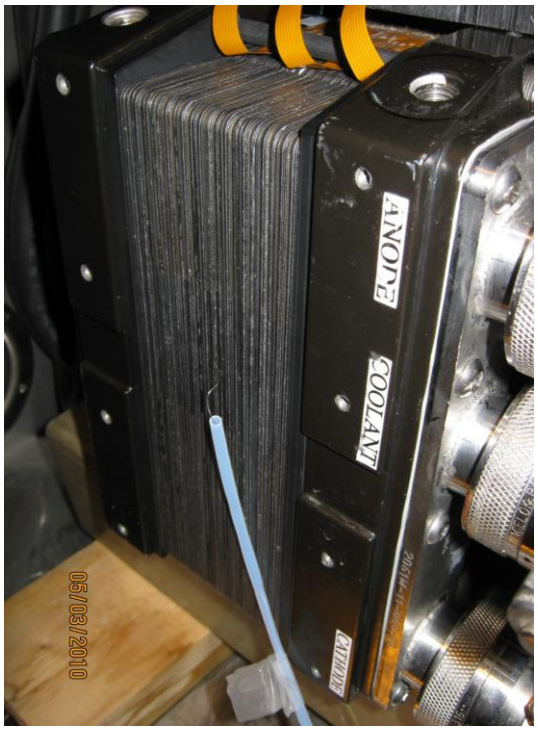

Figure 0-1: PEMFC stack

1.14. Fuel Cell Automated Test Station (FCATS™)

Stack testing is conducted with an automated test bench called FCATS. The stack can be operated with many different parameters for controlled and accelerated testing. The FCATS system is able to control the operation through the use of HyAl™ and HyWare™, a scripted programming language and automation control software, respectfully. These systems enable automated testing of various parameters by HyAl scripts, which enable reproducible operation of the stack.

Figure 0-2: Image of the FCATS™ system

The FCATS use various equipment to humidify, heat and cool the gas reactants and coolant as they are delivered to the stack. The FCATS system uses a supply of hydrogen, oxygen, nitrogen, steam and air to enable different mixtures of gas feeds. The pressure supplied to the stack is controlled by back-pressure regulators, that make measurements at the stack inlets and outlets. Thermocouples are also located at the gas and coolant inlets and outlets within the stack and at the endplate surfaces.

The coolant within the system uses a liquid with a freezing point below that of water. The coolant mixture also has low electrical conductivity to prevent the stack from short circuiting and wasting electrical power. The coolant consists of an ethylene glycol mixed with water at a 50:50 ratio. The mixture of ethylene glycol and water freezes at a temperature below -30°C. The trade-offs for the use of a non-freezing coolant are poorer thermal properties and an increase in the required pumping power. The FCATS can heat the coolant with an electric heater or cool it by the use of plate heat exchangers and plant chiller water. There is no circulation of coolant during sub-zero temperatures immersion or during start-up until a satisfactory internal stack temperature has been reached.

1.14.1. HyWare™

The FCATS™ use a computer software program known as HyWare developed by Hydrogenics Corporation for use with the FCATS. HyWare has an interface that allows user control of the FCATS integrated hardware. HyWare displays various parameters and pages that can be cycled through for the display and control of input and output variables. HyWare also measures and enforces safety limits during stack operation. The safety limits on the stack prevent potentially dangerous situations from occurring such as low voltage, cell reversal or pressure build-up.

1.14.2. HyAl™

HyAl™ is a scripted programming language that operates the automated testing. HyAl allows the execution of test protocols repeatedly with reproducible results.

1.15. Environmental Chamber

The ambient temperature of the stack is controlled by the use of an environmental chamber (Figure 0-3). The environmental chamber preconditions the stack to a desired sub-zero temperature. The stack is located inside the environmental chamber with the required piping and return lines connected to the FCATS. This permits continuous cooling of the stack and pre-condition supply gases. The temperature of

the stack during operation is still controlled by coolant recirculation in conjunction with heaters or heat exchangers.

The gases supplied to the stack are fed initially from the building supply into the FCATS unit, which heat or cool to the desired condition. The gases then pass into the environmental chamber and the stack before returning to the FCATS system. The system setup has been modified in order to simulate a true sub-zero temperature start-up, where the environmental chamber is used to further condition the supply gases. Two heat exchangers within the environmental chamber are used to chill the anode and cathode gas reactants to the environmental chamber set point. The gas conditioning in the stack will be discussed further in Section 1.15.1.

The FC stack has six connections: three for the supply and three for the returns. The connected lines pass through port holes located on the sides of the environmental chamber. The lines are wrapped with heat tracer cable to help control temperature while operating after start-up and at steady state. All lines are insulated to keep them warm or cool as the environmental chamber operates continuously.

Figure 0-3: Environmental cooling chamber

1.15.1. **Gas Conditioning**

To accurately simulate the unassisted start-up response, the inflow gases pre-cooled to the desired freezing set-point temperature matching that of the system. The gases are pre-cooled by the use of plate heat exchangers circulating a coolant medium of ethylene glycol and water mixture (Figure 0-4).

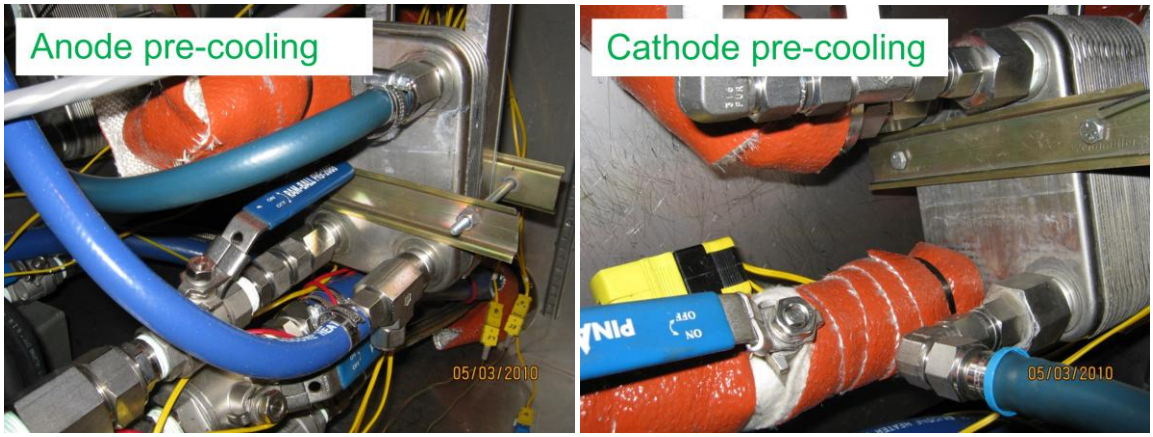

Figure 0-4: Gas reactant pre-coolers

The heat exchangers are installed in series. The coolant is circulated through two heat exchangers, a forced fan convection radiator using a small pump rated at 4 U.S. gallons per minute. The radiator uses the ambient temperature in the environmental chamber to cool the coolant. A process diagram illustrating the setup is presented in Figure 0-5.

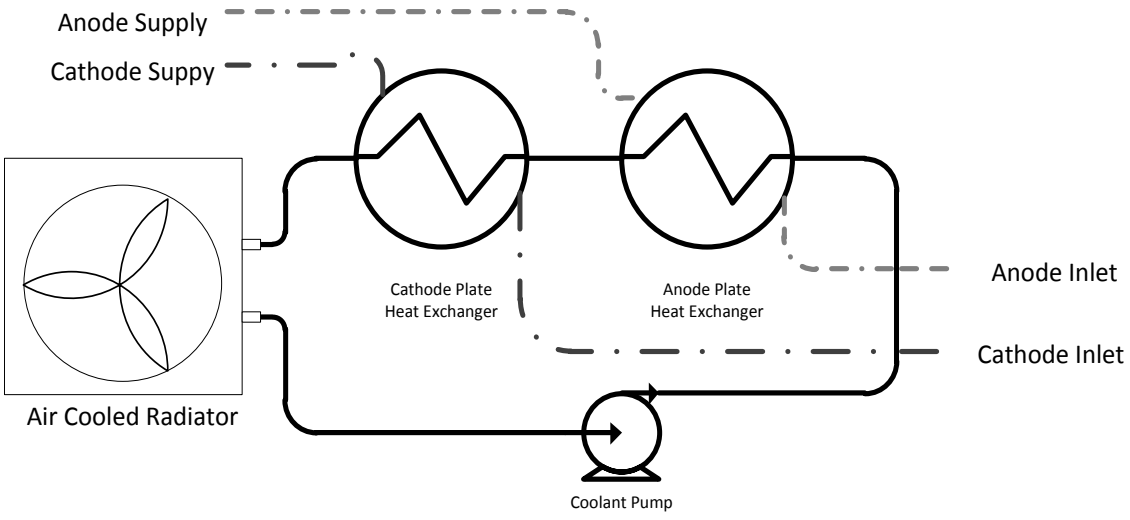

Figure 0-5: Gas reactant pre-Cooling process diagram

During longer start-ups where the initial power production of the stack may be delayed by ice, gas circulation from the exterior can warm up the supply lines and the stack. TCs located at the stack inlets determine the temperature of incoming gases. The associated temperature rise of the gas is low during start-up operation and confounded with the heat capacity of the supply gases, and the casings of the supply lines. The fan is turned on and off by the FCATS HyWare software during continuous cyclic testing. The resulting experimental stack set-up is shown in Figure 0-6.

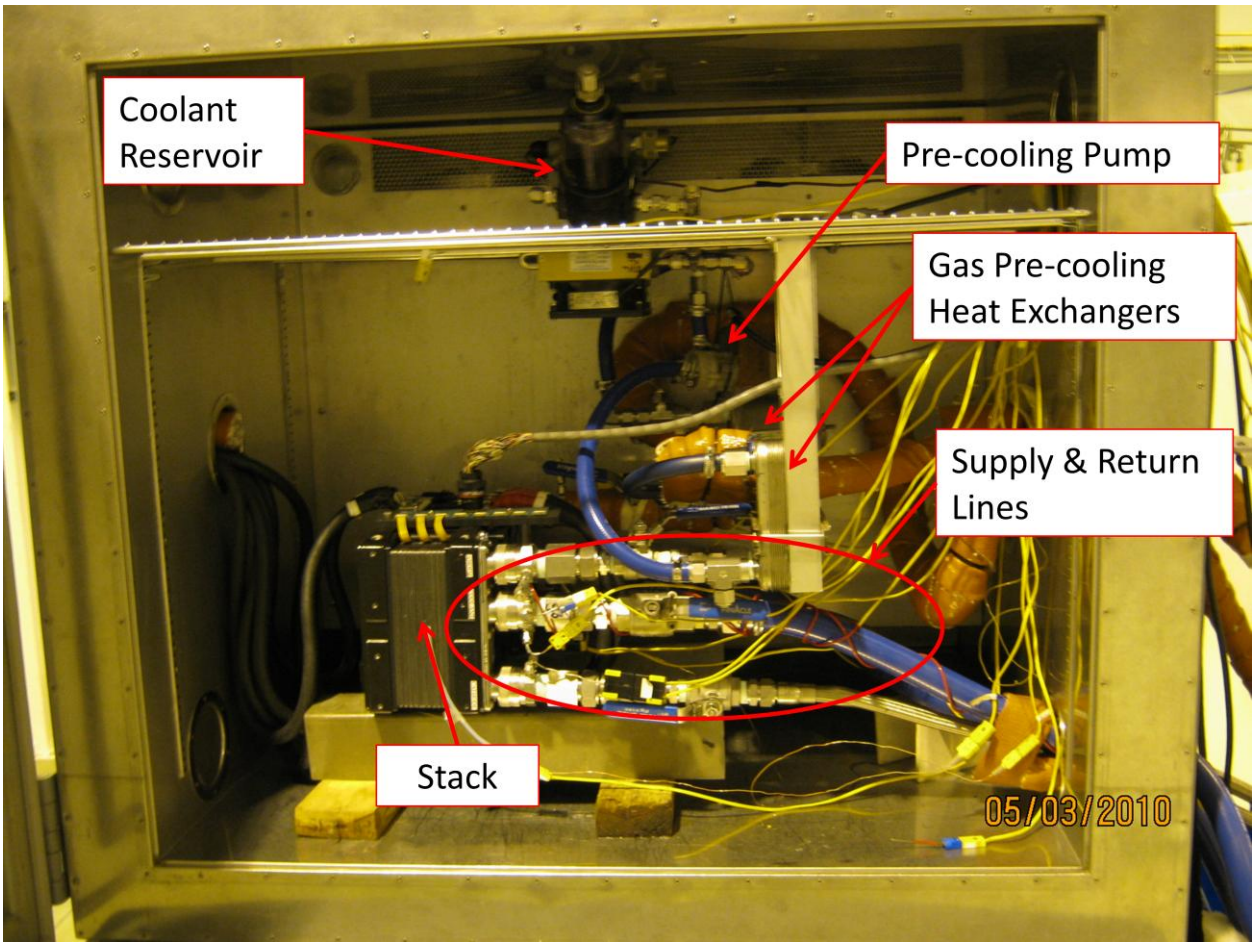

Figure 0-6: Experimental stack system setup in environmental chamber

1.16. Freeze Start-up Operation

A start-up from ambient temperatures (i.e. non-freezing) is easily conducted and can attain rated power delivery within seconds. The ability to start from sub-zero conditions requires attention as a result of the slower kinetics and residual water effects. Accelerated testing is completed by continuously operating the environmental chamber at a controlled set point. The generalised process for freeze stack cycling is

shown in Figure 0-7. The attempt to start-up of the stack is conducted with various changes to parameter values in order to define and locate improvements in stack start-up performance. This section discusses the various parameters that are important to stack operation such as the start-up procedure, flows at start-up, load regime, coolant activation, stoichiometry and humidification.

Operation of the PEMFC is very dependent upon the last residual state. Operational history has a direct impact on future operation since residual water may be frozen at start-up. In order to control the freeze start-up performance of the fuel cell stack, the method of shut-down is investigated in tandem.

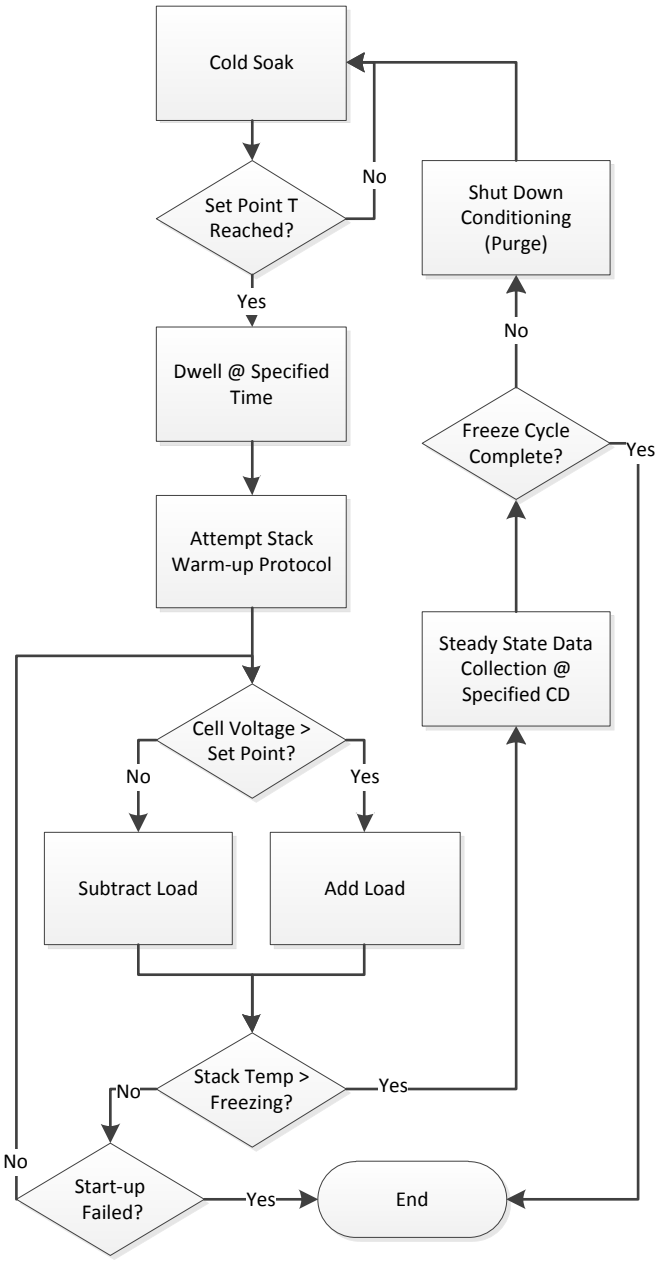

Figure 0-7: Freeze start-up cycle operation process flow diagram

1.16.1. **Gas Reactant Delivery**

Experimental investigation included examining gas reactant delivery rates at start-up. Sufficient fuel gas is critical to operate the fuel cell in order to avoid starvation. Gas reactant is supplied at a rate matching that of fuel consumption at an operating current density. In any situation where the amount of fuel gas required exceeds that of the amount delivered, then the system will automatically provide the required excess. Four main types of gas delivery are investigated:

constant, step, burst and ramping flow rates. ***Figure 0-8*** shows several examples of delivered flows to the stack.

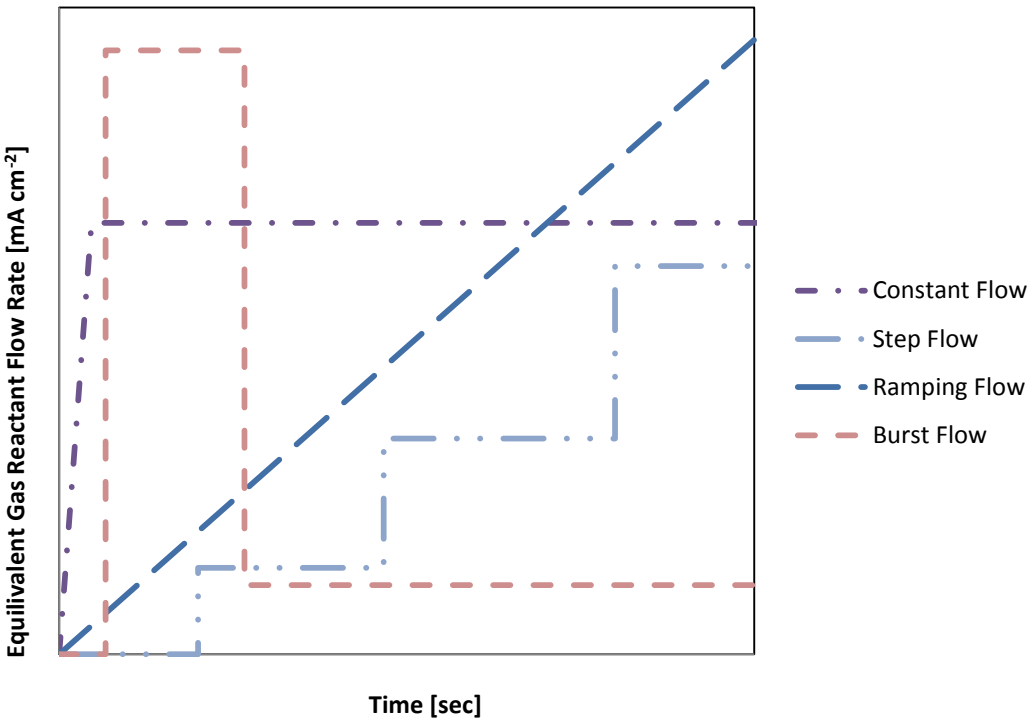

Figure 0-8: Configuration of gas reactant delivery

The effect of constant set point flow rates were initially investigated for successful start-up performance. Knowledge gained from these tests helped in the testing of the other configurations (Table 0-1), allowed the development of a step flow profile. Stack performance improved when a supply of reactant within the cells was available before an increase in load. Constant flows already in excess of the load are thought to cool the stack components and waste fuel during start-up. Trials completed with a step regime occur where by a known increase in flow is made at pre-determined times. Step flows require prior knowledge about the stack fuel usage and the rate at which performance improves. This lead to the concept of burst flows to deliver a fresh supply of reactant for a period of time before being halted to stop cooling. This mode of gas flow was investigated during one trial. The results of the first three types of gas flow delivery lead to the development of a ramp flow method to continually increasing the amount of supplied fuel.

Table 0-1: Start-up flow trial distributions

Start-up Flow Type	Number of Trials
Constant	80
Step	3
Burst	1
Ramp	7
Total	91

1.16.2. **Load Regime**

The start-up load is determined by a balance between the rate of heat generation which is highest when a fuel cell operates at its lowest voltage and the amount of water produced. Stack cell voltages depend on temperature, membrane water content, operating current density and the availability of gas reactant. A balance must be attained between the ability to heat up the cells as fast as possible without operating at a damaging cell voltage. In order to reduce the start-up time, cell voltages should be as low as possible while maintain a safe voltage in order to avoid cell reversal situations and corrosion of the catalyst support. During start-up, the generated heat must be conducted into the cell components to warm them above freezing before the generated water freezes and blocks the available reactive sites or gas supply. The load of the fuel cell can be applied with two different start-up types: amperostatic (i.e. current controlled) or potentiostatic (i.e. voltage controlled).

Amperostatic operation maintains the current drawn from the fuel cell stack at a constant rate. An amperostatic operation results in voltage measurements changing as the FC warms due to increasing performance. This type of load regime is typically used in power delivery and is easiest to implement with typical equipment. Amperostatic operation requires the correct current be available (i.e. can call for current in excess resulting in low cell voltages or cell reversal). In a sub-zero environment, the current drawn from the stack may not be available due to reactant delivery and product removal or may be unstable. A lack of available power in a cell may cause cell reversal or a failure to start-up.

Potentiostatic method has also been examined for its benefit in maintaining a constant desired low cell voltage, thereby eliminating possible cell reversal or corrosion of the catalyst support. Potentiostatic operation generates the greatest amount of heat for faster start-up times. During start-up the temperature will increase, resulting in an improved cell performance and allow greater loads. In order to maintain potentiostatic operation, the load must be modulated by continually turning it on and off. An increase in load during sub-zero start-up will increase the

rate of reaction that simultaneously generates more water that may form ice and increases the rate of heat generation that can warm up the cell. If water generation occurs faster than the transfer of heat, the water will freeze and block gas reactant and decrease cell voltages. A decrease in cell voltage below the maintained minimum will cause the stack current to diminish. Operation in a potentiostatic method is difficult to employ in typical applications since the cell response ends up changing the load. Modulation of a load during start-up requires a complex circuit that would normally not be available in typical installations.

1.16.3. Coolant Activation

Coolant circulation is a critical issue because the temperature of the cells in a stack can significantly increase in a short amount of time. High temperatures can damage the components and dry the PEM with continual operation. A dry PEM will lead to cell failure and inconsistent power production. The flow of cold coolant into the stack can cause a large thermal shock due to isolated cooler pockets that remain in the supply lines. At full operating temperatures, the desired internal temperature is 60°C to 80°C. Consequently the coolant is activated when these temperatures are reached or when the internal stack temperature measures the same as the temperature of the surrounding facility. Stationary coolant remaining in the supply lines will exist at the pre-cooled freezing temperature. The coolant within the stack will be warmed by attempting start-up operation. As coolant circulation starts, the stack coolant will be replaced by the low temperature region followed by the ambient warmed coolant (coolant within the facility). In order to examine the effects of coolant activation, the effect of various start-up temperatures ranging from 30°C to above 100°C was investigated.

1.16.4. Stoichiometry

The selected stoichiometry for operation of the fuel cell stack is chosen to match that of the steady state operation at a current density of 650 mA cm^{-2}. The start-up gas flow rates have been investigated by manipulating the overall gas delivery rates instead of manipulating both the flow and stoichiometry.

Table 0-2: Stack operational stoichiometry

Electrode	Stoichiometric Ratio
Anode	1.53
Cathode	2.16

1.16.5. Humidification

Freeze start-up operation of the stack is conducted with completely dry reactant feeds to eliminate the effects of water build-up in the supply lines. Humidity control of the fuel at the anode occurs when the outlet temperature has reached a minimum threshold or when the stack has reached a sufficient operating load/temperature condition.

1.17. Freeze Stack Conditioning at Shut-down

The aim of stack conditioning is to control the amount of residual water exposed to sub-zero temperature. This involves dry gas purging to remove water at shut-down. Several parameters including the duration of gas flows, temperature at which purge is started and the rate of gas flow through the stack are measured. In theory an increase in any of these parameters should remove a greater amount of water from the stack and increase the freeze start-up capability.

At shut-down, water will be present in the bipolar plate channels, between bipolar plate lands and the GDM, within the GDM, along the CL and within the membrane. Water uptake by the membrane is also a function of temperature [21]. As the membrane cools, water desorbs into the surrounding components and can potentially form ice [48]. In order to prevent this, the membrane should be dried out.

1.17.1. Purge Duration

Experimental investigation led to the development of seven classifications of purge duration presented in Table 0-3. During purging execution from the stack, some trials showed a higher than recommended pressure differential across the membrane or pressure that was above the recommended safety limits causing emergency shutdown. Emergency shut-downs resulted in uncontrolled/unplanned purge rates. These uncontrolled purges trials may then be able to freeze resulting in ice formation within the stack.

Table 0-3: Experimental stack purge duration

Purge Procedure Denomination	Total Anode Purge Time [sec]	Total Cathode Purge Time [sec]	Total Number of Trials
Purge A	150	150	67
Purge B	150	210	6
Purge C	210	210	5
Purge D	180	210	1

Purge E	90	90	1
Purge F	90	150	1
Uncontrolled purge			10
		Grand Total	**91**

Reducing the purge time or rate of gas flow is investigated by a purge reduction scheme to scope limits and measure the dependency for successfully start-up with the purge parameter. The effect of reducing purge was investigated by comparing purge conditions F and comparison to either purge C and D (all conditions are shown above in Table 5-3). A purge reduction is attempted in order to determine if one electrode purge time can be decreased in order to save fuel gas and power. The investigations into the reduction in purge were halted unfortunately due to time constraints and equipment availability.

1.17.2. **Purge Rate**

The investigation continued to examine the speed at which dry reactant is circulated through the stack. The various purge rates tested are shown in Table 0-4.

Table 0-4: Experimental purge rates

Anode Purge Rate [slpm cell^{-1}]	Cathode Purge [slpm cell^{-1}]	Number of Trials
0.9	9.5	13
1.4	12	1
1.8	16	53
1.8	19	1
2.7	15	12
3.2	18	1
5.0	26	1
Uncontrolled		9

1.17.3. **Purge Temperature**

Investigation revealed that the purge temperature is a critical parameter to assist in removal of water. Increased temperature enhances water mobility and the amount of water removal during a stack purge. Figure 0-9 shows the number of experimental trials aimed at exploring the effect of purge temperature. More trials were completed at the highest purge temperature due to the improved performance at these conditions.

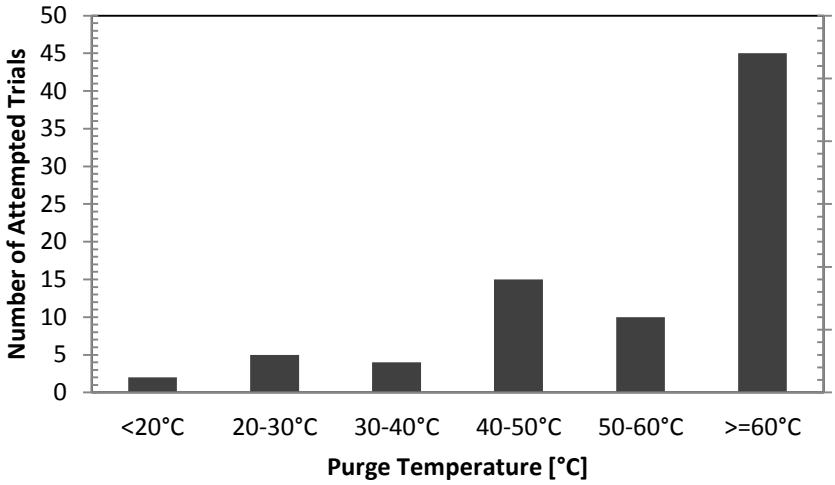

Figure 0-9: Distribution of experimental purge temperatures

The maximum purge temperature examined was 68°C. This temperature was manually controlled and voltage monitored in order to test the upper limit and remove as much water as possible without harming the stack. Generally, the open circuit voltage (OCV) remains constant during the purge. If the OCV showed signs of deviation, the purge was stopped. A drop in OCV indicates insufficient water availability that results in poor oxygen electrocatalysis, an increase in the resistance in the catalyst layers and an increase in membrane ionic resistance [49].

RESULTS AND DISCUSSION OF FREEZE START-UP

The number of successful and failed start-up experimental trials according to freeze start-up temperature can be seen in Figure 0-1. A start-up is successful when the stack achieves stable full power and full normal operating temperatures, neglecting time constraints. Some initial start-ups took in excess of 30 minutes to produce stable full power. A failure to start occurs when the stack is unable to maintain a stable load and thereby will never generate enough heat to sufficiently warm the stack above 0°C. The largest number of completed trials tested is at -20°C in order to compare with the DOE target for the adoption of fuel cell technology. Recall that these require that a freeze start-up for mobile FC applications at -20°C reach 50% power within 30 seconds.

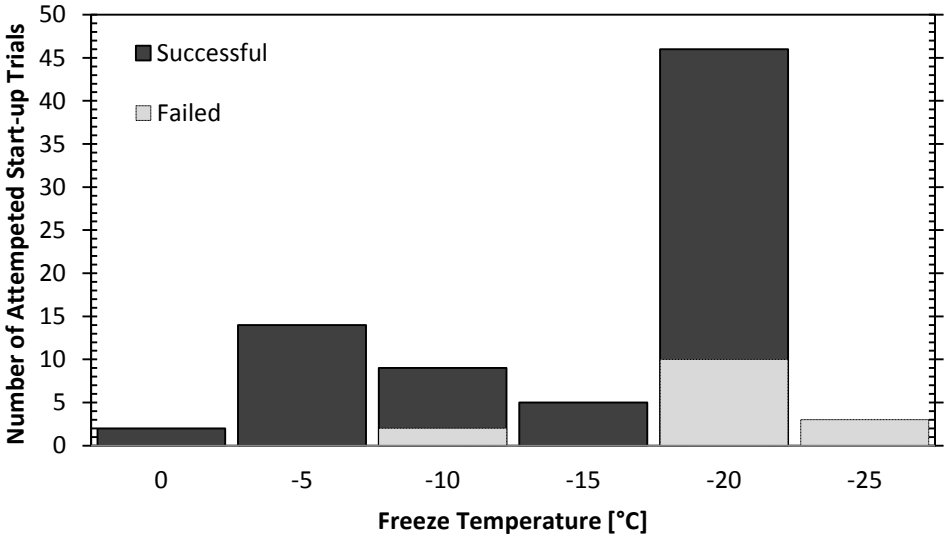

Figure 0-1: Experimental freeze start-up trials

The two start-up failures at -10°C occurred due to an experimental equipment error and electrode gas crossover from anode to cathode. The crossover leak was detected during a start-up from -10°C and after several low purge trials that failed resulting in a catastrophic and irreversible failure of specific cells within the stack. The EOL occurred after 42 freeze start-up trials, a prolonged period at OCV and several failed freeze start-ups. In order to continue testing, the affected cells located at positions 11, 15 and 16 were removed and the stack was reassembled. The cell failures all occurred within the stack and not at the ends. The end cells receive the coldest flow and lose the most heat so that this is where ice would most likely form during start-up. The cell failures in the middle of the stack show that degradation occurs from water being present during shutdown rather than during start-up. After the removal of the cells, the addition of three new cells was disregarded due to time

constraints and discrepancies between performance of the new and used materials. The investigation continued after the stack was rebuilt with further examination into the purge procedure.

1.18. In-Situ Investigation

1.18.1. Stack Temperature Conditioning

During start-up operation a temperature distribution occurs in the stack that results from the thermal conductivity of the gas manifold connections to the exterior of the environment, the load cables and the endplate. Thermocouples (TC) located at various positions measure the temperature distribution across the stack (i.e. inlets, outlets, internally and endplate surface temperatures). The inlets and outlets are situated on the same side of the stack as the wet endplate. The connections from the stack into and out of the environmental chamber allow pathways for heat into and out of the stack. Heat transfer causes a thermal gradient to exist within the stack from the dry endplate to the wet endplate.

In order to gain the correct freeze temperature, the environmental chamber set point temperature was decreased below the freezing set point. The temperature values are shown below in Table 0-1, for the case where the stack has been cooling for 60 hours at an environmental chamber set point temperature of -23.2°C. The middle of the coolant compartment cell temperature measured by the internal TC reached -20.94°C, whereas the wet endplate and dry endplate have a temperature differential of 0.8°C across the stack. This is an example of a freezing temperature at -20°C. An attempted start-up trial occurs after the internal cell TC measures a temperature at or below the set point for 5 minutes. Typically the stack requires four hours to achieve the desired freezing temperature.

Table 0-1: Stack freezing equilibrium temperature values

Collection Point	Temperature [°C]
Environmental Set Point	-23.3
Chamber interior	-22.00
Chamber Wall	-20.16
Anode Inlet	-21.25
Anode Outlet	-21.44
Cathode Inlet	-21.38
Cathode Outlet	-21.81
Coolant Inlet	-16.27
Internal Cell	-20.94
Coolant Outlet	-17.74
Coolant Out Stack Control	-17.80
Wet Endplate Surface	-20.48
Dry Endplate Surface	-21.32

1.18.2. **Reactant flows at start-up**

Once the stack has achieved the desired temperature, reactants are delivered to the stack and the cell voltages increase. Gas flow rate at start-up depends on the desired freezing temperature as the water in the stack is removed by evaporation. Water generated during operation may accumulate in the stack and freeze as a result of the lower temperature of the stack thermal mass. Freezing temperatures decrease the amount of humidity that can be supplied to and removed from the fuel cell. The colder the temperature the lower in the amount of water that evaporates when saturation is reached. As the stack temperature increases, so does the gas reactant temperature and the amount of water storage capacity that can be carried away as humidity. Increasing the amount of water removed from the stack aids in decreasing the amount that may form ice.

The gas flow rates are presented here in terms of their equivalent consumption rate at a defined current density. (0-1) presents the conversion from a current density to an equivalent volumetric flow delivered to the electrode at start-up. Calculations are based at standard temperature and pressure. The delivery gas will exist at this constant rate until the current density exceeds the set point, at which time the flow with increase to match.

$$\text{Equivalent } Gas\ Flow \quad \frac{mA}{cm^2} = \frac{Fn_e}{A}\ \frac{y_i Q_{H_2} P}{\lambda RT} \tag{0-1}$$

The temperature of the fuel cell depends on the heat that is generated in the stack since unassisted start-up is employed. Heat may be removed by convective/conductive gas flows circulated through the stack and conductive/convective flows from the environment. Heat removed during start-up increases the amount of time required for the stack to reach full performance. From the attempted start-ups, a subset is selected to examine the effect of gas flow rate, as shown in Figure 0-2. The figure shows how the output power varies with time. All trials occur from -20°C but with variations in start-up flow rate. Supply gases are delivered in excess (by the stoichiometric ratio) of the rate of consumption. It is important to note that for the lower flows, a point will be reached where the consumption of reactants exceeds their initial setting, as can be seen by the cases of 200, 350 and 500 $mAcm^{-2}$ equivalent at the 2 kW to 4 kW range. The best start-up flows for the current system are between 770 and 900 $mAcm^{-2}$ equivalent. Comparison of the results at flow rates of 900 and 1000 mA cm^{-2} shows a slight decrease in the power production rate roughly between 100 and 300 seconds at the higher current. This reduction may be the result of heat loss by the higher gas flow.

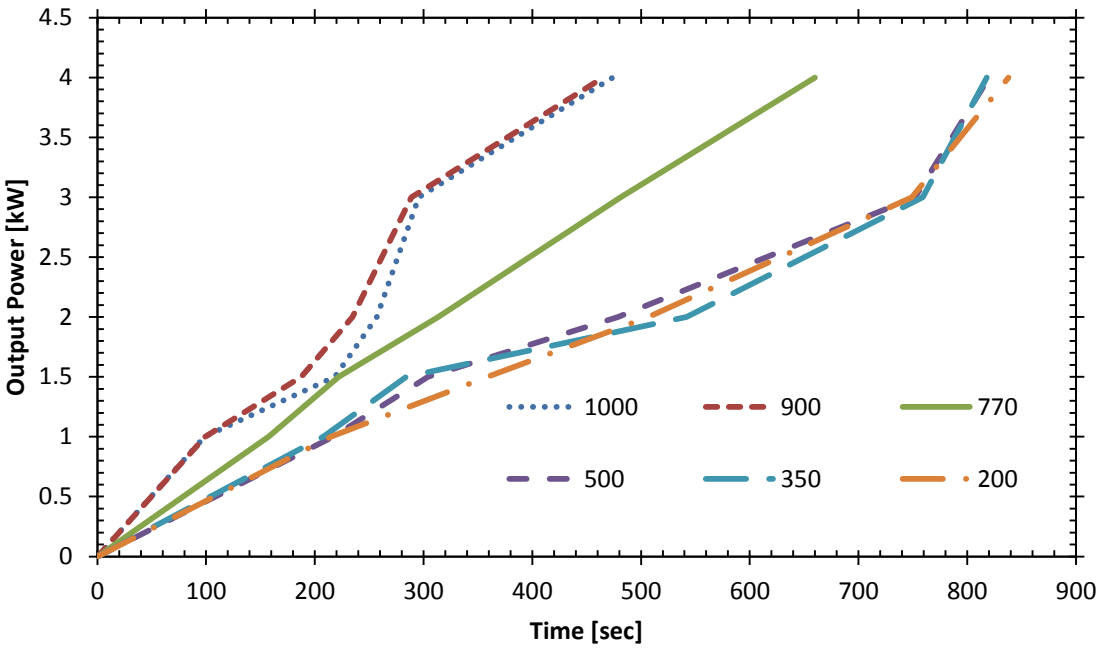

Figure 0-2: The effect of constant flow rates ($mAcm^{-2}$) on freeze start-up showing power production versus time for -20°C trials

Burst flow trials involve the use of a short burst of gas flow followed by reduction to the stoichiometric level. This mode shows an overall decrease in performance in comparison to the constant, steps or ramping flow mode. The execution of the burst procedure was somewhat difficult as the mass flow controllers took time to respond. A 15 second burst will almost reach the required set point at the end of the flow (depending on set point) and follow another 20-25 seconds down to the new set point. The performance of this trial show an overall porrer performance compared to that of a constant 900 mA cm^{-2} start-up.

The results using step flow and burst flow are similar although placement and timing of steps can be difficult to implement and may not follow the supply exactly. The default supported load overrides the amount of gas delivered in order to maintain the current density. Ramping flows lead to greater capability by maintaining a surplus above the consumption rate.

The use of ramping flow show an improvement in comparison with the use of constant flow rates by consuming less gas at start-up. Figure 0-3 shows an improved peak performance at 900mAcm^{-2}, but lower at flows above and below this value. There exists a flow where the generated water is removed before it can freeze, but increasing beyond a certain point may cause cooling of the stack by convective gas flows due to the higher rate. The cooling of the stack causes increase in the time required before full performance can be achieved. The curves converge at higher operating currents due to the operating protocol. The activation of the stack coolant flow typically occurs at the 2 to 3 kW power output region and thereafter the heat carried out by gas circulation is insignificant.

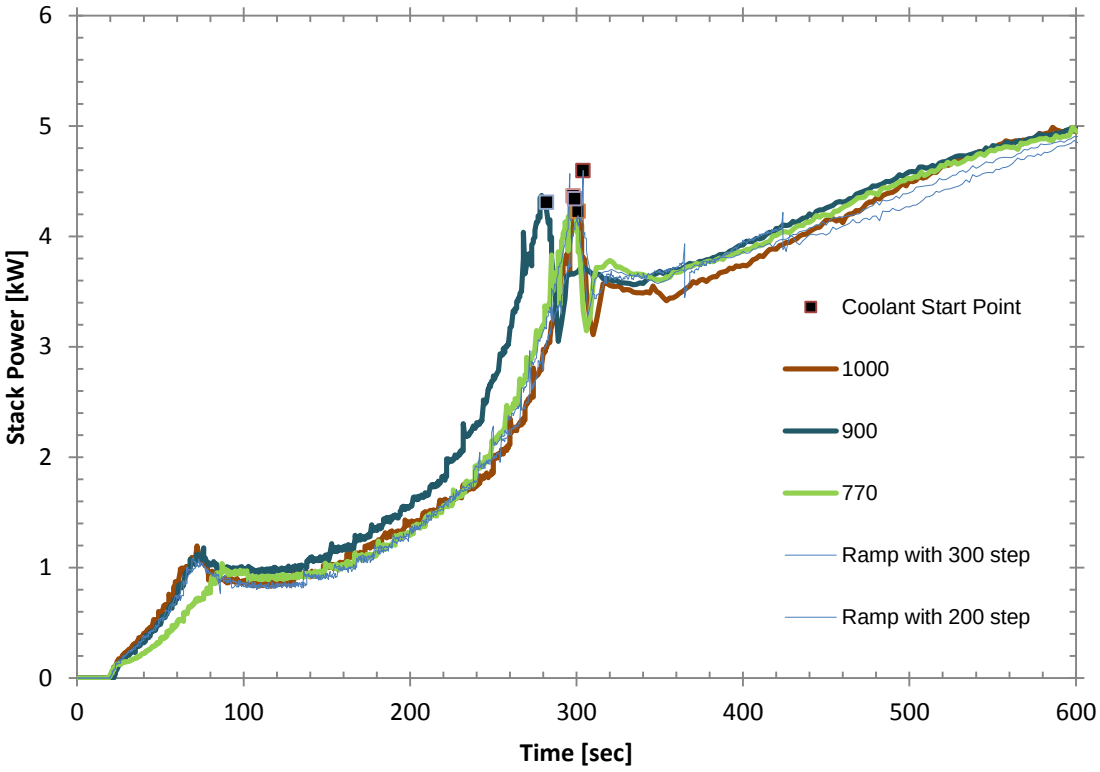

Figure 0-3: Effect of and ramping with step flow ($mAcm^{-2}$) rate on start-up power versus time at -20°C

1.18.3. **Dwell at Freeze Temperature**

In approaching the freezing temperatures, the aim of the experimental simulations was to bring the temperature down as fast as possible. Two methods were used to in freezing the stack: continuously running the environmental chamber at the required freeze temperature or if the environmental chamber was at idle conditions (i.e. not running) the chamber would go to the set point temperature as fast as possible. As an example, a fuel cell in mobile applications may travel outside in the winter and then be shut-down. This will cause a sudden immersion at sub-zero temperatures. Insulation on a fuel cell stack is typically not used due to thermal management difficulties (i.e. the insulation would result in stack overheating during operation). The amount of time and the temperature at which the fuel cell is immersed will affect the location and state of water within the system. As the stack freezes, water may migrate from the centre and warmer regions towards the outer cooler edges as the stack is exposed to the

environment. As the stack remains at suppressed temperatures, water may equilibrate across the MEA surface. Water within the membrane that does not freeze as a result of the acidic environment may travel and equilibrate across the MEA surface. As the membrane cools, water will leak out due to the contraction of the polymer and pores that contain water. The water that desorbs will initially be present at the membrane interface and may be transported away.

The results in Table 0-2, show the effect of dwell time (time spent at freezing temperature without fuel cell operation) at fixed freeze temperature, similar purge temperature and flow rate. A relationship between freeze dwell time and the ability to start may exist at higher and lower dwell times, as there is a large variation between start-up performances. For times ranging from 0 to 5 hours, no obvious trend is apparent. As testing continued, the longer dwell times of about 60 hours present a larger effect for the start time performance. In comparison between trials, a longer dwell time increases the amount of time required to reach full power. This indicates that there may be a relationship between the amount of dwell freeze time and performance.

Table 0-2: Dwell freeze temperature results

Freeze Temperature [°C]	Dwell Freeze Temperature [hrs]	Flow rate [equivalent mA cm^{-2}]	Purge Temperature [°C]	Time to 50% Power [sec]	Time to Rated Power [sec]
-20	1.0	900	65.9	209	407
-20	2.0	900	66.5	248	447
-20	2.0	900	66.5	228	432
-20	3.0	900	66.3	216	414
-20	3.0	900	66.3	200	414
-20	5.0	900	66.3	179	384
-20	5.0	900	66.5	195	394
-20	59.8	900	66.4	312	537
-20	60.7	1000	66.5	302	506

If the membrane is purged at a high temperature, this will remove water from the channels, GDL and CL before the membrane starts to dehydrate. Once purging is halted and the temperature begins to decrease, the water uptake in the membrane decreases, causing water to be expelled from the membrane. An unsaturated membrane during temperature decline may become supersaturated causing the water to desorb and migrate outwards and freeze along the GDM or CL interface. As the stack cools, the water will diffuse outwards towards colder regions and may accumulate along the surface and eventually redistribute across the MEA. Ice may not be fully

formed at the desired freezing point, even if the desired freeze temperature has been achieved by the stack. Water may be in the process of freezing through the pores in the GDM and may migrate to various areas by capillary effects. A distribution of ice across the MEA surface will provide multiple sites for crystal growth upon start-up.

1.18.4. Temperature Responses at Start-up

For a fuel cell to reach full power production, a minimum temperature must be attained to enable full power production without causing degradation to the membrane. The generation of heat during a start-up allows the fuel cell to perform at increasing power densities and generate more heat as the stack starts to generate electrical power. The production of heat can hinder operation when it causes dehydration of the membrane, and thus reduces performance. The activation of coolant is an important parameter to adjust as the temperature declines. Experimental testing proceeded with multiple runs at various coolant activation temperatures. The results shown here are in decreasing temperature and are not related to the sequence of testing that was performed.

1.18.4.1. Coolant Activation

Lower freezing temperatures increase the amount of time required before full power can be generated. The generation of heat occurs rapidly once the stack is above freezing temperature. Although cell performance may still be low as a result of maldistribution of reactant flows, lower amount of available catalyst sites and/or the thermal temperature gradient across the stack. Coolant circulation is necessary to prevent excessive drying of the stack during operation. The circulation of coolant will cause an increase in thermal load, increasing the amount of material that must be heated, therefore resulting in an overall increase in start-up time. Temperature and water variations across the cells will exist due to reactant flow, ice formation, reactant delivery and product removal. Coolant can help to flatten the temperature gradient across the cells.

The activation of coolant circulation occurs at various temperatures and operating states. Typically this occurred when the ambient room temperature of the coolant (25°C) was reached inside the stack (as measured by the ultra thin TC inserted in the centre of the stack). A 25°C internal stack coolant temperature would be similar to the temperature within FCATS system (i.e. outside of the environmental chamber). Stagnant

portions of coolant in the supply and return lines will remain chilled at the environmental freezing condition. Upon coolant circulation it would then be moved through the stack causing a large shift in temperature. Conceivably the situation in practice would be cold coolant being heated by the electrochemical reaction until it reaches the desired temperature at which time the coolant circulation is activated. This would cause a large amount of continuous cold coolant to be circulated.

Activating coolant circulation causes a shift in the temperature of the stack components. Heat generated in the stack by the electrochemical reaction heats the stack faster if the coolant is retained in the cells (i.e. not circulated). Without activation of the coolant circulation, the internal cell temperature can reach above the boiling point of water causing extensive drying and damage to the membrane. The effect of coolant activation on the performance of the stack can be seen in the start-up performance in Sections 1.18.4.5 and 1.18.4.6. The point at which the coolant activates the system is no longer simulating a true unassisted stack start-up condition. The circulation of cold coolant is not possible with the current experimental setup. The FCATS system can manage the circulation of coolant by taking into account the exiting coolant temperature and heating the incoming coolant to that desired point. However, the transient conditions that cannot be simulated by the stack operation must be acknowledged.

Temperatures at which coolant activation occurs were investigated and it is noted that higher temperature coolant activation will allow the stack to reach greater power in shorter time. Activation of coolant at a higher temperature allows more heat to be retained within stack, warming the cell components before the coolant takes effect. Unfortunately, this heat is not well distributed across cells or within cells and may lead to dehydration and potential damage of the MEA. However, when the coolant does activate, the cold circulation of coolant causes a drop in temperature. The reduction in the temperature of the cells causes a reduction in cell performance. Trials have shown that when the stack was delivering rated power the stable power output dropped to as low as one-quarter of its initial value upon coolant activation (see Figure 6.8 and 6.9).

1.18.4.2. Response at 0°C

The FC start-up performance at 0°C gives an indication of the performance based on the script and temperature effects, without the effect of sub-zero temperature and ice formation. Start-up from suppressed temperatures will be based on the results at 0°C with the added combination of water/ice formation hindering gas reactant and product flows. The lower temperature also reduces the rate of electrochemical reaction.

One start-up trial at 0°C is shown in Figure 0-4. This start-up was completed with initial gas flows equivalent to 10 mA cm^{-2}, with a Type A purge at 59.2°C (as measured by the internal thermocouple). The environmental chamber is set to simulate a -5°C freezing stack start-up response. Figure 0-4, presents the cell voltage response and the current density versus time. Upon activation of the gas reactant feeds, voltage is generated and once it rises above the minimum voltage the load is ramped on. As the load increases, the voltage drops forcing the operator to decrease the load in order to maintain cell voltage.

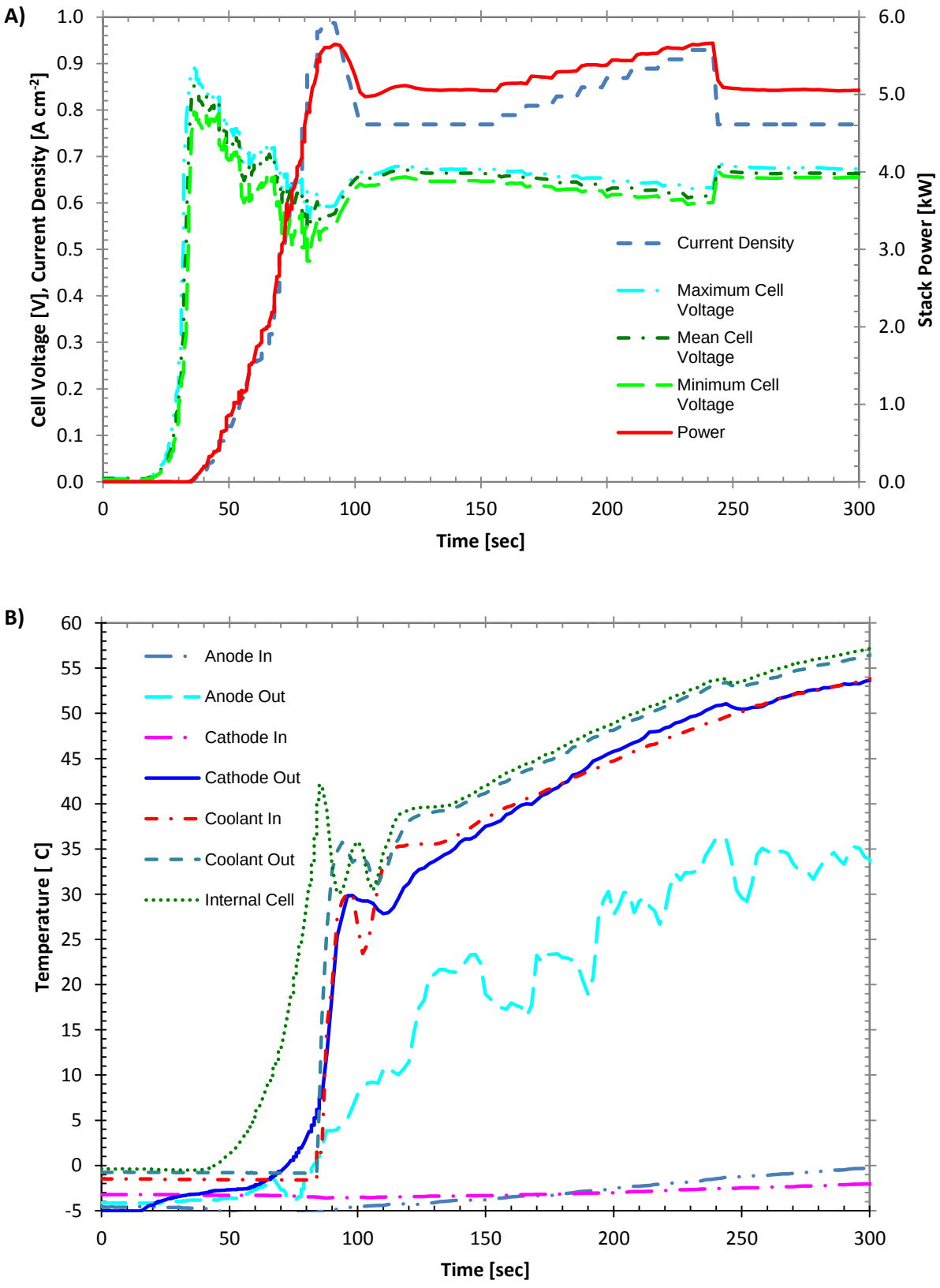

Figure 0-4: Reponse at 0°C, a) cell voltage, current density with power against time and b) the temperatures of the stack flows and internal cell.

Maintenance of the minimum cell voltage at 0.3 volts by adding and subtracting the load in stages is the current procedure. The response of the voltage is taken into account and the load is modified. The figure shows that during start-up the cell voltage is always above the minimum voltage. The execution of the current script cannot add the load at a fast enough rate to keep the cell voltage at the desired level. Manipulating the load fails to correctly constrain the cell voltages, and as such the start-up performance at this temperature can be improved. Figure 0-4 B) shows the temperature response of the stack during freeze start-up. The horizontal axes of Figure 6-4 A) and B) are the same to easily visualise the progression of heat generation as the stack produces power. The anode outlet shows a large variation in temperature that may be due to the maldistributions of flow through the stack channels.

After the current density reaches 1 Acm^{-2}, a large drop in performance occurs due to the rise of the cell temperature and activation of coolant. The load is maintained at 770 mA cm^{-2} for a period of time while temperatures reach a steady state. Steady state data is collected for performance with the life of the stack, but is not shown here.

1.18.4.3. Response at -5°C

No start-ups failed when evaluating the stack response at -5°C. This agrees with the work by Hou *et al.* [50] who reported no performance losses from repeated start-up cycling at -5°C. Freeze *s*tart-up should be possible at this temperature as long as large amounts of water have not been retained at shut-down.

In Figure 0-5, a response can be seen where the minimum voltage of the cell during the start-up decreases to about 0.5 V. The start-up performance can be improved from this basis, as shown in the results for the response at 0°C.

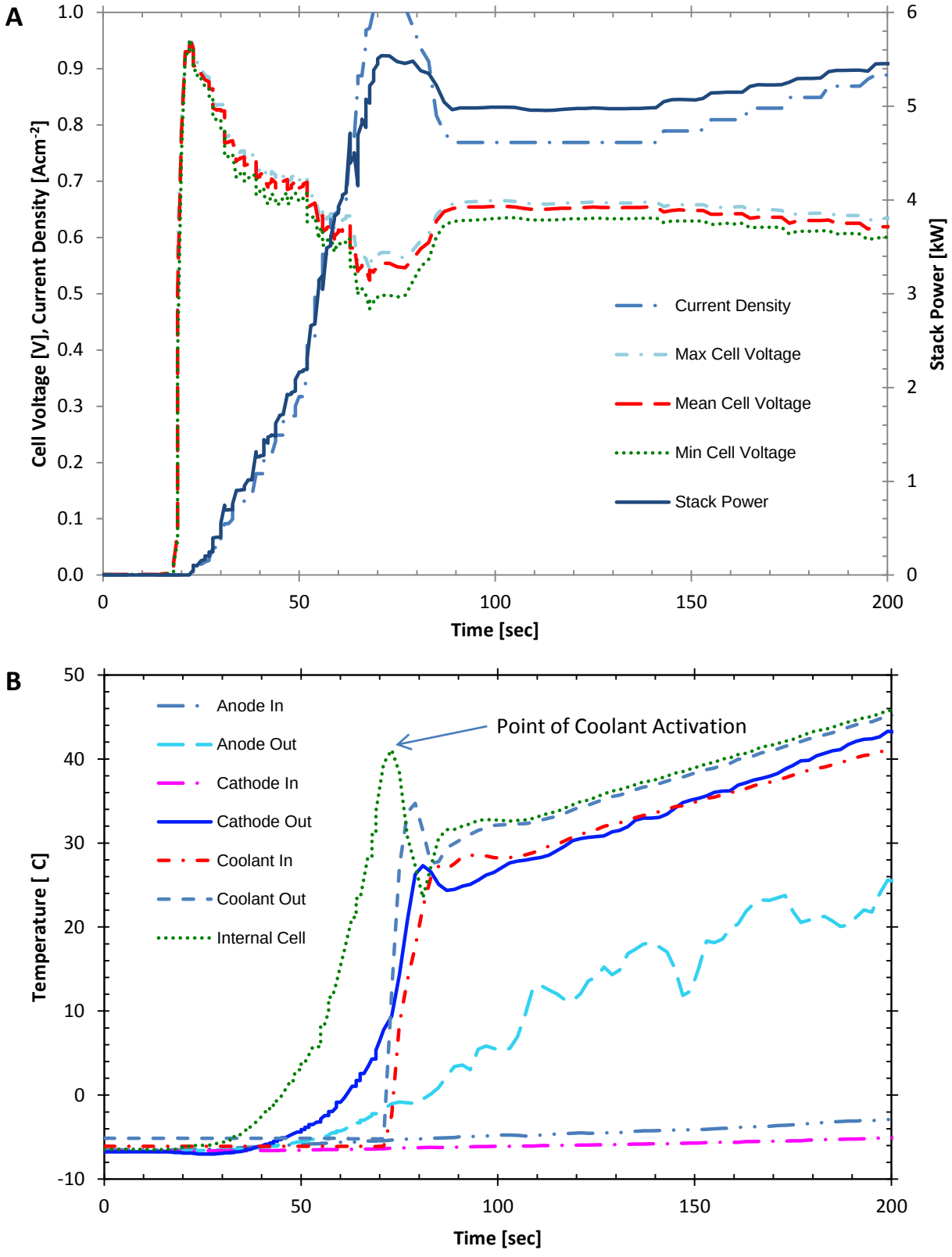

Figure 0-5: Reponse at -5°C, a) cell voltage, current density with power against time and b) the temperatures of the stack flows and internal cell.

The times to reach 50% and full power in this case are 36 and 48 seconds, respectfully. Type A purge was employed at a temperature of 59.3°C and higher initial constant gas flows of 900 $mAcm^{-2}$. The anode outlet temperature shows a large fluctuation during the warm-up period to steady state data collection.

1.18.4.4. Response at -10°C

The stack response at -10°C also showed the first start-up failures. These failures are attributed to the performance of the testing equipment and the heavy damage the stack had already sustained as a result of a gas crossover leak causing an EOL condition. Two experimental results are presented here: 1) a successful start-up trial at -10°C and 2) the failed trial that results from the stacks EOL gas crossover.

Figure 0-6 shows the results of the successful freeze start-up at -10°C. The trial was executed with 900 mA cm^{-2} gas flows, purged at 65.3°C at rates of 1.8 and 16.0 slpm $cell^{-1}$. The stack reached 50% and full power within 55 seconds and 73 seconds before coolant activation.

A faster start-up trial at -10°C and a lower purge temperature of 53.3°C was able to reach to 50% and full power within 41 seconds and 61. The effect of purge temperature will be discussed in Section 1.18.8.2.

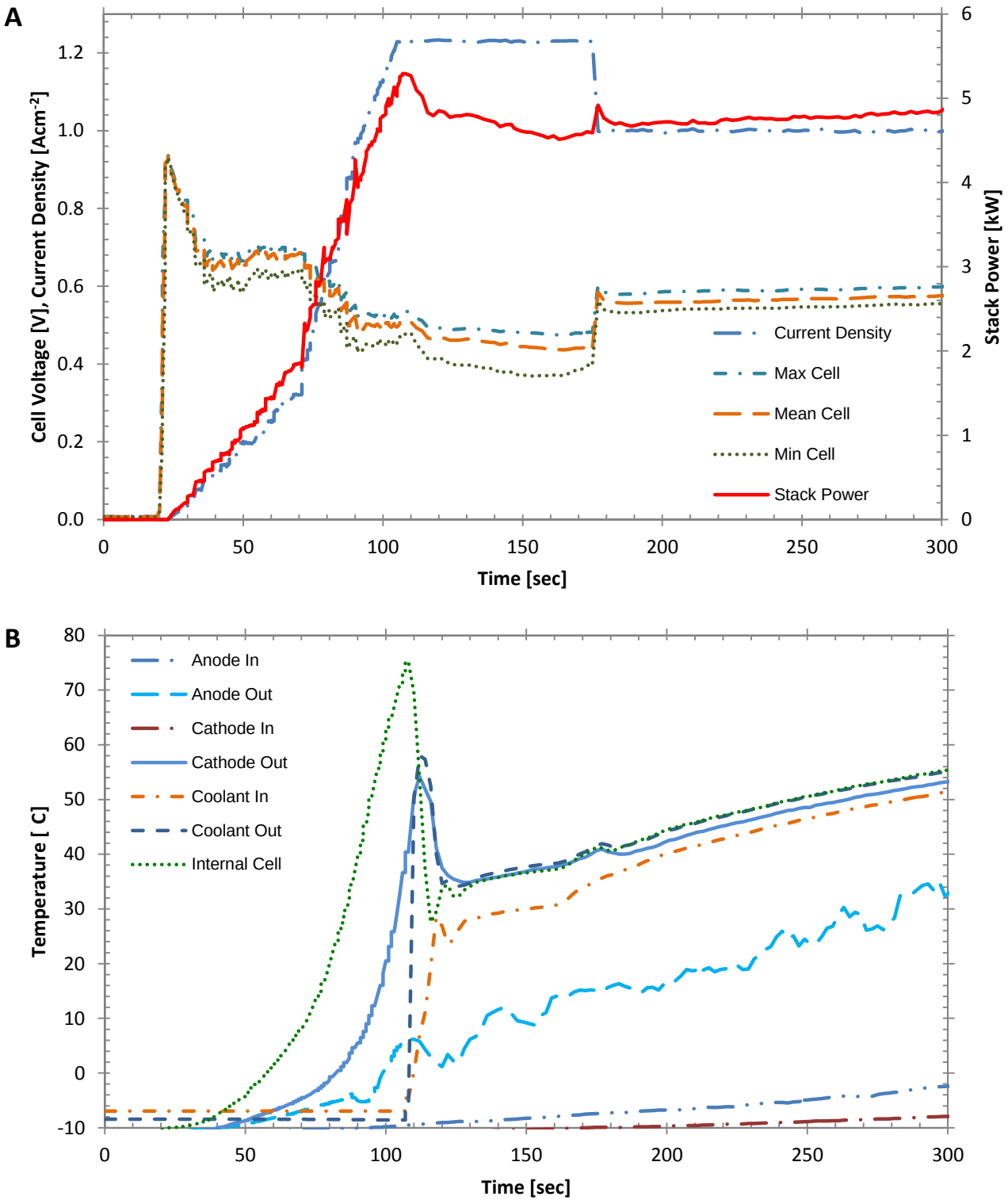

Figure 0-6: Reponse at -10°C, a) cell voltage, current density with power against time and b) the temperatures of the stack flows and internal cell against time.

The two failures to start-up at -10°C were the result of errors: 1) an equipment malfunction, 2) a crossover leak that results in an EOL condition which is discussed in Section 1.18.9. The stack EOL occurred during the 43rd start-up trial. The trial proceeded after a severe dehydration conditions were reached resulting from an equipment malfunction. The failed start-up trial is shown in Figure 0-7. The lower cell voltages were measured in the middle of the stack from cells 11 and 15. The problem developed in the middle cells and prevented the cell potentials from increasing enough to generate enough current to for a successful start-up. This is of interest as a high gas crossover increases the amount of heat generation, but at too high a rate and the performance of the stack will decay. These failures inflict and present the degradation of the stack.

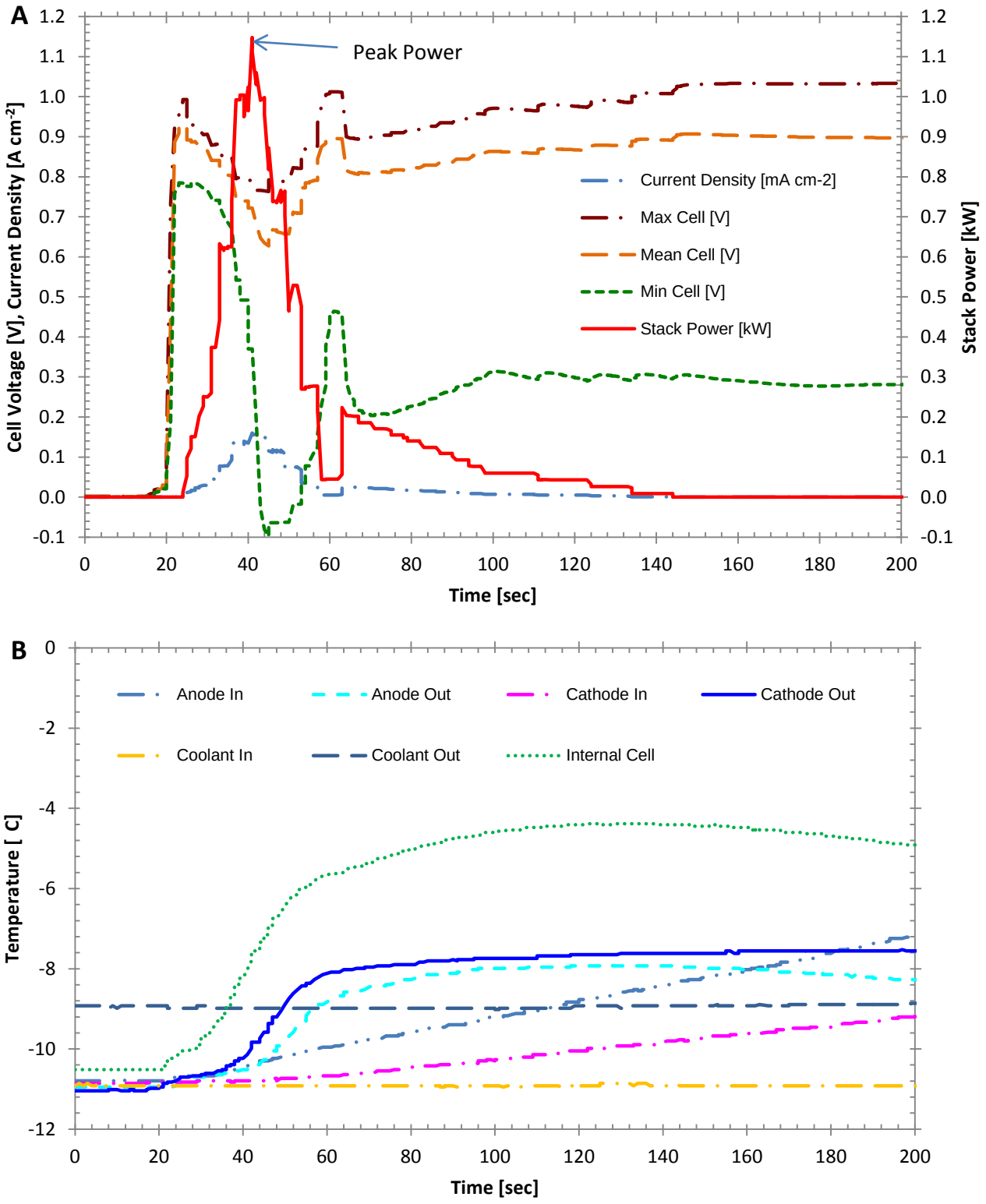

Figure 0-7: Failed freeze star-up at -10°C due to EOL gas crossover condition a) cell voltage, current density with power against time and b) the temperatures of the stack flows and internal cell against time.

1.18.4.5. Response at -15°C

Five trials completed at -15°C helped in the development of a successful start-up procedure. Data collected from the trials at -15°C were tested earlier in this study and therefore do not benefit from the knowledge this study gained in this study.

The start-up presented in Figure 0-8 had the best start-up performance at -15°C, but the employed purge was type A at a temperature of 24°C. Figure 0-8 A) shows the variations of cell voltage and power generation versus time. The results show that the current increases in steps in order to stabilize the cell voltage. A drop in current occurs around 21 seconds due to the increasing current density and again at around 62 seconds possibly due to the formation of ice. The cell voltages show a larger distribution during start-up. Lower cell voltages occur at either end of the stack. The voltage of the cells is shown vary until about 470 seconds when the temperature of the stack reaches 54°C. Activation of coolant circulation occurs at about 125 seconds, leading to a slight disruption to the generation of power as a result of the cold coolant being pushed though the stack. A large decrease in temperature is observed at the cathode and anode outlets as the heat generated in the stack is now warming the circulated coolant. The performance at this level shows that the 2kW is reached after about 126 seconds and full power at 408 seconds.

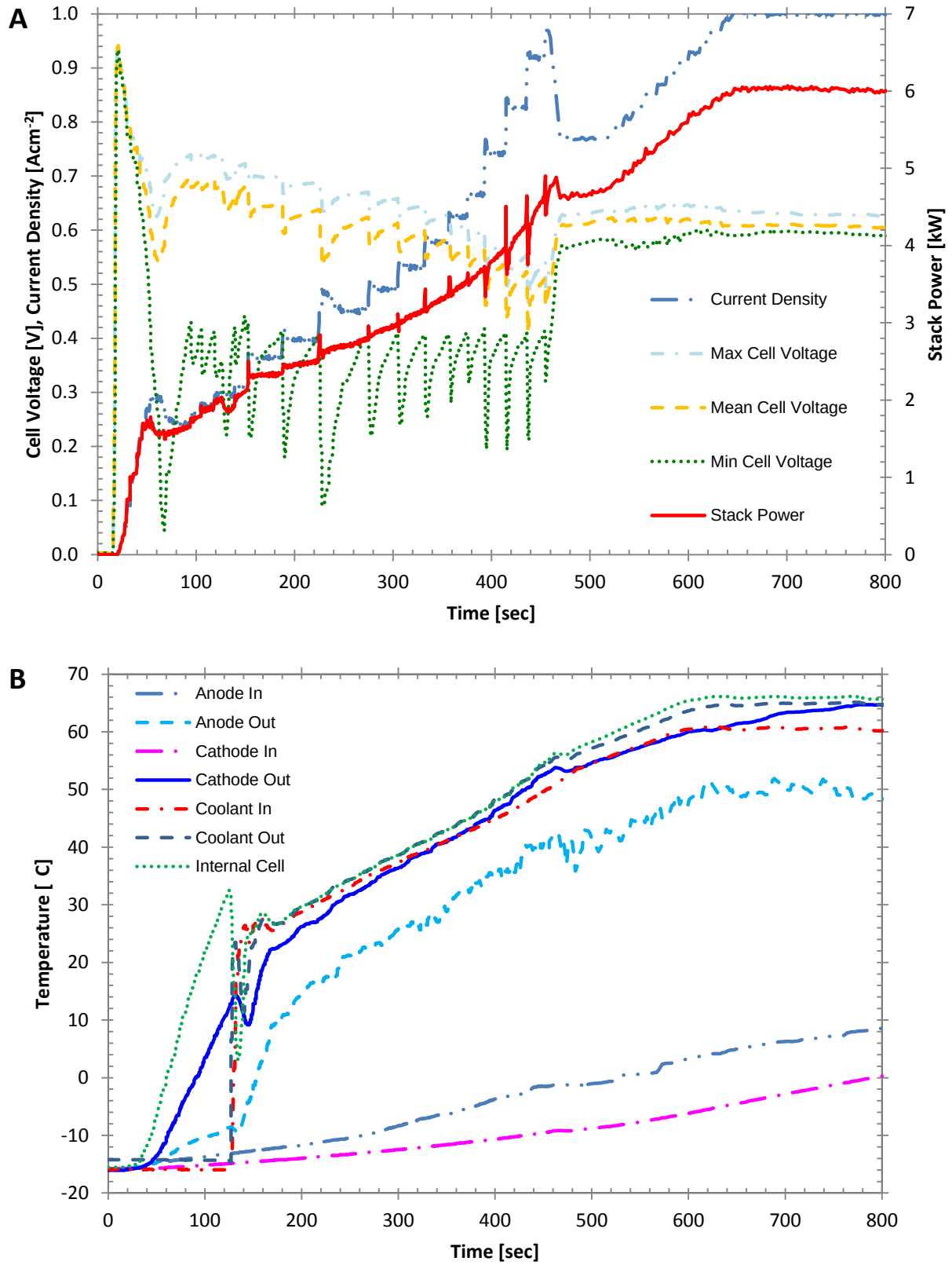

Figure 0-8: Reponse at -15°C, A) cell voltage, current density with power against time, B) the temperatures of the stack flows and internal cell.

1.18.4.6. Response at -20°C

Investigation of freeze start-up at -20°C initially showed comparable results, but with further investigation problems arose with achieving a successful start-up. Further investigation showed that a minimum purge temperature on shut-down was necessary in order to allow removal of sufficient water for the stack to achieve a successful start-up.

A sample start-up performance can be seen in Figure 0-9. The power noticeably drops after about 80 seconds into the start-up as the result of ice forming and hindering the increase in voltage response by blocking reactants. The cell voltages declines when the load is further applied and take longer to recover in comparison to the situation at warmer start-up temperatures (i.e. longer to warm components to free up reactant channels). The cell voltages vary widely across the stack with the minimum and maximum cell voltages difference by as much as 0.6 volts. The lower performing cells are typically the end cells, as discussed in Section 1.18.7, or cells that have ice hindering gas reactant delivery. The spread of the cell voltages over the stack decreases as time progresses and the stack temperature increases. The start-up reaches 50% power at 229 seconds and full power at 474 seconds. The activation of coolant at 274 seconds into the trial occurs when the internal cell temperature reaches above 60°C. A much faster ramp rate of power occurs before the activation as a result of the much faster increase in temperature due to melting ice freeing up pathways for reactant delivery. The circulation of coolant causes a large thermal shock whereby the internal thermocouple readings measure about 60°C to around 10°C in a matter of seconds.

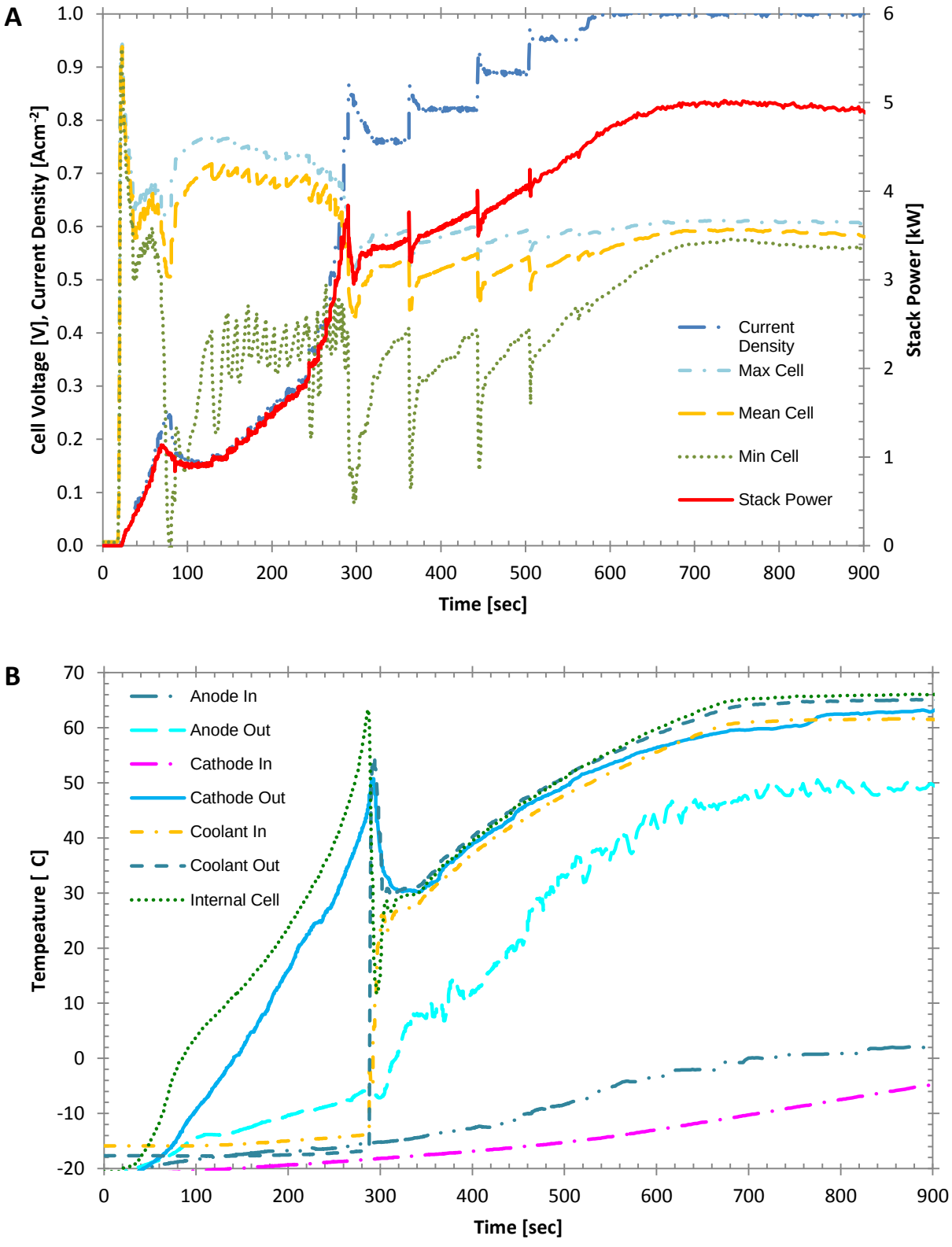

Figure 0-9: Reponse at -20°C, a) cell voltage, current density with power against time and b) the temperatures of the stack flows and internal cell.

1.18.4.7. Response at -25°C

Three experimental trials were conducted at -25°C, but all failed to achieve successful start-up operation. Figure 0-10 presents one of the attempted trials at -25°C. This specific trial was conducted with a type A purge at a rate of 1.8 and 16.0 slpm $cell^{-1}$ for the anode and cathode, respectfully. The previously conducted purge measured a peak temperature of 66.1°C. At start-up, constant flows are delivered at an equivalent set point up to 900 mA cm^{-2}. Delivery of the reactants allows the reactant to occur even at the lower temperature, increasing cell voltages. As the voltages response, the load again cycles on and off responding to the minimum cell voltage. The start-up current density peaks at around 0.22 A cm^{-2} at 68 seconds into the start-up. The generation of heat in the stack increased with the load and peaks since the cell voltage is unable to recover. Any load maintained at this level will decrease cell voltages and can lead to carbon corrosion or cause cell reversal. The temperature as measured by the internal thermocouple peaks at about 90 seconds at a value of -3.66°C. The cathode outlet shows a temperature increase with the attempted start-up but does not rise above -11°C. The gas reactants flows do show a small increase over the 200 second start-up as the flows carry heat into the chamber since a larger gradient exists at this temperature.

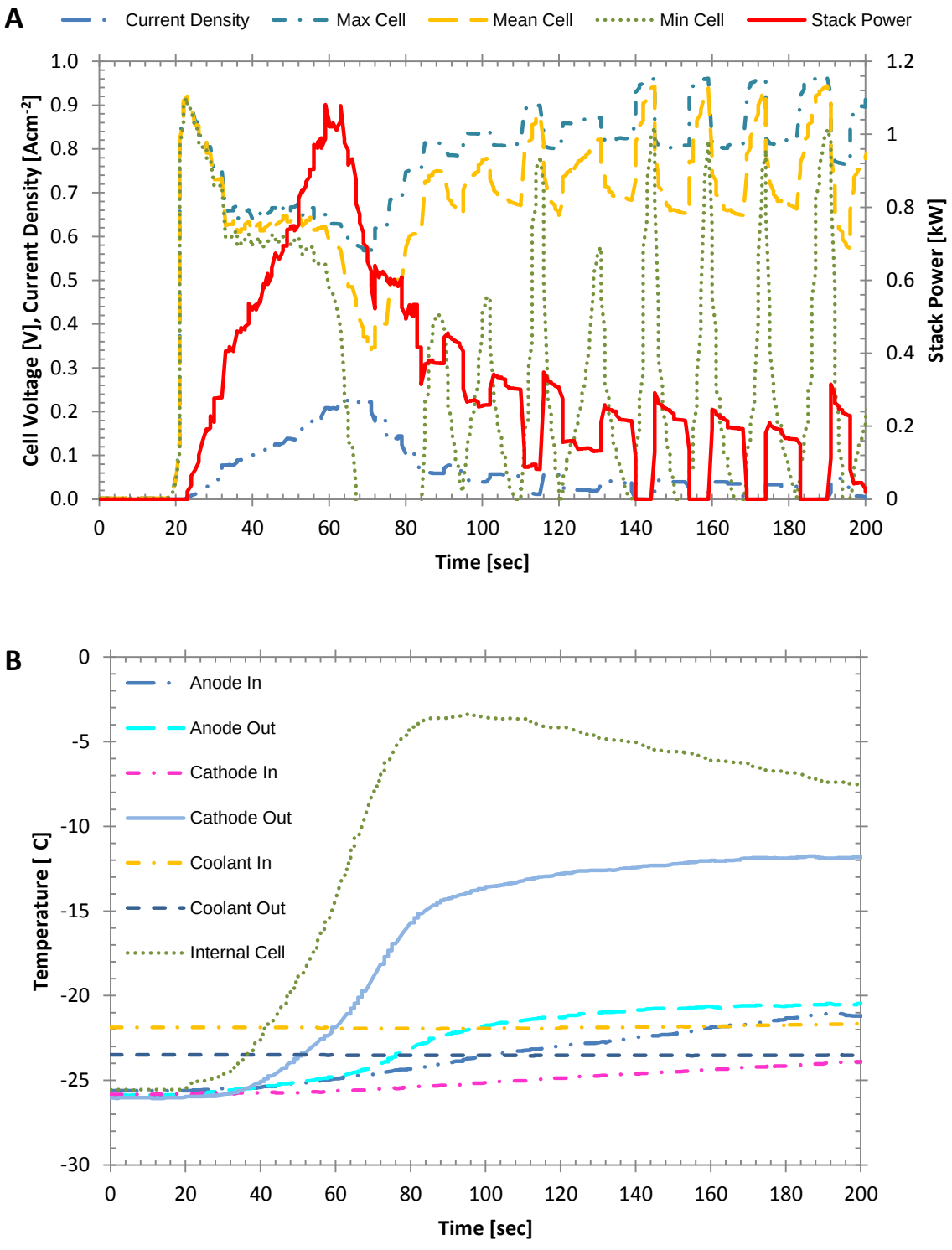

Figure 0-10: Reponse at -25°C, a) cell voltage, current density with power against time and b) the temperatures of the stack flows and internal cell.

1.18.5. **Power Production and Ice formation during Start-up**

Power production increases with increasing temperature. The onset of the current increases heat and generates water, which can freeze hindering reactant flows. As ice forms, the amount of gas distribution is disrupted and causes a large increase in resistance to the delivery of reactants. As ice growth continues the cell voltage will decrease as pore and channel openings become blocked. In this situation, OCV loss indicates that ice is blocking the pores and that start-up will not be possible. In order to achieve a successful start-up, the stack must maintain a minimum load to generate enough heat to melt the ice and warm the cell.

Trials at each of the various temperature levels were selected with other conditions maintained reasonably similar (Table 0-3). The only exception was at -15°C due to the fewer number of trials conducted at this temperature.

Table 0-3: Power production in selected purge type A trials

			Purge				Time to Power	
Temperature [°C]	Selected Data file	Initial Flow Set Point [mA cm^{-2}]	Internal Cell TC [°C]	Temperature Cathode Outlet [°C]	Ca Purge Rate [slpm $cell^{-1}$]	An Purge Rate [slpm $cell^{-1}$]	Time to 50% Power [sec]	Time to 100% Power [sec]
0	100526-205154.csv	10	59.0	54.6	1.8	16.0	53	65
-5	100602-140930.csv	770	58.5	52.9	1.8	16.0	35	49
-10	100708-062445.csv	900	65.3	58.8	1.8	16.0	52	73
-15	100615-132137.csv	900	24.0	25.7	2.7	15.1	126	408
-20	100603-122358.csv	900	59.1	53.2	1.8	16.0	268	581
-25	100617-192615.csv	900	66.1	60.2	1.8	16.0	-	-

In Figure 0-11 the power production is presented versus time for various temperatures. The decrease that results from the presence of ice occurs 40 to 80 seconds into the start-up. The power production shows that the rate of power production is steady for -5°C and -10°C. This shows that the generation of heat within the stack is enables power production without ice formation. The power response at -15°C and -20°C shows a deviation from that at the higher temperature. The power reaches a peak before decreasing briefly and then steadily rising above the first peak. This is related to the formation of ice along the surface of the MEA interfering with the delivery of reactant as a result of the resistance increasing and in turn the performance

of the cells can't maintain the desired operating range at the current density. The -25°C trial fails to start, as the suppressed temperature greatly affects performance.

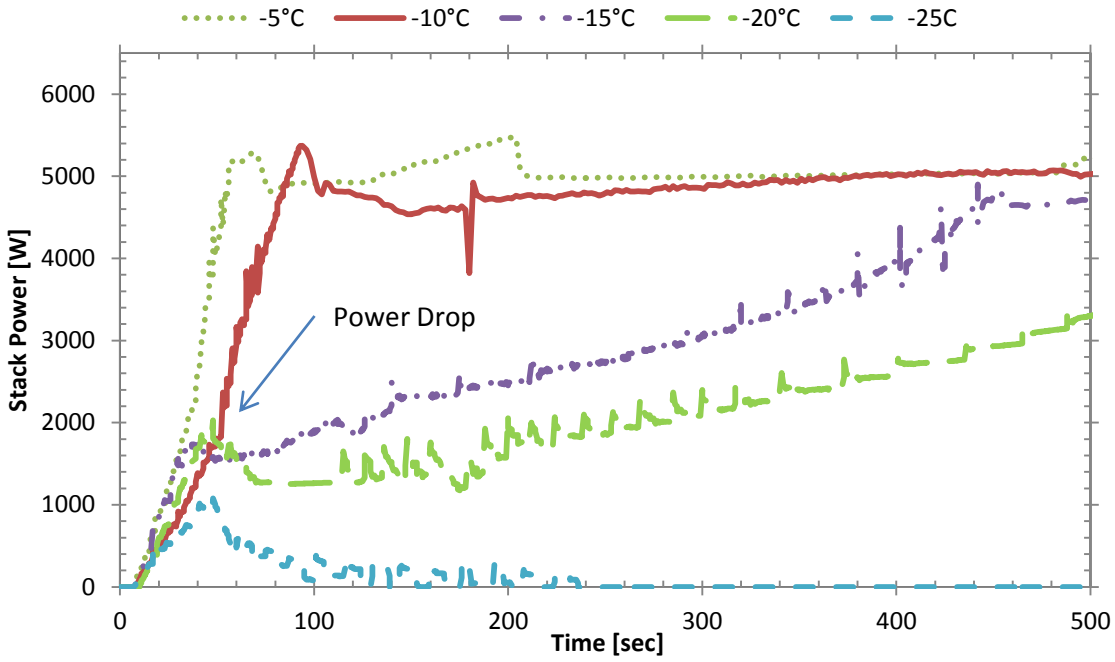

Figure 0-11: Start-up procedure initiation presenting power generation of various start-up temperatures against time

1.18.6. Failure to Start

The inability to operate the fuel cell stack arises due to the inability to maintain a constant current. When current is drawn from the cell the voltage drops. OCV be maintained at low temperatures for prolonged time even if the ability to deliver power is unattainable but not indefinitely. This shows that pathways for gas delivery may still exist but they cannot transfer reactant fast enough to enable start-up operation. Thompson *et al.* has presented findings about the time delay for OCV drop out by flowing gases in a stack at isothermal temperatures [7].

A start-up failure in a freezing environment is signalled by decreasing cell voltages either due to cooler temperatures or the presence of ice. Trials have shown that a single cell, end cell or middle cell can control whether a stack can be start-up.

A failed start-up can still be recovered while remaining in a freezing environment. A freeze start-up was attempted at -25°C, but failed. To determine if operation could still be recovered, the

environment was warmed to -10°C and start-up retried. The start-up trial (Figure 0-12) was successful and reached full operation, but performance was hindered by the residual water generated in the stack by the previous attempted start-up. Figure 0-12 shows a vast amount of fluctuations in cell voltages with the load being cycled on and off completely in order to maintain the minimum voltage. At around 1200 seconds into the start-up, performance increases which can be the results of a sufficient temperature in the cells melting the formed ice and allowing pathways for reactant delivery.

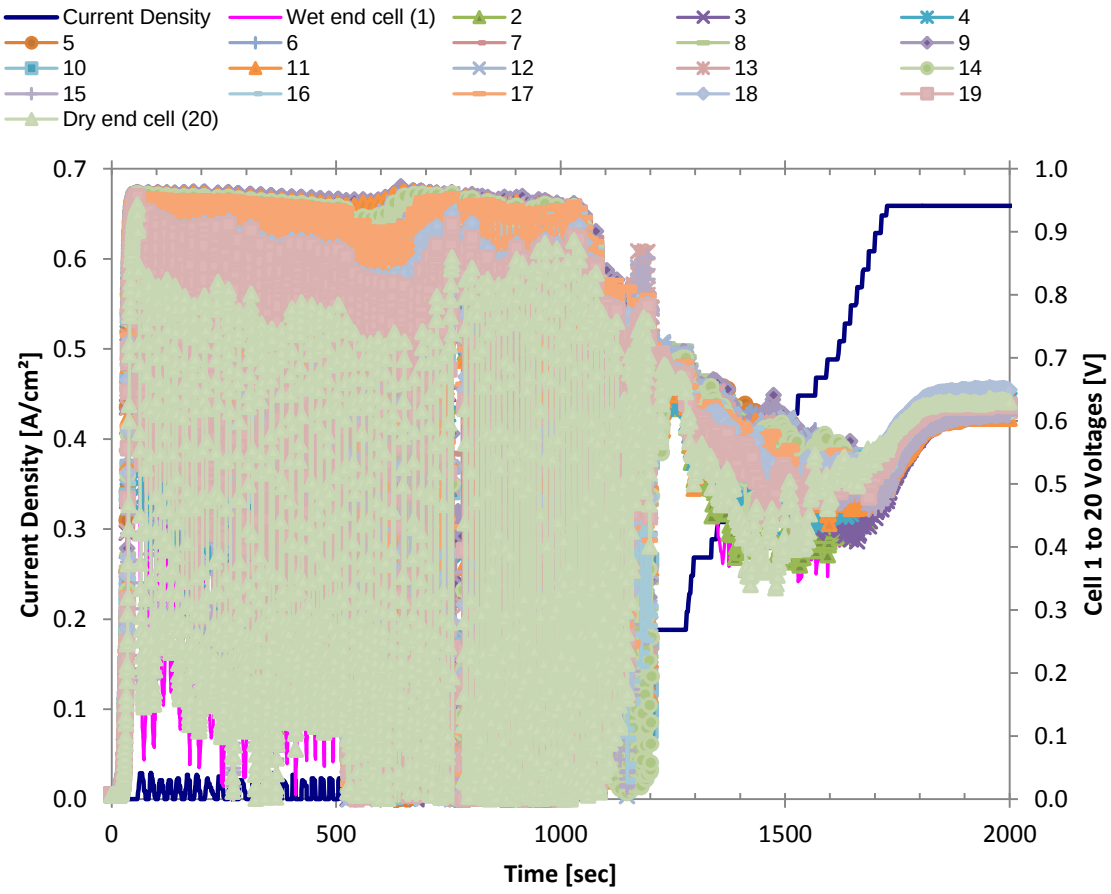

Figure 0-12: Start-up at -10°C after failed start-up at -25°C

Ice blockages can exist not only in the MEA but can build up along the channels in the bi-polar plates or in the return lines from the stack back to the FCATS. Freeze start-up trials have shown that a build-up of pressure on the exhaust can lead to the stack being shut down to prevent irreparable damage.

1.18.7. **End Cells**

The endplate is a large metal piece that supports the stack and maintains it rigid and compressed to prevent gas leakage into the surrounding environment. The endplate acts as a thermal sink to cool the end cells of the stack. Figure 0-13 presents the evolution of endplate temperature due to the large mass and the high thermal conductivity and heat capacity, considerable time is required before the endplates reach thermal equilibrium. From the figure, the temperatures of the endplates have stabilized only after 40 minutes. This is a typical trial result for the stack regardless of freeze temperature and start-up/shut-down procedure.

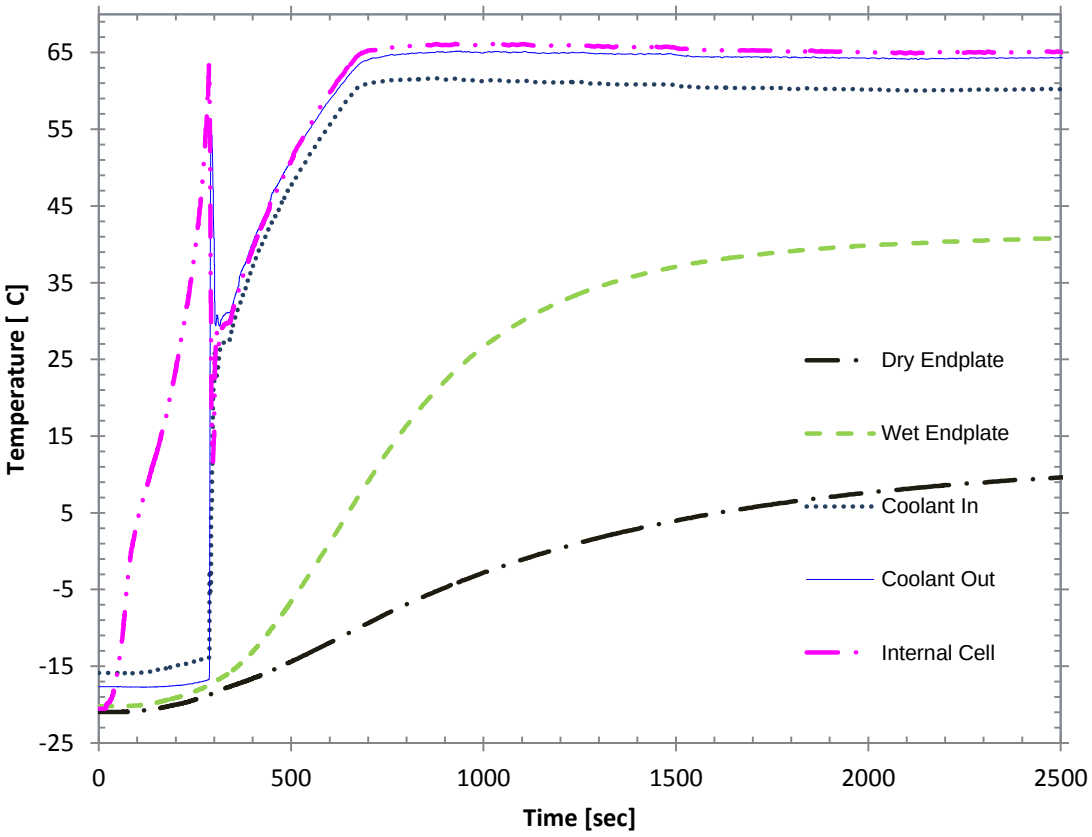

Figure 0-13: Stack temperature response at start-up

The voltages of end cells are lower than the others since they do not have a cell on either side to supply additional heat. Figure 0-14 shows the response of the cell voltages within the stack where cell 1 and cell 17 are the wet end cell and dry end cell, respectfully. The wet end cell operates at a lower voltage than the dry endplate cell due to the fact that it receives the coldest gas and has more thermal mass, due to the supply and return connections.

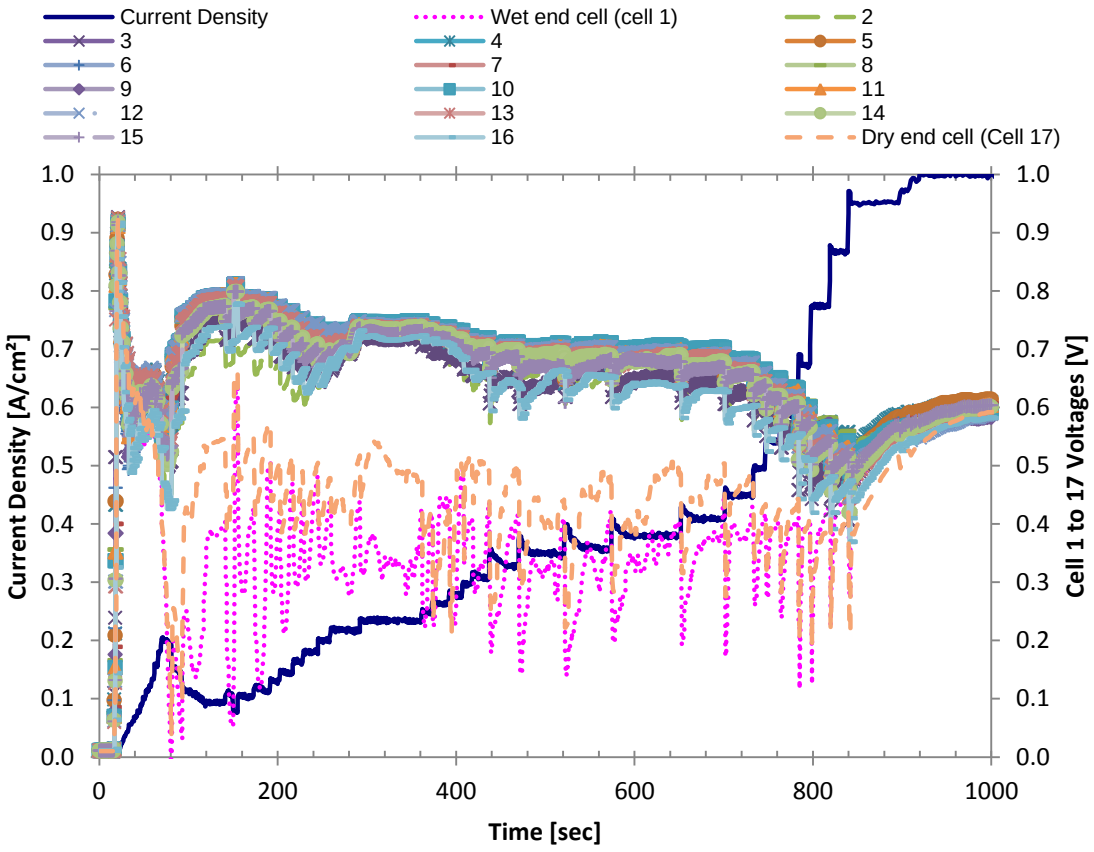

Figure 0-14: End cell performance during start-up at -20°C

1.18.8. **Results of Purge Stack Conditioning**

The purge of the stack is critical to freeze start-up performance. Increasing purge temperature or duration removes more water and gives the stack an increased ability to start successfully. Accordingly the effects of multiple purge rates, temperatures and types were investigated.

During start-up, the rate of power output will increase until an equilibrium is achieved and limitations in removal of water will hinder subsequent start-up. The decrease in proton conductivity from cell/membrane dehydration during the purge must be regained by the membrane before higher reaction rates can be reached. The reduction in water will make it easier for start-up to proceed from lower temperatures since the membrane contains less water.

In order to determine the start-up ability of the stack, a trial was conducted with the desire to remove as much water as possible without harming the stack components. The stack was operated at a high temperature in order to increase the amount of water leaving the stack during the purge. The following purge procedure was employed while monitoring the cell voltages. As the water was removed from the stack by purging with flowing dry gases, the amount of water hydrating the membrane decreased and caused the OCVs of the cells to drop. Reactant flows were then halted, decreasing the amount of purge time and gas required in comparison to previous trials.

A selected trial in an attempt to start-up at -10°C (***Figure 0-15***) shows that middle cells can control/limit start-up performance. Cell 16 and 19 control the start-up because their low cell voltage during potentiostatic start-up seeks to maintain a minimum cell voltage. This demonstrates that non-end cells can control the start-up due to inconsistent gas purge. This trial was conducted at a purge rate of 0.9 and 9.5 slpm $cell^{-1}$ for the anode and cathode, respectfully. Note, that these levels yield a lower purge in an attempt to save fuel gas and test limits of operation. A type A purge was conducted at a temperature of 27°C, as measured by the internal thermocouple. Cells 16 and 19 control the start-up because of the presence of ice. The maldistribution of gas flow during purge may cause water to remain in areas of the stack which can lead to this kind of performance.

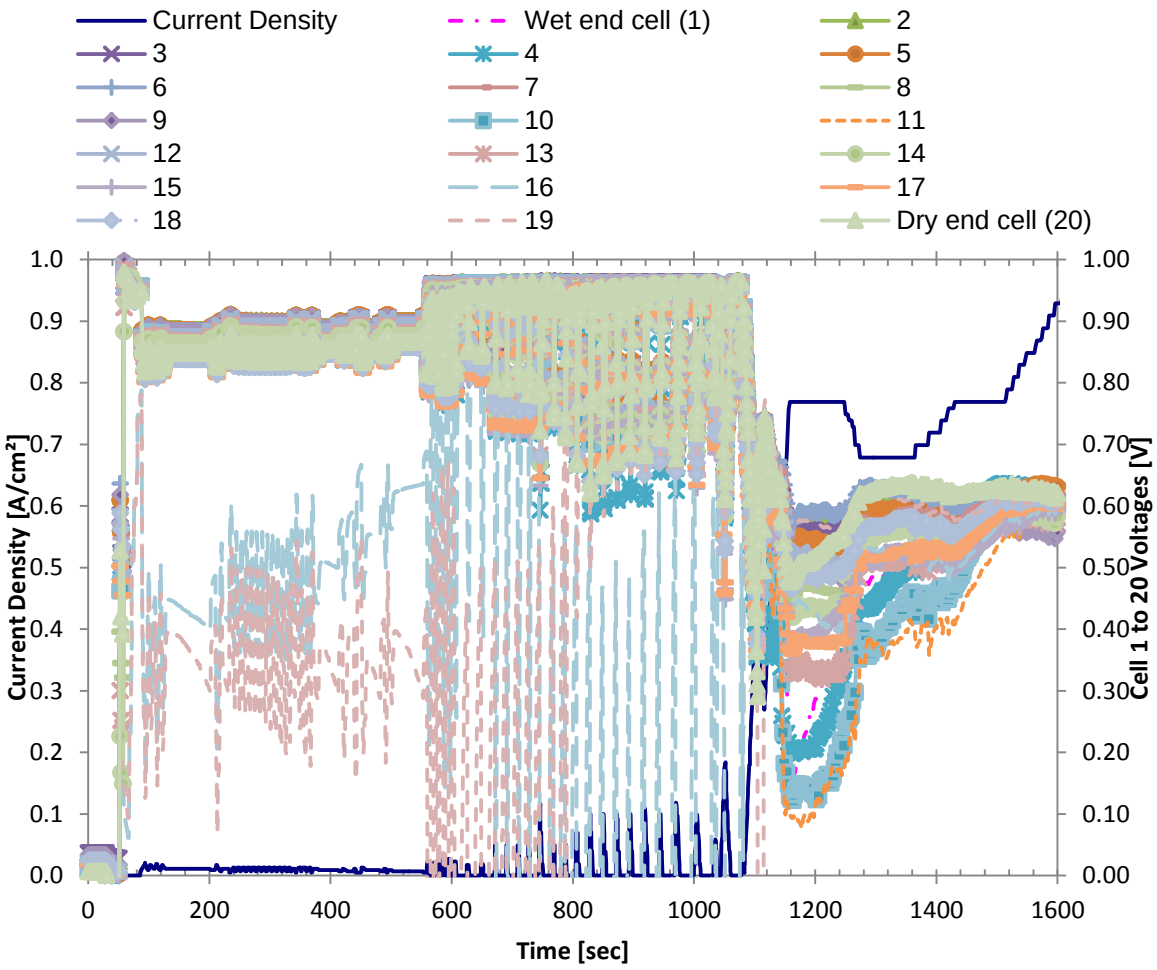

Figure 0-15: Middle cells limiting start capability at -10°C

The GDM selection may only allow for the removal of some of the water due to its hydrophilic properties, but more water may be removed from the stack at higher temperature.

Trial variations indicate that a point is reached where the lowest possible sub-zero temperature during start-up is limited by the amount of ice present and forming before the system could warm above freezing conditions. This shows a limit where a successful purge may be unable to be implemented for future operation. Note that the purge also drains the overall efficiency as it consumes reactants without generating energy.

1.18.8.1. Purge Type

The influence of purge type shows the effect the duration of purge flows through the stack has on performance. Electrodes were differentiated in order to determine if longer

purge time could be maintained through a single electrode and achieve similar or improved performance. Information presented in Table 0-4 shows the relation between purge type and the time to minimum stable power output.

Table 0-4: Summary of selected start-up trial purge type results at -20°C

Selected Start-up Label	Purge Type	Initial Flow Set Point [mA cm^{-2}]	Purge Temperature [°C]	Anode Purge Flow rate [slpm $cell^{-1}$]	Cathode Purge Flow rate [slpm $cell^{-1}$]	50% Power Minimum Start-up Time [sec]	100% Power Minimum Start-up Time [sec]
82	A	900	66.3	1.8	15.9	179	384
65	B	1000	62.6	1.8	16.0	237	422
71	C	1000	66.1	1.8	16.0	251	434
74	D	900	65.7	1.8	15.9	212	390
35	E	900	44.2	1.4	12.0		
85	F	900	66.4	1.8	16.0	259	464

Comparison of purge A, B and C shows that increasing the purge duration increases the start-up time at the current conditions. A possible explanation is that as more water is removed from the stack, resistance increases. The purge A trial shows the best performance reaching 50% power in 179 seconds.

The effect of reducing purge time was examined in trials E and F. A stable start-up could not be achieved in trial E. On the other hand, a successful start-up was attained in trial F. The resulting savings in fuel gas may be offset the increased start-up time required to reach full performance. Comparison of Purge C and D shows that a reduction in anode purge time (Purge D) decreases start-up time by 40 seconds. Conducted purge trials may be overly drying the PEM or removing insufficient water affecting the start-up performance. This shows that there is an optimum amount of water that has to remain within the cells to enable rapid start-up.

1.18.8.2. Purge Temperature

The number of successful/failed start-ups depending on purge temperature is shown in Figure 0-16. Operating at a lower temperature purge does not improve the ability of the stack to start-up from suppressed temperatures. Greater water removal will increase

the start-up capability from lower temperatures, but may compromise performance. Too much water removal causes a decrease in cell performance and an increase in start-up time from warmer freezing temperatures or normal operating temperatures.

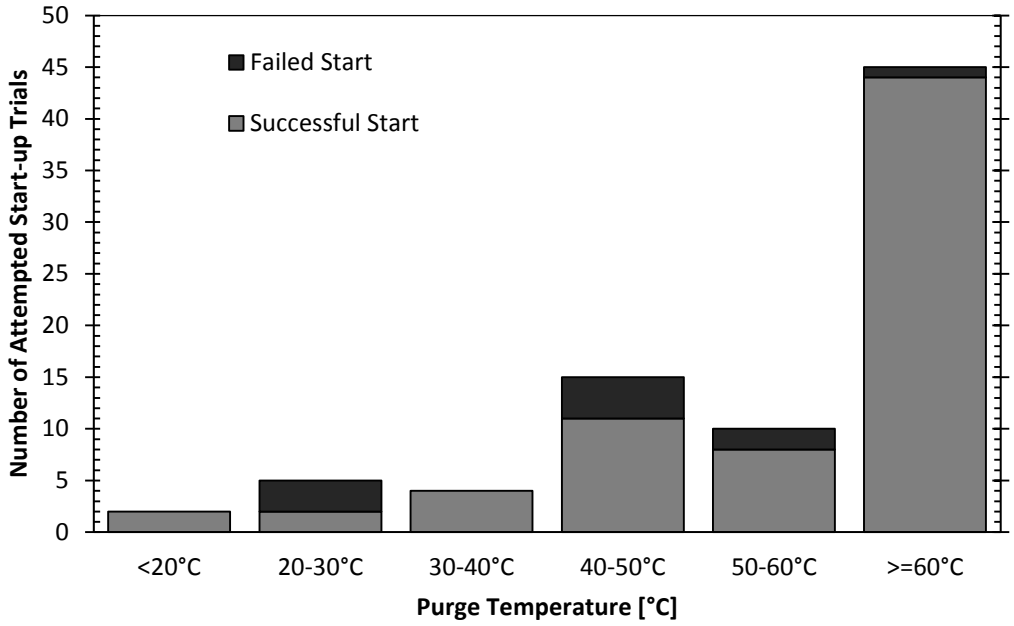

Figure 0-16: Freeze stack start-up ability by purge temperature

Selected results of the conducted trials have been summarised in Table 0-5. The trials shown are all conducted using a Type A purge, start-up flows at 900 $mAcm^{-2}$ and a freeze start-up temperature of -20°C. The result for Trial 45 is a specially selected case as the purge temperature is manually elevated.

Table 0-5: Selected trial results at -20°C showing purge temperature effect on start time

Start-up Temperature	Selected Trial Label	Internal TC During Purge [°C]	Cathode Outlet during Purge [°C]	Time to 50% Power [sec]	Time to 100% Power [sec]	Anode Purge Rate [slpm cell^{-1}]	Cathode Purge Rate [slpm cell^{-1}]
-5	20	26.8	19.5	904	1416	0.9	9.5
-5	19	40.1	38.7	72		0.9	9.5
-10	42	20.7	20.1	FAILED		2.7	15.2
-10	87	65.3	58.8	55	73	1.8	16.0
-20	36	22.7	22.6	FAILED		2.7	15.1
-20	33	24.0	15.7	FAILED		1.8	16.0
-20	64	49.0	44.8	1046	1530	3.2	18.1
-20	90	56.1	51.6	424	626	1.8	16.0
-20	31	59.1	53.2	268	581	1.8	16.0
-20	53	65.2	58.1	284	555	1.8	16.0
-20	54	66.8	58.4	229	474	1.8	16.0
-20	45	68.0	69.0	500	755	0.9	9.4

The results in Table 0-5 indicate that a low temperature purge may not allow a successful start-up and increasing purge temperature decreases time to attain the rated power. The results at -5°C, trial 19 do not present a time to 100% power, this is due to an equipment error resulting in shut down before it could be reached. For a successful start-up at -20°C a minimum purge temperature of 55°C is necessary. A point is reached at which purge temperature and purge rate causes a delay in start-up time, as shown by trial 45. Trials 53 and 54 show there is variability between runs. This variability may be the result of inconsistent water being removed across the stack resulting in ice being present prior to start-up.

Purging the stack at 49°C or below leads to an unstable start-up unless the load is ramped off entirely before sufficient temperature has been generated. The stability brought by purge temperature was only found after multiple trials were completed. Start-up was possible initially, at lower purge temperatures but after several freeze exposures this capability was lost. The changes in performance by purge temperature may have resulted from morphology changes to the structure of the GDM. These possible changes may have caused more water to be retained in the stack. The results in

Table 0-5 also enable us to examine start-up stability. If a low temperature purge is used, the load during start-up can be unstable (likely to require complete removal of load on and off).

1.18.8.3. Purge Rate

The effect of the rate of purge is examined in order to decrease the time necessary to reach full power performance by changing the amount of flow through the stack during purge. Experiment rates are listed in Table 0-4 and results presented below in Table 0-6. Trials have not been completed at all freeze start-up temperatures. It is important to assess the variations of start-up time attained with respect to purge temperature, type and the start-up flows during the trials.

Freeze start-up trial 29 at -5°C was halted during operation due to safety concerns with high pressure flows. The -5°C trials show that an increase in purge rate can improve the start-up response up to a certain point, depending on the temperature during purge. Overall the table indicates the results that an increase in the rate of purge decreases the time required to reach power production. Due to constraints at Hydrogenics facility, the complete examination of purge rate and the interaction with the necessary purge temperature and duration is incomplete.

Table 0-6: Data summary experimental results purge rates

Freeze Temperature [°C]	Selected Trial	Anode Purge Rate [slpm cell^{-1}]	Cathode Purge Rate [slpm cell^{-1}]	Start Flows [mAcm^{-2}]	Purge Type	Purge Temperature [°C]	Cathode Purge Duration [sec]	Anode Purge Duration [sec]	50% Power Min Start Time [sec]	100% Power Min Start-up Time
0	27	1.8	16.0	10	Purge A	59.2	150	150	53	65
-5	1	0.9	9.5	900	Purge A	40.1	150	150	56	366
	23	1.8	16.0	900	Purge A	59.3	150	150	36	48
	25	2.7	15.0	900	Purge A	39.7	150	150	40	190
	29	5.0	26.0	770	Uncontrolled	64.9	Uncontrolled		45	59
-10	18	0.9	9.5	770	Purge A	39.6	150	150	268	773
	87	1.8	16.0	900	Purge A	65.3	150	150	55	73
	2	2.7	15.0	10	Purge A	40.3	150	150	143	223
-15	17	0.9	9.5	770	Purge A	40.0	150	150	890	1084
	11	1.8	16.0	10	Purge A	34.4	150	150	197	772
	41	2.7	15.0	900	Purge A	24.0	150	150	126	408
-20	8	0.9	9.5	900	Purge A	68.0	150	150	500	755
	9	1.4	12.0	900	Purge E	44.2	90	90	Failed	
	54	1.8	16.0	900	Purge A	65.7	150	150	507	780
	80	1.8	19.0	200	Purge A	66.8	150	150	239	515
	81	2.7	15.0	10	Purge A	40.3	150	150	912	1238
	85	3.2	18.0	1000	Purge A	49.0	150	150	1046	1530

1.18.9. **Leak Testing**

To test the integrity of the internal stack components (i.e. PEM and GDM) a mechanical pressure test was completed. The test is carried out on three different compartments to detect a leak from the stack to the environment, between electrodes, or from the coolant to an electrode. The compartment in question is isolated at a specified gas pressure and is monitored for any pressure build up.

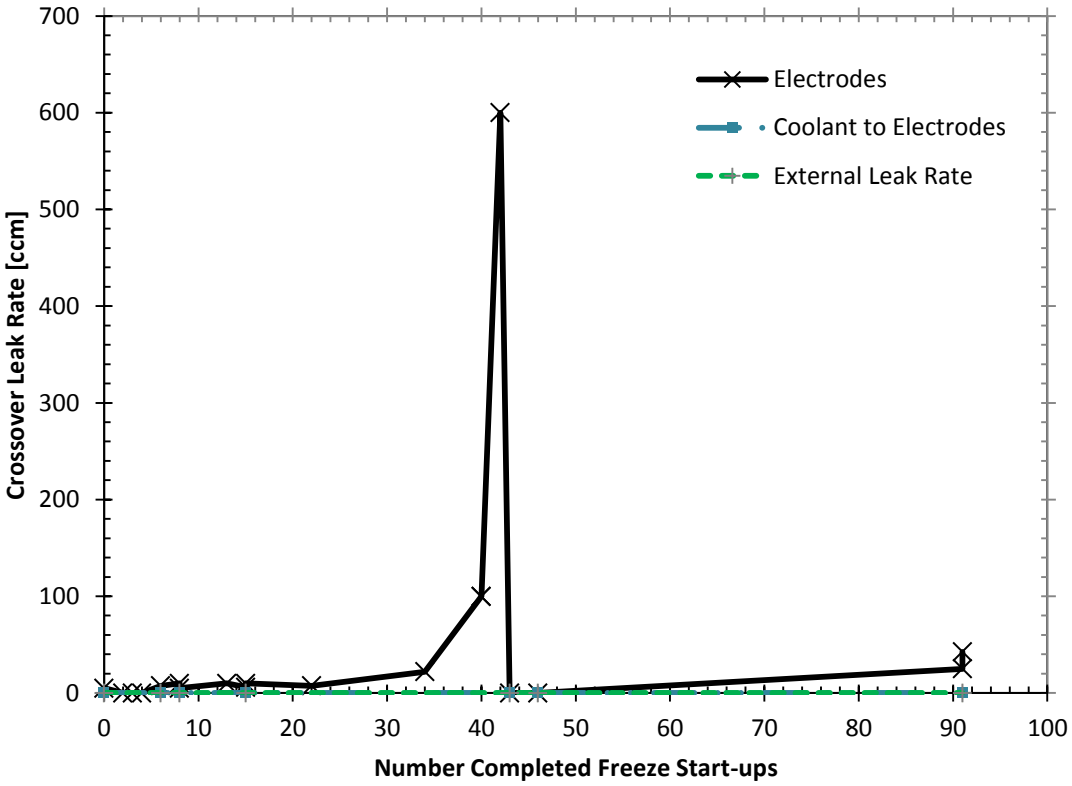

Figure 0-17: Stack gas crossover leak rate with start-up freeze trial number

From Figure 0-17, we can see that the coolant to electrode and external crossover leak rates never affected by freeze start-up trial. This shows that no losses occur as a result of thermal cycling in these two areas. The electrodes however do show a high crossover rate beginning around the 34th trial when a failure occurred during a cyclic freeze start-up because the stack refreezes with a low temperature purge. At the 39th trial, an error occurred with the FCATS preventing voltage measurements and gas flows across the stack for around 33 hours. High gas flow for prolonged duration is damaging to the stack. At trial 40, the stack was shut-down due to

the loss of nitrogen supply to the FCATS equipment. At the 41st trial, poor performance with increasing load resulted due to high gas crossover. The crossover rate was measured at 0.6 $L \cdot min^{-1}$ resulting in an end-of-life (EOL) condition. Analysis of the system led to the idea that three specific cells contributed to the crossover. The stack was disassembled and the three cells were removed. The rebuilt stack was reassembled without these three cell and testing continued. The effect of freezing the stack in an already conditioned state means that there may be no direct degradation to the mechanical properties. The crossover leak failure may not have been related to a single event but to a series of events associated with the stack freezing in an unconditioned state.

1.18.10. **Degradation**

Polarization curves were collected initially and after freeze start-up trials. Fuel cell components may initially resist degradation that may arise as a result of changes in surface morphology, hydrophobic ability of the components or amount of water present at shut-down. Figure 0-18 shows an example of degradation that can occur after several freezing exposures, freezing start-ups and freezing with water present.

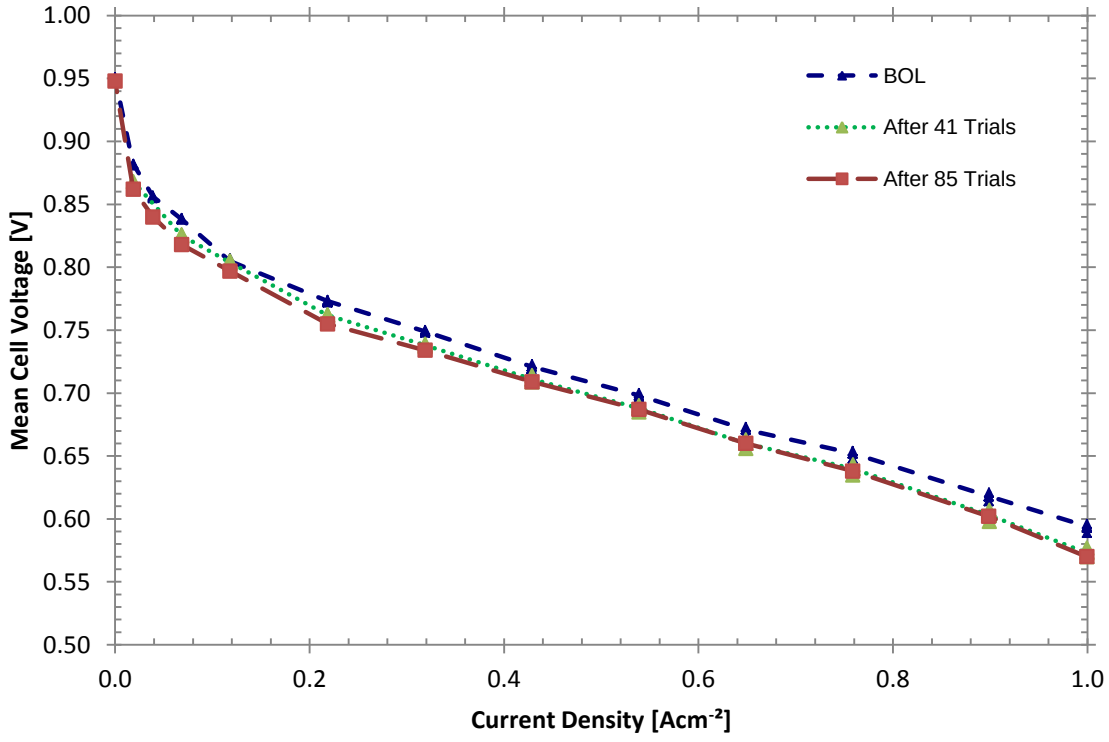

Figure 0-18: Polarization curve of stack by completed freeze start-up trials

Comparison of the plots within Figure 0-18 show the beginning-of-life (BOL) which is the original stack performance against polarization curves conducted after freeze testing. The stack performance degrades as a result of the testing by the decrease in output potential at a specified current density. Performance in the ohmic and concentration overpotentials is affected by freeze testing. The 41st trial denotes the last successful operation of the stack before the leak crossover causes the EOL condition. Rebuilding the stack and progressive testing showed little loss in performance.

The freeze start-up trials shown in Section 1.18.4 shows the response of freeze start-up. The cell voltages displayed show some low values due to the aggressive start-up strategy employed to warm the stack as fast as possible. Low cell potential due to localized reactant starvation can lead to the loss of carbon support for the catalysis and increase degradation through the cells [51,52]. The stack was also exposed to a prolonged duration at OCV conditions as a result of equipment failing to measure any cell voltage while gases were flowing across the electrodes. The gas flowed for a period of 33 hours before halting. The prolonged result of open circuit conditions can cause drying of the membrane and degradation to the stack [53,54].

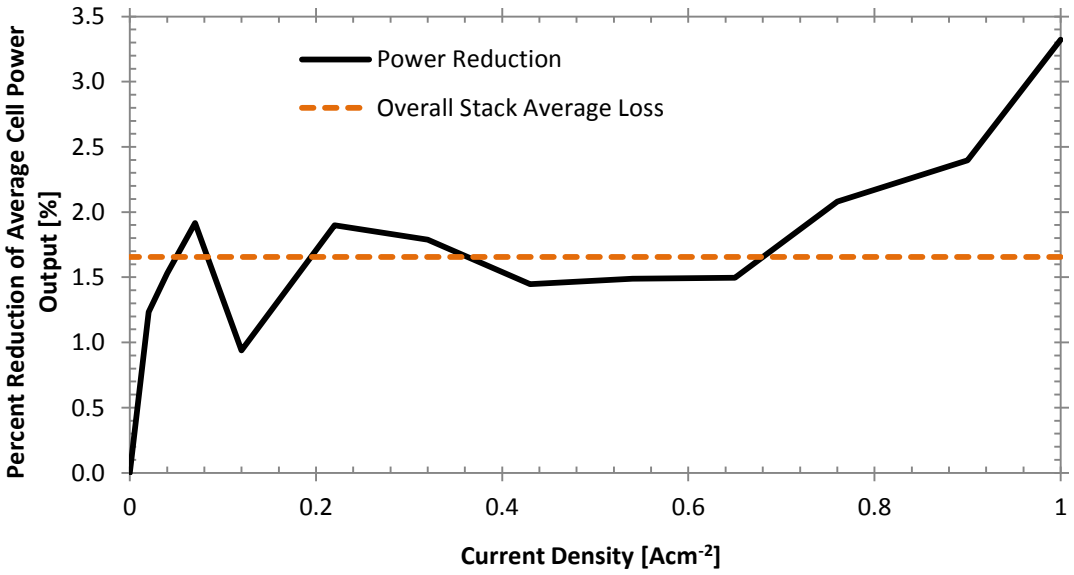

Figure 0-19: Average percent reduction in performance from polarization curve

The reduction in the performance from BOL and the last polarization curve is shown in Figure 0-19. The loss is greatest at the highest current densities where more mass transfer limitations

occur. The reduction of the stack performance accounts for 1.6% on average over the range of the operating current densities.

The degradation may also be reflected in steady state data from the polarization curves (Figure 0-20). The rate of degradation can be inferred by the reduction of the performance of the cells by the progression of the day of operation. In total the cumulative running time of the stack is around 280 hours which includes operation after the stack was rebuilt. A variation occurs on the 19th day that due to deviations in the environmental chamber temperature set point deviated from normal operation. The set of data shows some points missing at the 62nd polarization curve as a result of a manual safety shut-down.

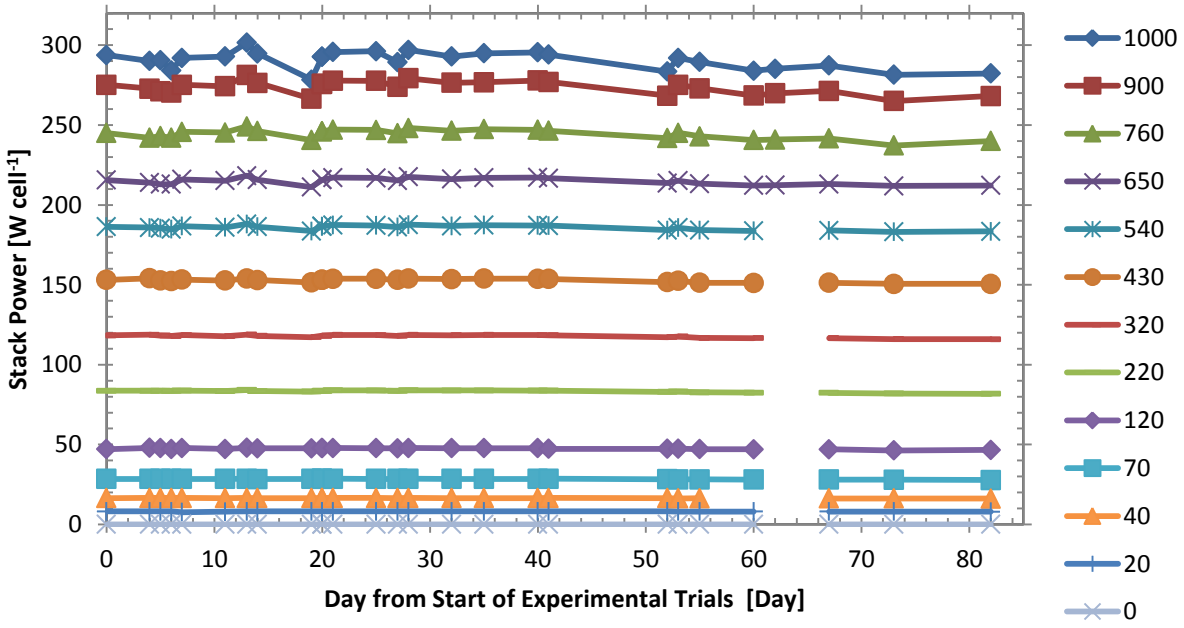

Figure 0-20: Average stack power output by current density (mA cm^{-2}) measurements from PC versus initial start day of the experiment at multiple current density measurements

Decay voltage measurements for Gore™ Primea® series 57 MEAs are published [55]. We can directly compare the results of accelerated freeze start tests to normal decay rates. The operation of the stack varied in current density and the published decay rates at 200, 400 and 800 mA cm^{-2} are 28, 30 and 28 µVhr^{-1}, respectfully. Any operation above 800 mAcm^{-2} will have a decay rate of >50 µVhr^{-1}. Operation of the stack from freezing exposure has resulted in an average decay rate of

53.7 $\mu V hr^{-1}$. This decay rate aligns with the normal rate of the stack since stack operation went above 800 mA cm^{-2}.

1.19. Ex-situ Investigation

Freeze testing of the stack and the vigorous stack start-up operations accelerated gas crossover. Diagnosis determined that three cells contributed to the high crossover leak rate. The cells were removed and further analyzed by visual inspection and by scanning electron microscopy (SEM).

1.19.1. Visual Inspection Results

The cells removed from the stack were examined visually, by removing the GDL to expose exposing the MEA. Removal of the GDL by peeling it off from the membrane was generally very easy. The fresh MEA surface appears black as a result of the carbon catalyst support. Visual examination revealed various pinholes and larger holes present.

The freeze-cycled, freeze-started PEM in Cell 15 is shown in Figure 0-21. The figure was generated by placing the MEA on a scanner bed and scanning the image. This method shows the larger portions of the MEA that has been lost but fails to note the finer pinholes present. The larger holes present in the MEA are indicated. Once smaller pinholes have formed the may grow as a result of local hot spots from the unrestricted reaction to occur without powering an external load (i.e. by simple combustion reaction between H_2 and O_2 in air). The combustion reaction generates local hot spots and burns away sections of the MEA by the increase in temperature. As the fuel mixes and oxidizes, the temperature around the pinhole rises and causes it to grow larger.

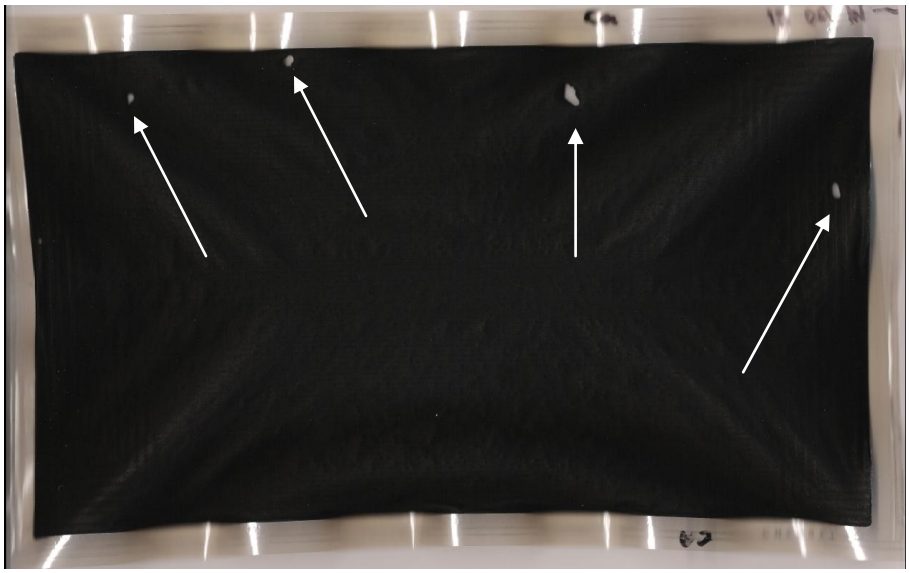

Figure 0-21: Visual image of freeze start-up cycled MEA

The image can be better captured by using a light table with a digital camera. Figure 0-22 shows an expanded image of the holes present in the MEA. The larger holes in the MEA vary in diameter but measure approximately 5 mm to 8 mm. Finer pinholes can be seen around these larger areas.

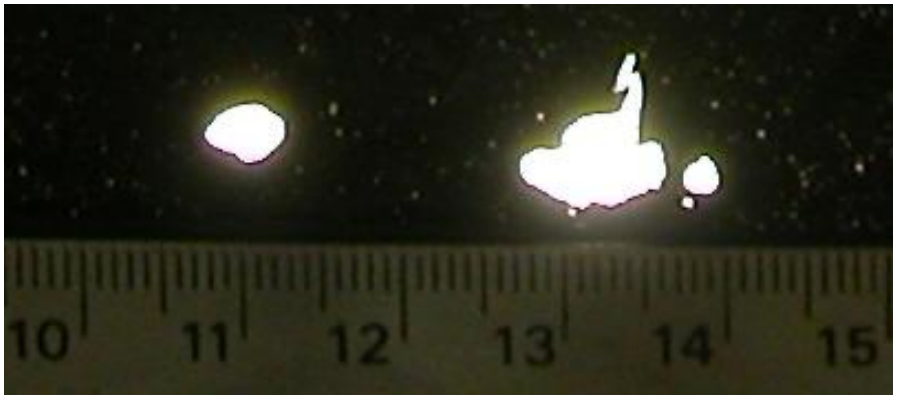

Figure 0-22: Freeze start-up cycled MEA focusing on formed pinhole

The accelerating freeze-cycled testing and vigorous start-up operation of the stack causes an increase in the rate of degradation. The central region of the MEA in Cell 11 is shown in Figure 0-23. The large number of pinholes set against the black catalyst support shows a “starry night sky”. Any spot that is not black corresponds to a pinhole.

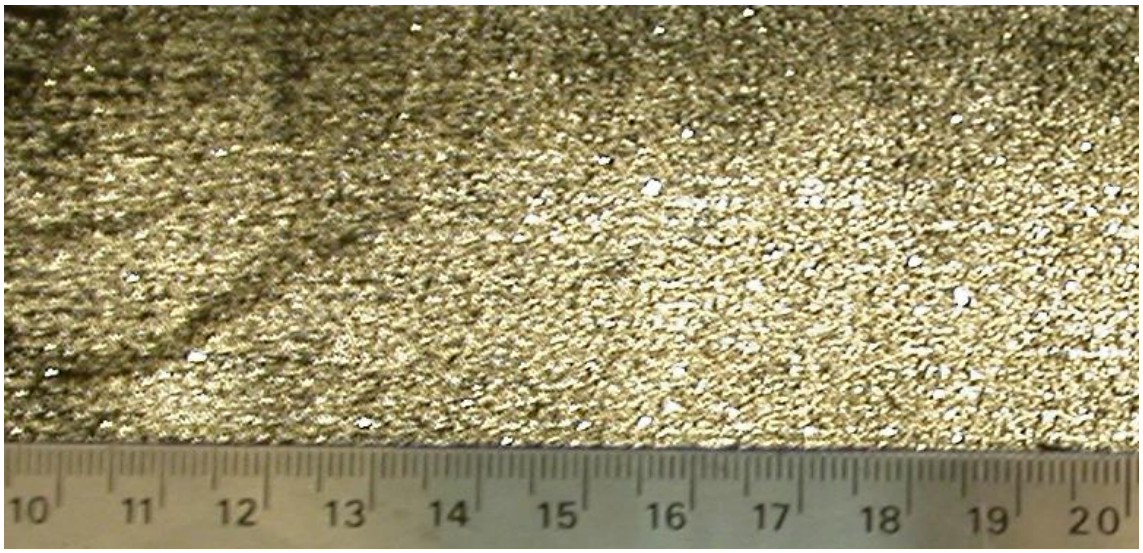

Figure 0-23: Visual image of cell 11 captured by light table, locally emphasised for smaller pinholes

Figure 0-23 shows many pinholes that form along cell 11 membrane. The examination of the pinholes shows that they follow a pattern in the PEM. Pinholes are grouped into regions near open channels (i.e. no land support) corresponding to the bipolar plate gas delivery field configuration. Ice may form under the lands and protect these areas from pinhole formation. The increase of gas reactant delivery at the open channels may have accelerated the local reaction and escalated degradation due to the generation of current density during sub-zero freeze start-up.

The catalyst support was shown to be missing around the outer edges of the MEA and only remaining the central membrane (i.e. catalyst lost). This may occur due to frost heave formation in these local regions. As an ice lens or a frost heave occurs, the freezing of pooled water generates an expansion force that increases stress that dislodges portions of the membrane surface. The inlets receive the coldest flows and the highest concentration of oxygen. This means rapid and early formation of ice before the rest of the cell or stack can warm.

1.19.2. **SEM Results**

The affected cells that were removed from the stack were sampled at various positions and analysed by SEM. Samples were prepared by cutting out a small section from the MEA in an area of interest. Selected regions of the membrane examined: inlets, outlets and central positions. Two types of samples were prepared and tested, 1) surface, and 2) cross-sections. Surface images can display how the morphology of the catalyst layer surface may be affected. Cross-

section images present information about catalyst migration, cracking, delamination of the PEM and through-plane morphology changes. Cross-sections of the MEA were prepared by cutting out a rectangle measuring approximately 1 cm x 1-2 cm. The sample was immersed in liquid nitrogen to rapidly freeze the sample. The frozen MEA section was then snapped into two pieces with two tweezers. A frozen sample is easy to cleanly fracture and provides a level image for the microscope to capture.

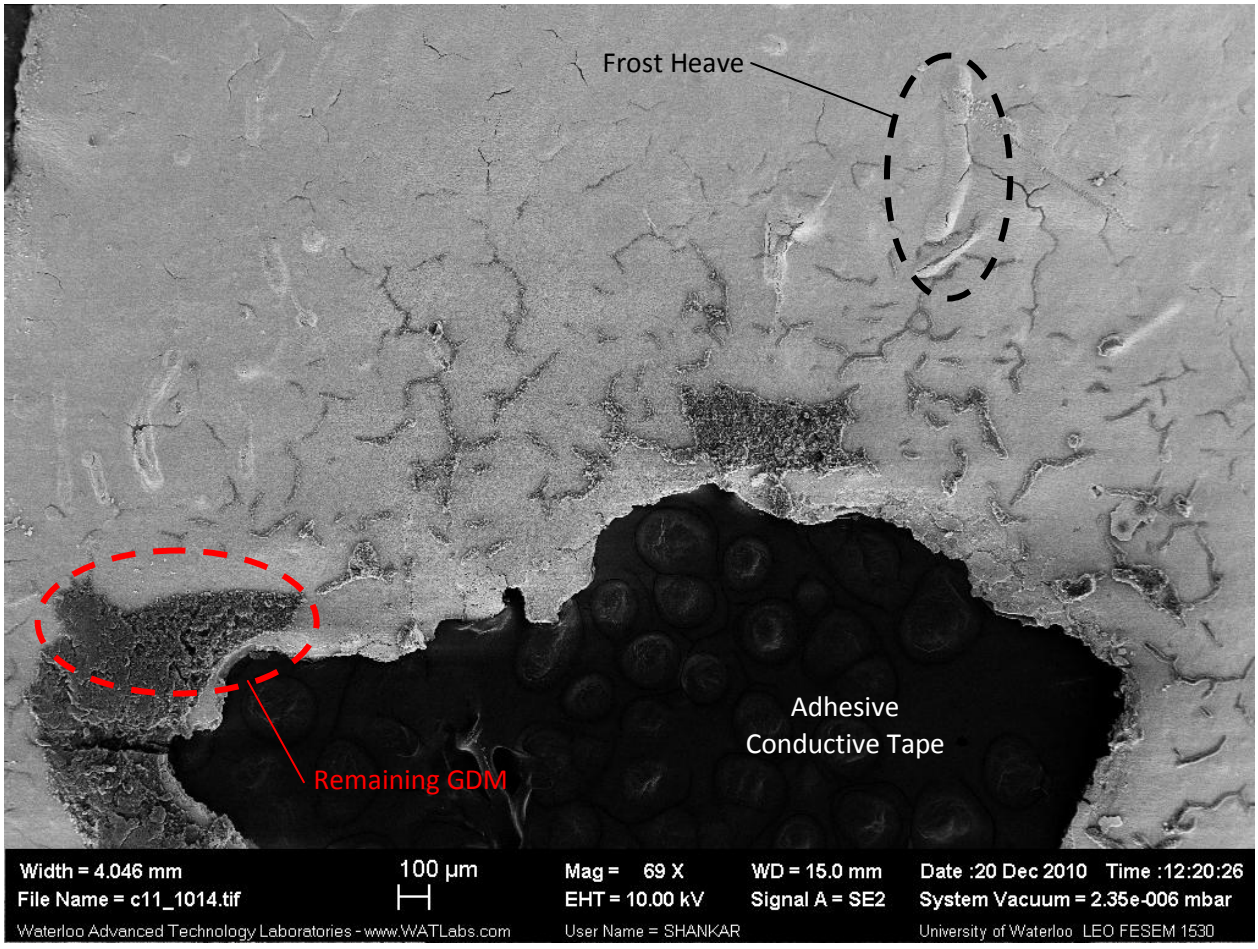

Figure 0-24: SEM surface near a pinhole

Figure 0-24 shows an enlarged view of a pinhole. The tape used to adhere the sample can be seen in the lower central black area. Some pieces originally from the GDM that have been left as a result of fusing and/or burns to the MEA, appear near the pinhole that may have resulted from higher temperature exposure. Fractures in the CL form near the pinhole, while evidence of CL lifting or bubbling due to frost heave formation and delamination appear further away.

A fresh un-used sample of the GORE™ PRIMEA® Series MEA is shown in Figure 0-25. The MEA has several characteristics of note: it is composed of five layers and is symmetrical. The layers include an outer catalyst layer, an ionomer layer and the central reinforcement. The ionomer layers and the reinforcement make up the membrane of the PEM, and combine with the anode and cathode CL defines to make up the CCM.

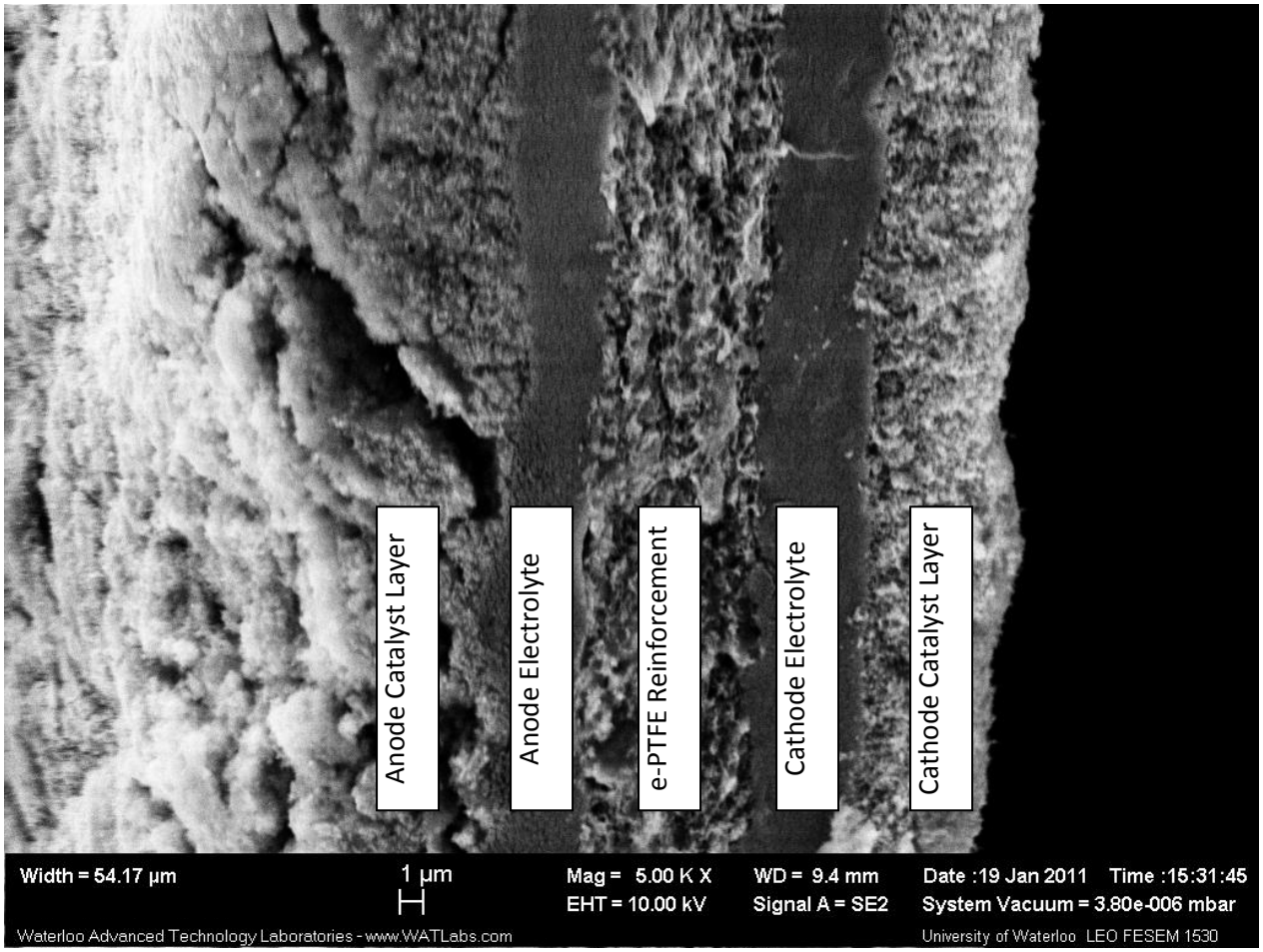

Figure 0-25: SEM cross-section of fresh GORE™ PRIMEA® Series MEA

Figure 0-26 shows the cross-section of the MEA in Cell 15. The cross section shows evidence of delamination between the CL and the electrolyte. Cracks in the catalyst layer appear where water may pool during operation and freeze cycling. This area may be a likely location for an ice lens to form. A large crack (black arrow in figure) runs through both the CL and the electrolyte into the e-PTFE reinforcement. In Figure 0-26 A) a region in which expansion between the CL and electrolyte has occurred is noted with a circle. Figure 0-26 B) shows the area of interest in higher magnification. This expansion could be the result of frost heave formation. If this expansion occurs between two different layers, then it leads to delamination. A frost heave

increases the pressure in the through-plane and lateral positions of the membrane forcing an expansion. The increase in pressure along the membrane may have compressed the ionomer and e-PTFE and caused the cracking of the CL, delamination and the non-uniformity in the e-PFTE layer.

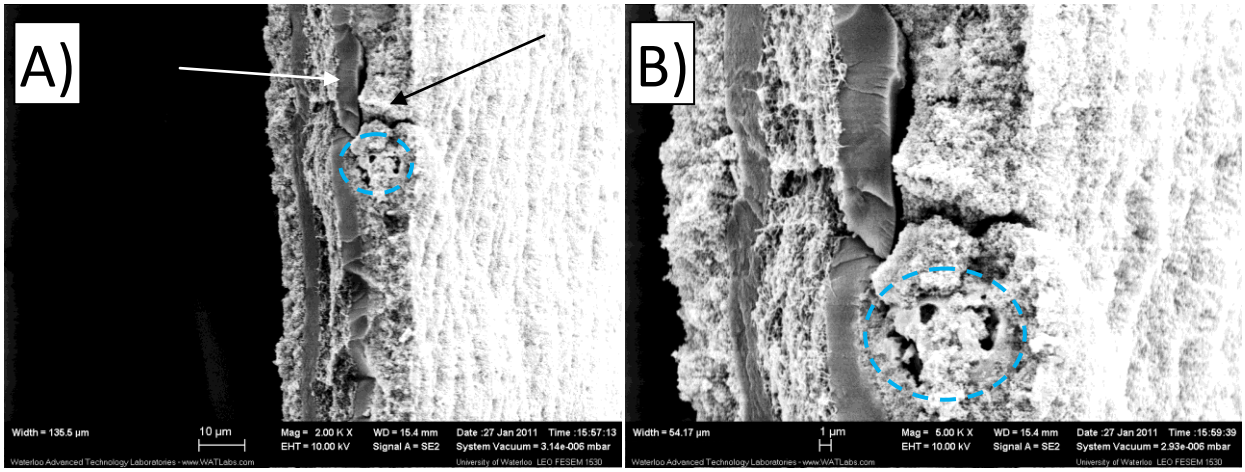

Figure 0-26: SEM cross-section image Cell 15, A) magnification at 2000x showing overall decay present, B) increased magnification 5000x centred on delamination and frost heave formation

Figure 0-27 below shows a prepared cross-section from Cell 16. The image shows that the CL on the left has delaminated and separated from the membrane. The e-PTFE reinforcement of the membrane appears to have expanded into and through the electrolyte. The expansion could result from a frost heave expansion inside the PTFE strands. PTFE has low wetting contact angles and is classified as a non-wetting substance. This should facilitate removal of water but it will not prevent any remaining water from freezing in the structure. Lower temperatures can also cause water to be expelled by the resulting contraction of the polymer. This water may lead to a frost heave between the electrolyte layers. Cycling may allow for the continual occurrence of these phenomena and lead to the structures such as in Figure 0-27.

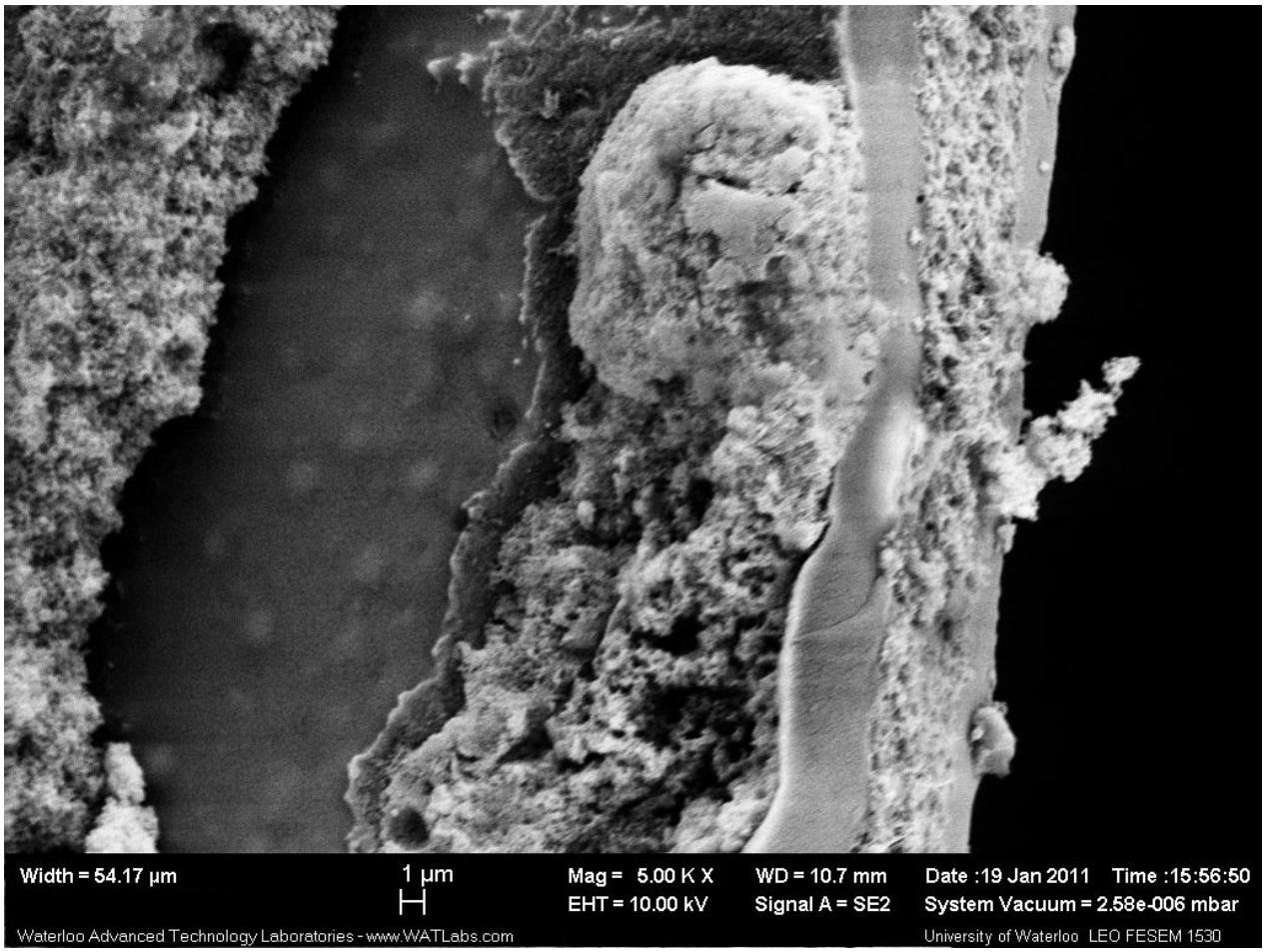

Figure 0-27: SEM cross-section cell 16 showing expansion of e-PTFE through electrolyte and catalyst layer delamination

Figure 0-28 below shows similar characteristics of the above figure, the loss of CL around an area where the expansion due to a frost heave has caused delamination of the surrounding area and expansion of the pores in the CL. The expansion appears to have expanded the pores in the CL and caused it to expand into the electrolyte layer. The non-uniform thickness of e-PTFE reinforcement, electrolyte and CL (on left) may occur as a result of the forced expansion causing deformation of the membrane.

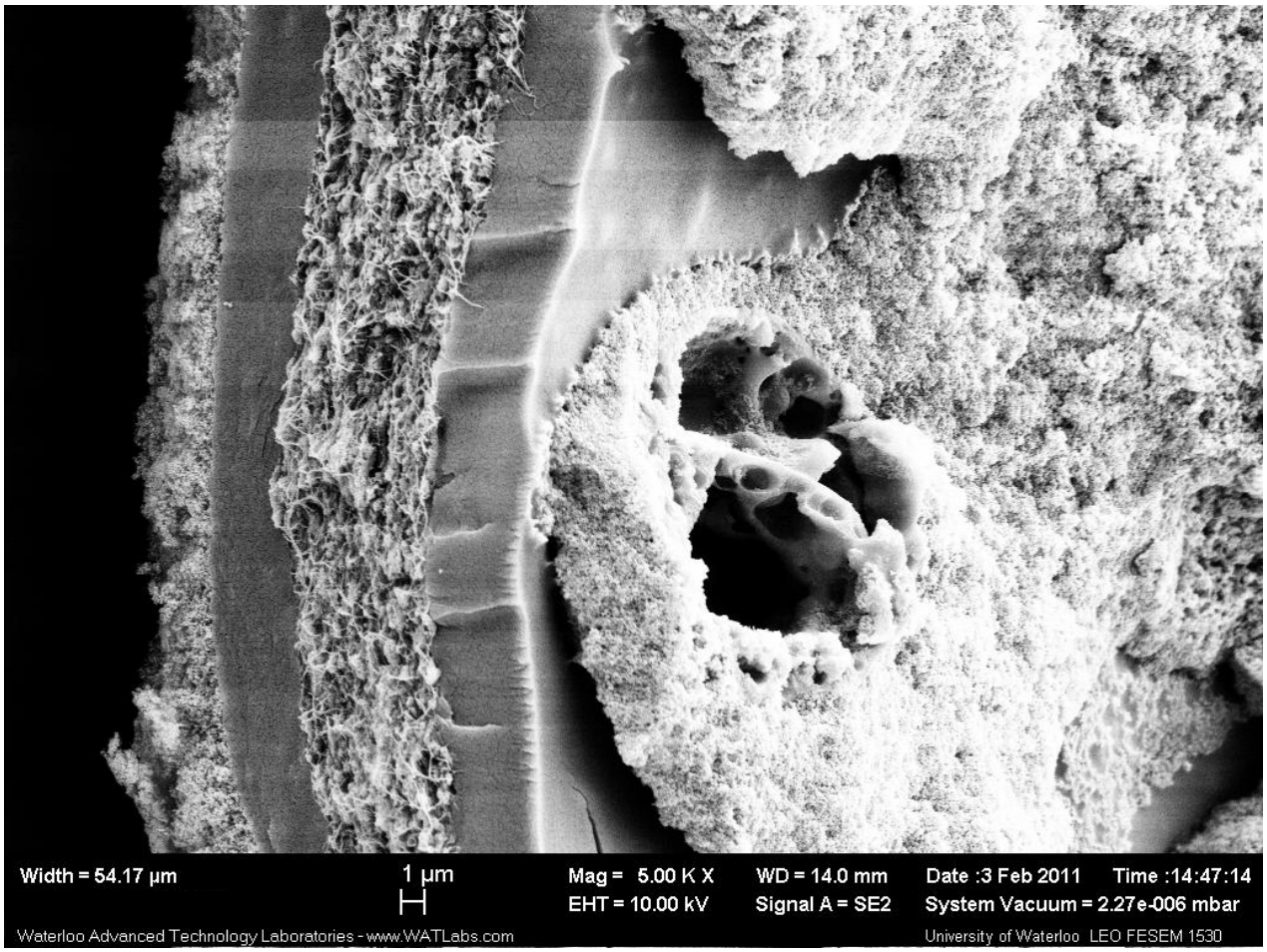

Figure 0-28: SEM cross-section of cell 16 with hole through catalyst layer

CONCLUSIONS & RECOMMENDATIONS

1.20. Conclusion

In order for fuel cells to be adopted by industry and fully applicable, they must meet the requirements of within our environment. The ability to start-up in freezing temperatures is a practical application for both mobile and stationary fuel cell installations. Minimization of start-up time and performance loss increases product durability, life and ease of implementation.

The effect of freeze start-up on PEMFC was examined by various methods to determine the ability to start-up and resulting performance of the stack without assistance. Factors associated with the start-up procedure are gas reactant flows, start-up load profile, point of coolant activation, shut-down purge duration, shut-down purge temperature, shut-down purge rate and start-up temperature. The damage that results due to sub-zero exposure may be reduced by removing water prior to shut-down. Water generated during start-up in freezing temperatures may lead to the formation of frost heaves and to delamination of the MEA. Delaminations result in permanent degradation which causes performance loss and ultimately cell failure. The current purge method examines the effects of circulating dry reactants and removing residual water by evaporative gas flows.

A balance occurs between freeze start-up temperature, purge temperature and purge rate on their effect on the start-up performance. Increasing water removal improves start-up performance at lower temperatures, but decreases start-up performance from ambient (non-freezing) temperatures.

1.20.1. Freeze Stack Start Operation

Unassisted start-up shows that the response of the cells in generating power is diminished at lower temperatures. A freezing temperature exists below which the stack is unable to start, due to slow electrode kinetics and the formation of ice that blocks reactant. A failed start-up may still be capable of starting while remaining at freezing conditions but at a warmer temperature.

During start-up, end cells exhibit the lowest performance since they operate at lowest temperatures. If stack purge occurs homogeneously across the cells, the end cells will control the maximum start-up load imposed on the stack during start-up.

1.20.2. **Freeze Start-up Procedure**

Examination of freeze start-up allowed several successful freeze start-up procedures to be developed and implemented with varying degrees of success. Here are improvements that can be made in general to improve the overall start-up procedure at sub-zero temperatures:

- Increasing initial gas reactant supply improves the start-up performance and the rate of power generation. This should be increased to the point where a balance is achieved between the removal of product water and the cooling effect of the incoming gas.
- The start-up capability of the fuel cell stack is temperature-dependent. If previous stack operation doesn't enable full temperature operation freeze start-up will be limited and hindered by remaining water.
- The lowest performing cells will control start-up. A controlling cell will either have water remaining from the purge-conditioning process or those cells that are the coldest.
- Delaying the activation of coolant, increases the rate of temperature rise until a point where dehydration may occur. At higher initial temperatures, ice melts which will result in improved gas transfer and distribution within cells.
- Upon coolant activation cell temperatures will decrease causing a reduction in cell performance.

1.20.3. **Purge Stack Shut-down Conditioning**

The ability to start stack operation is highly dependent upon the remaining state at shut-down. The results show that purging is necessary in order to successfully start-up in sub-zero freezing environments. The results show that by increasing the purge temperature, rate and duration, enhances water removal.

- Start-up at sub-zero temperature is affected by the remaining water hydrating the membrane.
- Start-up and shut-down procedures should be employed in combination with the operating temperature of the stack. If stack operation is only used for a short period of time, the stack temperature may be too low for a properly conducted purge.
- Currently a lower purge temperature has a lower performance. Increasing the length of purge may remove more water that hinders the stacks ability to start-up successfully and/or stably.

- A minimum purge temperature is necessary in order to execute a stable start-up at sub-zero temperatures.
- Decreasing water content will increase proton resistances prolonging the time required to start-up but is necessary at low temperatures. As water is generated, it can be absorbed by the membrane and improve performance. An excessively purged stack (i.e. very dry during shut-down) is more difficult to start-up as a result of lower membrane water content.
- Purging the stack improves the overall start-up by removing remaining water, decreasing the overall thermal mass of the system and freeing up locations for water retention and accumulation.
- As the external temperature decreases, the importance of stack conditioning increases for the successful start-up operation. An increase in purge temperature or rate increases the amount of time required for successful operation regardless of temperature.

1.21. Recommendations and Future Work

- Consideration should be given to employing a limited volume coolant or employing a bypass coolant loop. The bypassed coolant will improve performance and heat distribution across the cells improving stability and controlling the temperature ramp.
- Assisted start-up can be examined with the addition of pre-heaters on the inlet gases in order to determine the degree of improvement in start-up times if any and/or allow for start-up at lower freeze temperatures.
- Adjustment of gas reactant stoichiometry may improve start-up if hydrogen is allowed to operate with minimal excess. It will be useful to determine the optimal performance by varying the stoichiometry.
- A purge of the stack is critical for freeze start-up but may be possible by further reducing by the anode purge time. Extending the cathode purge time may allow a shorter anode purge and still remove the required amount of water to start-up successfully.
- Start-up at a prolonged low current density may allow successful sub-zero start-up below the current limit. If the heat that is generated in the stack is allowed to remain by limiting the speed of the exiting gas flows while removing product water the stack may be able to transfer enough heat within the cells to enable increased performance. This may be approached by an increased flow on the cathode side while having a reduced anode flow rate.

- Investigation can be conducted on start-up procedure modification. Start-up flows delivered to the anode may be reduced and save fuel since the ORR and water build-up in the cathode GDM make the largest contribution to a decrease in performance. The amount of water generated in the PEMFC stack is limited by the amount that can be absorbed by the membrane and accumulate between the CL and MPL before 'break though' leading to ice. Some work has been completed, but a more comprehensive study would further the understanding.
- System can be modified replacing or reducing the thermal mass of the system components to make it easier to heat them during start-up. The graphite bi-polar plates could be replaced with stainless steel and reduce the heat capacity by about three times for the same mass. The use of stainless steel plates enables less mass to be used due to their improved strength.
- Modification of the endplates can be done in order to lighten, insulate or reduce their cooling effect.
- Note that gas purging wastes reactants, power and increases cell resistance during a non-freezing temperature start-up. Rapid start-up of a stack at non-freezing conditions will no longer be possible. As such, the employment of a gas purging procedure should only be used when required. Limiting the use of a purging procedure will require tracking the temperature of the stack environment for potential freeze situations.

BIBLIOGRAPHY

1 The National Hydrogen Association. The Energy Evolution: an analysis of alternative vehicles and fuels to 2010. The National Hydrogen Association; 2009.

2 EG&G Technical Services, Inc. Fuel Cell Handbook ed. 7. Morgantown: U.S. Department of Energy; 2004.

3 Bose S, Kuila T, Nguyen T, Kim N, Lau K, Lau K. Polymer membranes for high temperature proton exchange membrane fuel cell: Recent advances and challenges. Progress in Polymer Science. 2011 813-843.

4 Gottesfeld S, Wilson MS. High performance catalyzed membranes of ultra-low Pt loadings for polymer electrolyte fuel cells. Journal of the Electrochemical Society. 1992 February;139(2):L28-L30.

5 Morozan A, Jousselme B, Palacin S. Low-platinum and platinum-free catalysts for the oxygen reduction reaction at fuel cell cathodes. Energy and Science. 2011;4:1238-1254.

6 U.S. Department of Energy. 2007 DOE Hydrogen Program Merit Review and Peer Evaluation Meeting.; 2007.

7 Thompson EL, Jorne J, Gu W, Gasteiger HA. PEM Fuel Cell Operation at −20°C. II. Ice Formation Dynamics, Current Distribution, and Voltage Losses within Electrodes. Journal of The Electrochemical Society. 2008;155(9):B887-B896.

8 Japan Hydrogen & Fuel Cell Demonstration Project. About FC. [Internet]. 2011 [cited 2011 March 25]. Available from: http://www.jhfc.jp/e/beginner/about_fc/.

9 Gostick J. Multiphase Mass Transfer and Capillary Properties of Gas Diffusion Layers for Polymer Electrolyte Membrane Fuel Cells. PhD Thesis. Waterloo, Ontario: University of Waterloo; 2008.

10 Qi Z, Kaufman A. Improvement of water management by a microporous sublayer for PEM fuel cells. Journal of Power Sources. 2002;109:38-46.

11 Ramasamy RP, Kumbur EC, Mench MM, Liu W, Moore D, Murthy M. Investigation of macro- and micro-porous layer interaction in polymer electrolyte fuel cells. International Journal of Hydrogen Energy. 2008;33:3351-3367.

12 Kandlikar SG. Microscale and Macroscale Aspects of Water Management Challenges in PEM Fuel Cells. Heat Transfer Engineering. 2008 July;29(7):575-587.

13 Larminie J, Dicks A. Fuel Cell Explained. 2nd ed. Chichester, England: John Wiley & Sons; 2003.

14 Yi JS, Puhalski J, King C. Porous Bipolar Plate with Interdigitated Flow Fields. [Internet]. [cited 2011 June 21]. Available from: www.electrochem.org/dl/ma/202/pdfs/0812.PDF.

15 Litster S, Buie CR, Fabian T, Eaton JK, Santiago JG. Active water management for PEM fuel cell. Journal of The Electrochemical Society. 2007;154(10):B1049-B1058.

16 Weber A. Gas-Crossover and Membrane-Pinhole Effects in Polymer-Electrolyte Fuel Cells. Journal of the Electrochemical Society. 2008;155(6):B521-B531.

17 Kreuer KD. On the development of proton conducting polymer membranes for hydrogen and methanol fuel cells. Journal of Membrane Science. 2001;185:29-39.

18 Nguyen TV, Mack W K. A liquid water management strategy for PEM fuel cell stacks. Journal of

Power Sources. 2003;114:70-79.

19 Chen J, Matsuura T, Hori M. Novel gas diffusion layer with water management function for PEMFC. Journal of Power Sources. 2004;131:155-161.

20 Canut JML, Abouatallah RM, Harrington DA. Detection of Membrane Drying, Fuel Cell Flooding, and Anode Catalyst Poisoning on PEMFC Stacks by Electrochemical Impedance Spectroscopy. Journal of The Electrochemical Society. 2006;153(5):A857-A864.

21 Zawodzinski TA, Derouin C, Radzinski S, Sherman RJ, Smith VT, Springer TE, Gottesfeld S. Water Uptake by and Transport Through Nafion 117 Membranes. Journal of the Electrochemical Society. 1993;140(4):1041-1047.

22 Gurau V, Bluemle MJ, Castro ESD, Tsou YM, Mann JA, Zawodzinski TA. Characterization of transport properties in gas diffusion layers for proton exchange membrane fuel cells: 1. Wettability (internal contact angle to water and surface energy of GDL fibers). Journal of Power Sources. 2006 October;160(2):1156-1162.

23 Ge S, Wang CY. Characteristics of subzero startup and water/ice formation on the catalyst layer in a polymer electrolyte fuel cell. Electrochimica Acta. 2007;52:4825–4835.

24 Mauritz KA, Moore RB. State of Understanding of Nafion. Chemical Review. 2004;104:4535-4585.

25 Yoshida H, Mirua Y. Behavior of water in perfluorinated ionomer membranes containing various monovalent cations. Journal of Membrane Science. 1992;68:1-10.

26 Thompson E, Capehart T, Fuller T, Jorne J. Investigation of Low-Temperature Proton Transport in Nafion Using Direct Current Conductivity and Differential Using Direct Current Conductivity and

Differential. Journal of The Electrochemical Society. 2006;153(12):A2351-A2362.

27 Mukundan R, Kim YS, Garzon F, Pivovar B. Freeze/Thaw Effects in PEM Fuel Cells. ECS Transactions. 2006;1(8):403-413.

28 Nandy A, Jiang F, Ge S, Wang CY, Chen KS. Effect of Cathode Pore Volume on PEM Fuel Cell Cold Start. Journal of The Electrochemical Society. 2010;157(No. 5):B726-B736.

29 Wang Y, Mukherjee PP, Mishlera J, Mukundan R, Borup RL. Cold start of polymer electrolyte fuel cells: Three-stage startup characterization. Electrochimica Acta. 2010;55:2636-2644.

30 Owejan JP, Gagliardo JJ, Falta SR, Trabold TA. Accumulation and Removal of Liquid Water in Proton Exchange Membrane Fuel Cells. Journal of The Electrochemical Society. 2009;156(12):B1475-B1483.

31 Ito H, Maeda T, Kato A, Yoshida T, Ullebergd Ø. Gas Purge for Switching from Electrolysis to Fuel Cell Operation in Polymer Electrolyte Unitized Reversible Fuel Cells. Journal of The Electrochemical Society. 2010;157(7):B1072-B1080.

32 Hiramitsu Y, Mitsuzawa N, K. Okada MH. Effects of ionomer content and oxygen permeation of the catalyst layer on proton exchange membrane fuel cell cold start-up. Journal of Power Sources. 2010;195:1038–1045.

33 Cho E, Ko JJ, Ha HY, Hong SA, Lee KY, Lim TW, Oh IH. Characteristics of PEMFC repetitively brought to temperatures below 0°C. Journal of The Electrochemical Society. 2003;150(12):A1667-A1670.

34 Jiang F, Wang CY, Chen KS. Current Ramping: A Strategy for Rapid Start-up of PEMFCs from Subfreezing Environment. Journal of The Electrochemical Society. 2010;157(3):B342-B347.

35 Ge S, Wang CY. Cyclic Voltammetry Study of Ice Formation in the PEFC Catalyst Layer during Cold Start. 2007;154(12):B1399-B1406.

36 Oszcipok M, Riemann D, Kronenwett U, Kreideweis M, Zedda M. Statistic analysis of operational influences on the cold start behaviour of PEM fuel cells. Journal of Power Sources. 2005;145:407-415.

37 Kim S, Mench MM. Investigation of Temperature-Driven Water Transport in Polymer Electrolyte Fuel Cell: Phase-Change-Induced Flow. Journal of The Electrochemical Society. 2009;156(3):B353-B362.

38 Guo Q, Qi Z. Effect of freeze-thaw cycles on the properties and performance of membrane-electrode assemblies. Journal of Power Sources. 2006;160:1269-1274.

39 Hou J, Yu H, Zhang S, Sun S, Wang H, Yi B, Ming P. Analysis of PEMFC freeze degradation at −20◦C after gas purging. Journal of Power Sources. 2006;162:513-520.

40 Lee SY, Kim HJ, Cho E, Lee KS, Lim TH, Hwang IC, Jang JH. Performance degradation and microstructure changes in freezeethaw cycling for PEMFC MEAs with various initial microstructures. International journal of hydrogen energy. 2010 December;35(23):12888-12896.

41 Kim S, Mench MM. Physical degradation of membrane electrode assemblies undergoing freeze/thaw cycling: Micro-structure effects. Journal of Power Sources. 2007 November;174(1):206–220.

42 He S, Mench MM. One-Dimensional Transient Model for Frost Heave in Polymer Electrolyte Fuel Cells. Journal of The Electrochemical Society. 2006;153(9):A1724-A1731.

43 Lee C, Merida W. Gas diffusion layer durability under steady-state and freezing conditions. Journal of Power Sources. 2007;164:141-153.

44 Lee SY, Kim SU, Kim HJ, Jang JH, Oh IH, Cho EA, Hong SA, Ko J, Lim TW, Lee KY, et al. Water removal characteristics of proton exchange membrane fuel cells using a dry gas purging method. Journal of Power Sources. 2008;180:784-790.

45 Meng H. A PEM fuel cell model for cold-start simulations. Journal of Power Sources. 2008;178:141-150.

46 Kandlikar SG, Zijie L. Fundamental Research Needs in Combined Water and Thermal Management Within a Proton Exchange Membrane Fuel Cell Stack Under Normal and Cold-Start Conditions. 2009;6.

47 Bruijn FAd, Dam VAT, Janssen GJM. Review: Durability and Degradation Issues of PEM Fuel Cell Components. Fuel Cells. 2008;1:3-22.

48 Álvarez-Gallego Y, deHeer MP. Sub-Freezing Conductivity of PFSA Membranes. Fuel Cells 09. 2009;4:421-431.

49 Springer TE, Zawodzinski TA, Wilson MS, Gottesfeld S. Characterization of Polymer Electrolyte Fuel Cells Using AC impedance spectroscopy. Journal of the Electrochemical Society. 1996 February;143(2):587-599.

50 Hou J, Yi B, Yu H, Hao L, Song W, Fu Y, Shao Z. Investigation of residedwater effects on PEM fuel cell after cold start. International Journal of Hydrogen Energy. 2007;32:4503 – 4509.

51 Taniguchi A, Akita T, Yasuda K, Miyazaki Y. Analysis of electrocatalyst degradation in PEMFC caused by cell reversal during fuel starvation. Journal of Power Sources. 2004;130:42-49.

52 Argonne National Laboratory. Development and Application of GREET 2.7 - The Transportation Vehicle-Cycle Model. Oak Ridge: Energy System Division ; 2006.

53 Sumit K, Fowler M, Simon L, Abouatallah R, Beydokhti N. Open circuit voltage durability study and model of catalyst coated membranes at different humidification levels. Journal of Power Sources. 2010;195(21):7323-7331.

54 Kundu S, Fowler MW, Simon LC, Abouatallah R, Beydokhti N. Degradation analysis and modeling of reinforced catalyst coated membranes operated under OCV conditions. Journal of Power Sources. 2008;183(2):619-628.

55 W. L. Gore & Associates. GORE™ PRIMEA® SERIES 57 MEAs. W. L. Gore & Associates, Inc.; 2003.

56 Ramousse J, Lottin O, Didierjean S, Maillet D. Heat sources in proton exchange membrane (PEM) fuel cells. Journal of Power Sources. 2009;192:435-441.

57 Zhao TS,KKD,NTV. Advances in Fuel Cells. Elsevier Science; 2007.

58 Yan Q, Toghiani H, Lee YW, Liang K, Causey H. Effect of sub-freezing temperatures on a PEM fuel cell performance, startup and fuel cell components. Journal of Power Sources. 2006;160:1242-1250.

59 Wheeler D. 2007 Status of Manufacturing: Polymre Electrolyte Membrane (PEM) Fuel Cells. Golden: National Renewable Energy Laboratory; 2008.

60 Wang H, Hou J, Yu H, Sun S. Effects of reverse voltage and subzero startup on the membrane

electrode assembly of a PEMFC. Journal of Power Sources. 2007;165:287-292.

61 Thomas S,ZM,&GD. Fuel Cells - Green Power. 2006.

62 Tang H, Peikang S, Jiang SP, Wang F, Pan M. A degradation study of Nafion proton exchange membrane of PEM fuel cells. Journal of Power Sources. 2007;170:85–92.

63 Tajiri K, Tabuchi Y, Kagami F, Takahashi S, Yoshizawa K, Wang C. Effects of operating and design parameters on PEFC cold start. Journal of Power Sources. 2007;165:279-286.

64 Sederquist, A. R, inventors. 1988. 4766044.

65 Schmittinger W, Vahidi A. A review of the main parameters influencing long-term performance and durability of PEM fuel cells. Journal of Power Sources. 2008;180:1-14.

66 Saito M, Hayamizu K, Okada T. Temperature Dependence of Ion and Water Transport in Perfluorinated Ionomer Membranes for Fuel Cells. Journal of Physical Chemistry. 2005;109:3112-3119.

67 Saito M, Arimura N, Hayamizu K, Okada T. Mechanisms of Ion and Water Transport in Perfluorosulfonated Ionomer Membranes for. Journal of Physical Chemistry B. 2004;108:16064-16070.

68 Ryan O'Hayre R,CSW,PFB,CW. Fuel Cell Fundamentals. John Wiley & Sons; 2009.

69 R. C. McDonald CKMaELT. Effects of Deep Temperature Cycling on Nafion 112 Membranes and Membrane Electrode Assemblies. Fuel Cells. 2004;4(No. 3):208-213.

70 Pineri M, Volino F, Escoubes M. Evidence for Sorption Ddesorption Phenomena during Thermal Cycling in Highly Hydrated Perfluorinated Membranes. Journal of Polymer Science. 1985;23:2009-2020.

71 Pesaran AA, Kim GH, Gonder JD. PEM Fuel Cell Freeze and Rapid Startup Investigation. National Renewable Energy Laboratory; 2005.

72 Oszcipok M, Riemann D, Kronenwett U, Kreideweis M, Zedda M. Start Up and Freezing Processes in PEM Fuel Cells. Fuel Cells 07. 2007 135-141.

73 Mehta V,CJS. Review and analysis of PEM fuel cell design and manufacturing. Journal of Power Sources. 2003 32-53.

74 Lee JS, Quan ND, Hwang JM. Polymer Electrolyte Membranes for Fuel Cells. 2006;12, No. 2.

75 Lanz A. Hydrogen Fuel Cell Enginers and Related Technologies. Palm Desert: College of the Desert; 2001.

76 Karian HG. Handbook of polypropylene and polypropylene composites. CRC Press; 2003.

77 Karakoussis V,LM,VR,HD,LJ,PP,KJ. Environmental Emissions of SOFC and SPFC System Manufacture and Disposal. Crown; 2000.

78 Kandlikar SG, Lu Z. Thermal management issues in a PEMFC stack – A brief review of current status. Applied Thermal Engineering. 2009;29:1276–1280.

79 Fowler MW, Mann RF, Amphlett JC, Kundu S, Wheeldon I, Peppley BA. Issues Associated with Material Characteristics in PEM Fuel Cells. 135-157: The Institution Mechanical Engineers; 2004.

80 Fenton J. M. RMP,SDK,HX,BLF,RK. Membrane Degradation Mechanisms and Accelerated Durability Testing of Proton Exchange Membrane Fuel Cells. Journal of the Electrochemical Society. 2009;216(25):233-247.

81 Cortese A. DuPont's Teflon Dilemma. [Internet]. 2003 [cited 2009 April 4]. Available from: http://www.ewg.org/node/15788.

82 Cooper JS. Design analysis of PEMFC bipolar plates considering stack manufacturing and environmental impact. Journal of Power Sources. 2004 152-169.

83 C.H. Lee HBPCHPea. Preparation of high-performance polymer electrolyte nanocomposites through nanoscale silica particle dispersion. 2009;195.

84 Boyle N, McBrierty VJ, Douglass D. A Study of the Behavior of Water in Nafion Membranes. Macromolecules. 1983;16(No. 1):80-84.

85 Borup R, Meyers J, Pivovar B, Kim YS, Mukundan R, Garland N, Myers D, Wilson M, Garzon F, Wood D, et al. Scientific Aspects of Polymer Electrolyte Fuel Cell Durability and Degradation. American Chemical Society. 2007;107:3904-2951.

86 Barnes JE,EJD. Chemistry and Industry. 1982 151-155.

87 Barakat MAMMHH. Recovery of Platinum from Spent Catalyst. Hydrometallurgy. 2004 170-184.

88 Appleby AJ, Foulkes FR. Fuel Cell Handbook. 6th ed. Krieger Pub Co.; 2002.

89 Amphlett JC, Mann RF, Peppley BA, Roberge PR, Rodrigues A. A model predicting transient responses of proton exchange membrane fuel cells. Journal of Power Sources. 1996 July;61(1-

2):183-188.

90 Adamson AW. Physical Chemistry of Surfaces. New York: John Wiley & Sons; 1967.

91 Institute of Transportation Studies. Technical assessment of advanced vehciles for advanced energy pathways project. Institute of Transportation Studies; 2008.

92 Electricity Guide.org. Fuel Mix Information. [Internet]. [cited 2009 April 13]. Available from: http://www.electricity-guide.org.uk/fuel-mix.html.

93 Smithsonian Institution. Collecting the history of Proton Exchange Membrane Fuel Cells. [Internet]. 2004 [cited 2010 April 2]. Available from: http://americanhistory.si.edu/fuelcells/pem/pemmain.htm.

94 Industry Canada. Canadian Fuel Cell Commercialization Roadmap. Ottawa, ON: PricewaterhouseCoopers; 2003. ISBN 0-662-33769-7.

95 Cho E, Ko JJ, Ha HY, Hong SA, Lee KY, Lim TW, Oh IH. Characteristics of PEMFC repetitively brought to temperatures below 0°C. Journal of The Electrochemical Society. 2003;150 (12):A1667-A1670.

96 U.S. Department of Energy. DOE Hydrogen Program Merit Review and Peer Evaluation Meeting.; 2007.

97 Jiao K, Li X. Water transport in polymer electrolyte membrane fuel cells. Progress in Energy and Combustion Science. 2011;37:221 - 291.

98 Miller M, Bazylak A. A review of polymer electrolyte membrane fuel cell stack testing. Journal of Power Sources. 2011;196(2):601-613.

99 Yousfi-Steiner N, otéguy PM, Candusso D, Hisselb D. A review on polymer electrolyte membrane fuel cell catalyst degradation and starvation issues: Causes, consequences and diagnostic for mitigation. Journal of Power Sources. 2009;194:130-145.

100 Dincer I. Environmental and sustainability aspects of hydrogen and fuel cell systems. International Journal of Energy Research. 2006 29-55.

101 Gasteiger HA, Kocha SS, Sompalli B, Wagner FT. Activity benchmarks and requirements for Pt, Pt-alloy, and non-Pt oxygen reduction catalysts for PEMFCs. Applied Catalysts. 2004.

102 Cho E, Ko JJ, Ha HY, Hong SA, Lee KY, Lim TW, Oh IH. Characteristics of PEMFC repetitively brought to temperatures below 0°C. Journal of The Electrochemical Society. 2003;150(12):A1667-A1670.